Dissertation

Functional genomics of nodulins in the model legume *Lotus japonicus*

vorgelegt an der Mathematisch-Naturwissenschaftlichen Fakultät der Universität Potsdam

von Thomas Ott

geb. am 12.03.1975 in Marburg/Lahn

zur Erlangung des akademischen Grades

Dr. rer. nat.

Wissenschaftsdisziplin: Molekularbiologie der Pflanzen
Die Arbeit wurde am Max-Planck-Institut für Molekulare Pflanzenphysiologie in Golm angefertigt

Diese Arbeit wurde von folgenden Gutachtern bewertet:

1. Prof. Dr. Mark Stitt, Max-Planck-Institut für Molekulare Pflanzenphysiologie, Golm, Germany
2. Prof. Dr. Martin Parniske, Ludwig-Maximilians-Universität München, Germany
3. Prof. Dr. Peter Gresshoff, ARC Centre of Excellence, Queensland, Australien

Die Arbeit wurde am 03. Januar 2005 an der Universität Potsdam zur Begutachtung eingereicht.
Tag der mündlichen Prüfung war der 01. Juli 2005.

I. Contents

II. Figures

III. Abbreviations

A	adenosine
AA	ascorbic acid
ADP	adenosine diphosphate
AFLP	amplified fragment length polymorphism
AM	arbuscular mycorrhiza
AMP	adenosine monophosphate
AOX	ascorbate oxidase
APX	ascorbate peroxidase
AS	asparagine sythetase
Asp	aspartate
AT	aminotransferase
At	*Arabidopsis thaliana*
ATP	adenosine triphosphate
BNF	biological nitrogen fixation
bp	base-pairs
bv.	biovar
C	cytosin
CaMV	cauliflower-mosaic virus
CAT	catalase
Cd	cadmium
cDNA	complementary DNA
Cgs	cyclic glucan synthase
CO_2	carbon dioxide
cOMT	isoliquiritigenin-2'-O-methlytransferase
cpm	counts per minute
CTAB	Cetyl Trimethyl Ammonium Bromide
DEPC	diethylpyrocarbonate
DHA	dehydroascorbate
DHAR	dehydroascorbate reductase
DNA	desoxyribonucleic acid
Dpi	days post inoculation
ds DNA	double-stranded DNA
EDTA	ethlyenediaminetetraacetat
EMS	ethylmethane sulfonate
ENOD	early nodulin
EST	expressed sequence tag
et al.	and others
Fe	iron
FOL	fractional oxygenation of leghemoglobin
FW	fresh-weight
G	guanine
GDH	glutamate dehydrogenase
Gln	glutamine
Glu	glutamate
Gm	*Glycine max*
GOGAT	glutamate synthase
GR	glutathione reductase
GPX	glutathione peroxidase
GS	glutamine synthetase

GSH	reduced glutathione
GSSG	oxidised glutathione
Gus	β-glucurosidase
H_2O_2	hydrogen peroxide
Hpi	post inoculation
HPLC	high-pressure liquid chromatography
K	thousand
kDa	kilo Dalton
KDRI	Kazusa DNA Research Institute
KNO_3	potassium-nitrate
Lb	leghemoglobin
LCO	lipo-chitin oligosaccharides
Lj	*Lotus japonicus*
LPS	lipopolysaccharide
LRR	leucine rich repeat
MDA	monodehydroascorbate
MDAR	monodehydroascorbate reductase
MDH	malate dehydrogenase
MIPS	Munich information center for protein sequences
mM	milli-molar
Mo	molybdate
MPI-MP	Max-Planck-Institute of Plant Molecular Biology
MPSS	massively parallel signature sequencing
mRNA	messenger RNA
Mt	*Medicago truncatula*
MYA	million years ago
$N_{(2)}$	(gaseous) nitrogen
NAD(P)H	Nicotinamideadeninedinucleotide phosphate
NCBI	National Centre for Biotechnology Information
NEST	EST clones derived from a nodule library
NFR	Nod-factor receptor
NH_3	ammonia
NiR	nitrite reductase
nM	nano-molar
NO_3^-	nitrate
NR	nitrate reductase
NSG	non-symbiotic globin
O_2	gaseous oxygen
OCS	octopinsynthase
ODB	oxygen diffusion barrier
ORF	open reading frame
Os	*Oryza sativa*
PAGE	polyacrylamide gel-electrophoresis
PBM	peribacteroid membrane
PCR	polymerase chain reaction
PEPC	phosphoenolpyruvate carboxylase
PTGS	post-transcriptional gene silencing
PVPP	polyvinylpolypyrrolidon
RACE	3’ rapid amplification of cDNA ends
redox	reduced/oxidised
RNA	ribonucleic acid

RNAi	RNA interference
RNS	Root-Nodules Symbiosis
ROS	reactive oxygen species
RT	reverse transcription/ reverse transcriptase
SD	standard deviation
SDS	sodium dodecyl sulphate
SM	symbiosome membrane
SNF	symbiotic nitrogen fixation
SOD	superoxide dismutase
Sst	Symbiotic sulfate transporter
Sym	symbiotic
T	thymine
TAC	transformation-competent artificial chromosome
TC	tentative consensus sequence
TCA	tri-carbonic acid cycle
T-DNA	transfer DNA
TF	transcription factor
TIGR	The Institute for Genomic Research
wpi	weeks post inoculation
wt	wild-type

1.0. Introduction

1.1. The importance of biological nitrogen fixation

Nitrogen (N) is one of the major nutritional elements for plants and is cycled globally in the biogeochemical nitrogen cycle. There are a limited number of ways that nitrogen becomes available in soils for plant growth, including: Entry of oxides of N in rain produced by electrical discharge (lightening), biological nitrogen fixation of N_2 to ammonia, and a similar industrial process which provides fertilizer N for agriculture to the tune of 80 million tonnes per anum (Vitoursek et al., 1997). 50-70% of the worlds biological nitrogen fixation (BNF), leading to a terrestrial input of 40-50 million tons of nitrogen per year (Vitoursek et al., 1997), is carried out by symbiotic nitrogen fixation (SNF), mostly between bacteria of the family *Rhizobiaceae* and legume plants. Ammonia produced by biological and industrial reduction of N_2 can be used by most organisms. However, soil bacteria that derive their energy by oxidation of NH_3 to nitrite (NO_2^-) and nitrate (NO_3^-) are so abundant that nearly all ammonia in the soil is quickly oxidized to nitrate. This process is called nitrification. Plants and bacteria can reduce nitrate to ammonia by the action of nitrate reductases (nitrate assimilation). Ammonia is used for the biosynthesis of amino acids in plants and other autotrophs, which are eventually consumed by heterotrophs, including humans. Microbial degradation of proteins after the death of organisms returns ammonia to the soil, where nitrifying bacteria convert it to nitrate and nitrite again. A balance is achieved between mineral or fixed nitrogen and atomospheric nitrogen by bacteria that convert nitrate to N_2 under anaeobic conditions. In this process, called denitrification, soil bacteria use NO_3 as the final electron acceptor in a series of reactions that generates a proton gradient for ATP synthesis. In addition to inorganic, oxidised and reduced forms of N, soil biological activity also turns over large organic molecules containing N, liberating smaller organic N-molecules like amino acids that can be used by plants.

1.2. Legumes and evolution of SNF

The legumes are a diverse and important family of angiosperms. With more than 650 genera and 18,000 species, legumes are the third largest family of higher plants and are second only to grasses in agricultural importance (reviewed in Doyle, 2001). Legumes range from tiny herbs to giant trees, dominating many tropical rainforests. During symbiosis with bacteria of the root-colonising genera *Rhizobium* these plants form a novel organ called the root nodule that enables SNF. This feature makes legumes

relatively unique among land-plants. SNF in legumes was discovered in Germany over 100 years ago (Hellriegel and Wilfarth, 1888).

Ninety percent of all land plants are able to establish arbuscular mycorrhizal symbioses (AM) with zygomycete fungi, which provide plants with phosphorus and other nutrients. It is believed that AM symbiosis evolved 450 million years ago (MYA), at the time plants colonised the land (Brundrett, 2002). Root-nodule symbiosis (RNS) evolved much later, at around 65 MYA (Herendeen et al., 1999; Soltis et al., 2002). Today, RNS is confined to the clade Eurosid I that includes the orders Fabales, Fagales, Cucurbitales and Rosales. While the ancestors of nodulating plants might have had a predeposition for nodulation it seems possible that root nodules themselves evolved several times independently (Kistner and Parniske, 2002). Based on this genetic overlap, it is believed that features of the evolutionary older AM symbiosis were recruited during evolution of RNS (Albrecht et al., 1999; Gualtieri and Bisseling, 2000; Kistner and Parniske, 2002).

After map-based cloning of several S*ym* genes including *Nork* (Nodulation Receptor Kinase) and *Symrk* (Symbiosis Receptor-like Kinase) genes (Endre et al., 2002; Stracke et al., 2002) it was finally proven that common signalling components are required to establish both rhizobial and mycorrhizal symbioses (for review see: Albrecht et al., 1999; Kistner and Parniske, 2002).

1.3. Bacteria-plant signalling prior to SNF: plant flavonoids and bacterial Nod factors

Nitrogen limited legumes release flavone and flavonone compounds such as luteolin, a tetrahydroxyflavone, or daidzein, an isoflavone, into the surrounding soil. Each plant species produces a distinct mixture of flavonoids and isoflavonoids, and the quantity as well as the spectrum of the different compounds vary with age and the physiological status of the plant (for reviews see: Downie, 1994; Phillips and Streit, 1996; Spaink, 2000). Such flavonoids are perceived by the rhizobia as positive signals to which they respond by the production and release of signalling molecules called Nod factors. Because Nod factors consist of an oligosaccharide backbone of β-1,4-linked *N*-acetyl-D-glucosamine and a fragment of chitin *inter alia*, Nod factors are often called lipo-chitin oligosaccharides (LCOs). Rhizobial Nod factors elicit complex responses in legume root cells, including altered calcium fluxes and cell division (Felle et al., 1998; Albrecht et al., 1999).

1.4. Host specificity

Rhizobia-legume interactions exhibit specificity, whereby rhizobial strains nodulate a limited range of legumes. For example, *Mesorhizobium loti* infects *Lotus* most effectively, *Sinorhizobium meliloti* induces nodule development on *Medicago*, *Melilotus* and *Trigonella*. *Rhizobium leguminosarum* bv *viciae* initiates nodulation on *Pisum*, *Vicia*, *Lens* and *Lathyrus* ssp. Closely related to *Rhizobium leguminosarum* bv *viciae* is *R. leguminosarum* bv *trifolii*, which nodulates only some species of clover (*Trifolium*). However, not all rhizobia-legume associations are this tight. For example, *Rhizobium* strain NGR234 nodulates 232 species of legumes from 112 genera tested and even nodulates the non-legume *Parasponia andersonii*, a member of the elm family (Pueppke and Broughton, 1999).

Host specificity is determined in part by the Nod factors produced by different rhizobia, which differ in their R5 position of the reducing terminus of the Nod factors and other side-groups. Thus, mutations in *Nod* genes can impair nodulation and alter host specificity (reviewed in Spaink, 2000).

1.5. The infection process and nodule development

1.5.1. Morphological changes

Physical interactions between rhizobia and legumes typically begin by attachment of compatible rhizobial strains to root hairs, which lead to root hair swelling and curling, and to formation of a hook-like structure (sheperd's crooks) (reviewed in Gage, 2004). Rhizobia enter root hairs via the infection thread, an invagination of the cell wall and plasma membrane, that provides access to underlying cortical cells of the root. Rhizobia inside infection threads are topologically outside the root hair, as the infection thread wall is contiguous with the cell wall of the root hair. In parallel to the infection processes that take place in the root hair, de-differentiation and activation of cortical cells below infected root hairs result in the formation of the nodule primordia (Brewin, 1991; Gage, 2004). During primordial development in determinate nodules divisions are observed in the outer cortical cells while in case of the formation of indeterminate nodules the cells of the inner cortex divide (further discussed below).

Infection threads eventually penetrate root cortical cells and release rhizobia into the plant cells by endocytosis, resulting in a novel organelle called symbiosome. Symbiosomes consist of rhizobia surrounded by a plant membrane called the peribacteroid or symbiosome membrane (SM). Bacteria and symbiosomes continue to

grow and divide until host cells are packed with thousands of symbiosomes, each containing one or few bacteroids. Bacteroids are the differentiated nitrogen fixing form of the rhizobia. Results from biochemical and proteomic studies indicate that the SM harbours multiple transport systems that facilitate and control nutrient exchange between the plant cell cytoplasm and the bacteria (Panter et al., 2000; Udvardi and Day, 1997; Saalbach et al., 2002; Wienkoop and Saalbach, 2003).

1.5.2. Determinate and indeterminate nodules

Two types of nodules are formed on different legumes (Figure 1.1). Determinate nodules lack a persistent meristem and are typically spherical, as exemplified by nodules on *Glycine max* (soybean) and *Lotus japonicus*. Determinate nodules are ephemeral and have a life-span of a few weeks. When old nodules senescense new nodules are formed when the root grows further (for detailed information see: Rolfe and Gresshoff, 1988).

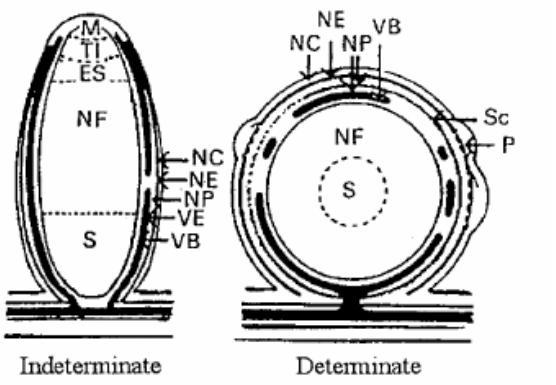

Figure 1. 1: Schematic cross-sections of anatomy of indeterminate and determinate nodules.

M= meristem; TI= thread invasion zone; ES= early symbiotic zone; NF= nitrogen fixing zone; S= senescent zone; NC= nodule cortex; NE= nodule endodermis; NP= nodule parenchyma; VE= vascular endodermis; VB= vascular bundle; SC= sclerenchyma; P=periderm (from Hirsch, 1992).

Indeterminate nodules have a persistent meristem, which results in nodules of cylindrical shape, as exemplified by nodules of *Pisum sativum* (pea) and *Medicago truncatula*. The apical meristem continuously produces new cells which become infected with bacteria provided from older cells. These nodules have a much more extensive vascular system than determinate nodules which surrounds the nitrogen-fixing in the center of the nodule.

1.5.3. Physiological changes during nodule development

Perception of the rhizobial Nod factors by the plant triggers downstream events to occur that are needed to establish the symbiosis. The receptor required for Nod factor perception was recently cloned in *Lotus japonicus* (Madsen et al., 2003; Radutoiu et al., 2003) and *Medicago truncatula* (Limpens et al., 2003). Within seconds after Nod factor addition, intracellular movement of Ca^{2+}, H^{+}, Cl^{-}, and K^{+} ions as well as membrane depolarization occurs (Ehrhardt et al., 1992; Felle et al., 1995; Felle et al., 1998; Kurkdjian, 1995). In the following minutes, changes in cytoplasmic Ca^{2+}-concentrations and calcium spiking occur (Ehrhardt et al., 1996; Catoira et al., 2000), which are believed to trigger further downstream events, including changes in gene expression. However, details of these processes remain unknown.

During nodule organogenesis large scale transcriptional and metabolic changes occur that set the scene for SNF. One of the major physiological changes during nodule developement is the reduction of free oxygen concentrations in the nodule tissue, which enables the oxygen sensitive enzyme nitrogenase to function. Leghemoglobins are believed to play an important role in this context.

1.6. Leghemoglobins are the most abundant proteins in nodules

Leghemoglobins (Lb) are the most famous and probably best characterised nodulins, or nodule-specific proteins (discussed below) in legumes. They were discovered in 1939 by Hideo Kubo, who described a protein present in extracts from soybean nodules that showed similar spectral behaviour to the hemoglobins from humans and mammals (Kubo, 1939). Kubo also showed that bacterial respiration and oxygen consumption were enhanced in the presence of the hemoprotein. Since then, extensive research has been carried out on hemoglobins from many organisms, including humans, mammals, plants, yeast and bacteria (Wittenberg and Wittenberg, 1990). Plant hemoglobins can be divided into three classes: The symbiotic hemoglobins (in the following text called leghemoglobins), the non-symbiotic hemoglobins (Bogusz et al., 1988; Trevaskis et al., 1997) and the truncated hemoglobins that are similar to non-symbiotic hemoglobins (Watts et al., 2001). Leghemoglobins are the most prominent proteins in root nodules and accumulate to millimolar concentrations in the infected cells of a nodule. Their backbone and the heme moiety of the protein are synthesised by the plant host (Santana et al., 1998).

The binding affinity of leghemoglobins was reported to be about 20-times higher than human myoglobin (Trent et al., 2001). The rate constant for O_2 binding for soybean Lb_a was determined to be 130 $\mu M^{-1}s^{-1}$ and the oxygen equilibrium constant to be 23 $\mu M^{-1}s^{-1}$ (Hargrove et al., 1997; Wittenberg et al., 1972). For respiration to occur in the presence of hemoglobin with a higher affinity for oxygen, a terminal oxidase is required. Indeed, k_m values for rhizobial cyctochrome-c-oxidase of 2-5 nM (Bergersen and Turner, 1993; Kuzma et al., 1993; Preisig et al., 1996) and of 20-44 nM for leghemoglobins (Appleby, 1984) have been reported. In addition, it was shown that the presence of leghemoglobin protein is directly correlated with respiration and nitrogenase activity (Dakora, 1995). These findings make leghemoglobins likely candidates for facilitation of oxygen diffusion at low oxygen concentrations in nodule cells. Nonetheless, the physiological role of leghemoglobins in nodules was not proven until now.

1.7. Nodule oxygen physiology: Solving the oxygen paradox

Low concentrations of free oxygen in the nodule tissue are necessary to protect the oxygen sensitive enzyme nitrogenase which is the key enzyme for symbiotic nitrogen fixation (Figure 1.2). On the other hand oxygen is essential for respiration and energy metabolism of rhizobia and plant cells in nodules. Solution of this apparent paradox requires low oxygen concentrations to be maintained around nitrogenase, but high fluxes of oxygen to the sites of respiration (Appleby, 1984). Leghemoglobins, which are present in concentrations of 3-5 mM in the cytoplasm of infected cells (Appleby, 1984; Becana et al., 2000), are believed to be important in both regards. The concentration of leghemoglobins in nodule cells is at least two-orders of magnitude higher than all concentration of free oxygen (5-60nM) (Hunt and Layzell, 1993), which means that the flux of O_2 carried out by Lb is greater than that of free O_2, despite the slower diffusion rate of Lb-O_2. The high affinity of Lb for O_2 also ensures that the O_2-concentrations are buffered at a low level. However, computer models estimated the buffering capacity of leghemoglobins in cells with normal leghemoglobins concentrations to be equivalent to only about 10 seconds of respiratory O_2-consumption under normal conditions (Denison and Harter, 1995). The flip-side of this result is that Lb could rapidly become saturated with O_2 if respiration is compromised, unless additional mechanisms exist to restrict oxygen entry into nodules (Figure 1.2). In fact, the presence of such restrictive site of oxygen entry in outer cell layers of nodules was

described in the early 1970s (Tjepkema and Yocum, 1974). The oxygen diffusion barrier (ODB) of nodules has been studied by a number of groups (Sheehy et al., 1985; Denison and Layzell, 1991; Webb and Sheehy, 1991; Witty and Minchin, 1998) leading to models of oxygen diffusion in nodules (Layzell et al., 1988; Denison, 1992; Moloney and Layzell, 1993; Thumfort et al., 2000). Several authors have concluded that the ODB is localised at the endodermis (Brown et al., 1997; Brown and Walsh, 1996; Streeter and Salminen, 1993; Witty and Minchin, 1994)

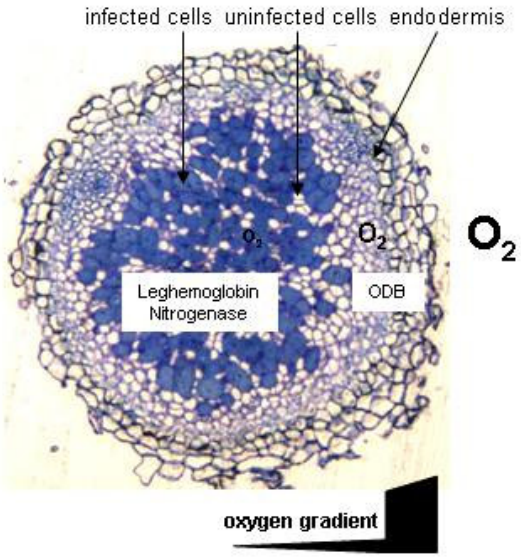

Figure 1. 2: Free oxygen concentrations decrease towards the center of the nodule.
Diffusion of oxygen into the nodules is blocked *via* an oxygen diffusion barrier (ODB). Inside the infected cells leghemoglobin proteins binds the free oxygen and deliver it to the site of respiration.

1.8. Nodule metabolism

1.8.1. Nitrogen fixation

At the heart of SNF is the reaction catalysed by the oxygen sensitive, bacterial enzyme nitrogenase :

$N_2 + 8H^+ + 8e^- + 16\ ATP + 16\ H_2O \rightarrow 2\ NH_3 + H_2 + 16\ ADP + 16\ P_i$

Reduction of N_2 requires an enormous investment of ATP and reducing equivalents, which are ultimately derived from oxidation of products of plant photosynthesis (see later). Another pre-requisite for SNF is a low-oxygen environment around the nitrogenase enzyme which is inactivated by free oxygen.

The bacterial nitrogenase protein complex is encoded by the *NifH*, *NifD* and *NifK* genes. The latter two genes encode the α- and the β-subunits of the FeMo protein, respectively, which functions as a heterotetrameric complex called dinitrogenase (component I). *NifH* produces the homodimeric Fe protein which is called dinitrogenase reductase (component II). The FeMo and the Fe proteins assemble to form the functional nitrogenase enzyme (for review see Fischer, 1994). Other genes are also required for SNF, such as *FixL* encoding a hemoprotein kinase and *FixN* which is believed to be an oxygen sensor. *Nif* and *Fix* genes in rhizobia are mostly organised into clusters of operons which are either located on megaplasmids, as in *Bradyrhizobium meliloti* or on symbiotic islands on chromosomes like in *Mesorhizobium loti*. It was shown that a mutation in any of the genes of the *FixABCX* operon leads to the inability of SNF. Therefore these genes are essential for a functional symbiosis (Earl et al., 1987; Gubler and Hennecke, 1988). Similar results were obtained for *FixR* and *NifA*, latter one is a positive regulator of several *Nif* and *Fix* genes (Thony et al., 1987). Most of the *Nif* genes are induced upon low oxygen conditions in the bacterial surrounding. This induction is mainly achieved by the action of the *NifA* gene product (Thony et al., 1987; Buikema et al., 1985).

1.8.2. C- and N-metabolism

The energy for nitrogenase activity in the bacteroids derives from photosynthesis in leaves. Sucrose from the shoot is thought to be the major source of reduced carbon for the nodules. It is delivered via the phloem and serves as an energy source as well as for supply of carbon skeletons, which are necessary for ammonium assimilation and export from nodules. Sucrose is metabolised mainly in the cytoplasm of cells in the infected zone of the nodule *via* the action of sucrose synthase which was shown to be active in nodules of soybean (Thummler and Verma, 1987), broadbean (Kuster et al., 1993) and *Medicago truncatula* (Hohnjec et al., 1999). Enzymatic and expression data indicate a higher capacity of glycolysis in nodules compared to uninfected roots, and enzymes involved in this pathway, including glyceraldehyde-3-phosphate dehydrogenase, phosphoglycerate kinase and phosphopyruvate hydratase were found to be induced during nodule development (Colebatch et al., 2002a; Copeland et al., 1995; Copeland et al., 1989; Vance and Gantt, 1992).

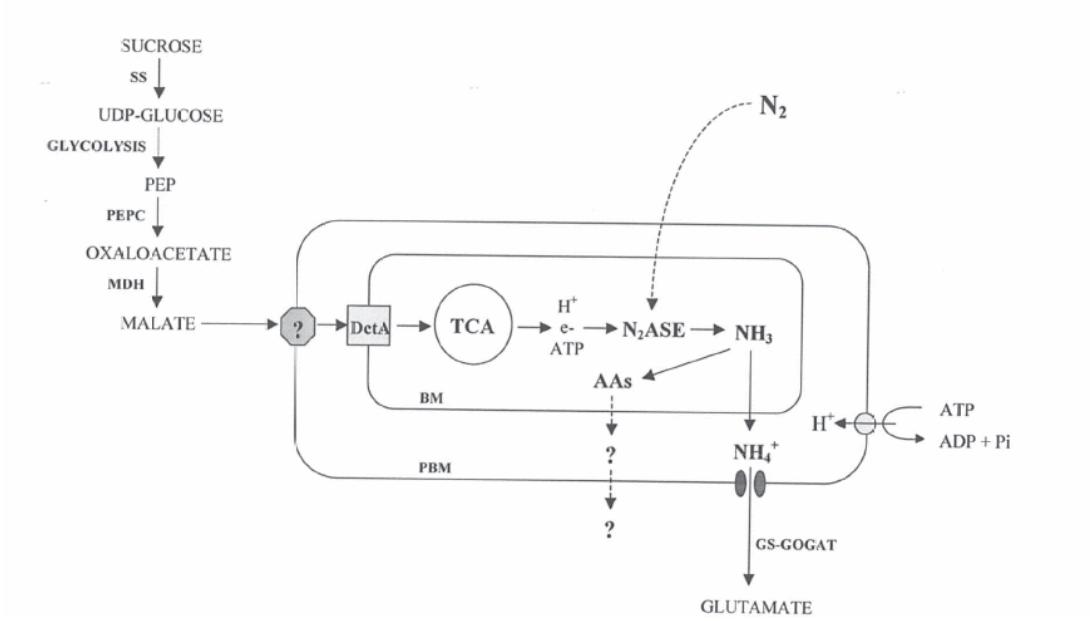

Figure 1. 3: Schematic representation of metabolism and nutrient exchange between a nitrogen fixing bacteroid and the plant cell.

As: amino acids; BM: bacteroid membrane; GS-GOGAT: Glutamine synthetase-Glutamate synthase; MDH: malate dehydrogenase; PBM: peribacteroid membrane; PEP: phosphoenolpyruvate; PEPC: phosphoenolpyruvate carboxylase; SS: sucrose synthase; TCA: tricarboxylicacid cycle (figure and legend from Lodwig and Poole, 2003)

C_4-dicarboxylates, rather than sugars or glycolytic intermediates are the primary carbon and energy source for bacteroids (Udvardi and Day, 1997). Dicarboxylates like malate are metabolized *via* the tri-carboxylic acid (TCA) in bacteroids (Bergersen and Turner, 1967; Kurz and Larue, 1977; Stowers and Elkan, 1983) (Figure 1.3) and mutations in genes of the bacterial dicarboxylate transport system lead to the formation of ineffective nodules (fixation minus mutants known as fix^- mutants) (Ronson et al., 1981; Finan et al., 1983; Arwas et al., 1985; Bolton et al., 1986; van Slooten et al., 1992). Malate itself is produced in the plant from the glycolytic intermediate phosphoenolpyruvate (PEP), via PEP carboxylase which produces oxalacetate (OAA), and malate dehydrogenase (MDH), which converts OAA to malate (Figure 1.3). Transcripts of genes encoding these enzymes are typically induced in nodules (Xu et al., 2003; Yoshioka et al., 1999).

Ammonia produced by the bacteroids is transported to the plant cytoplasm, where it is assimilated by GS, GOGAT and asparagine sythetase (AS). Genes encoding these plant enzymes as well as their activity are amongst those that are induced during

nodule development (Cullimore and Miflin, 1984, Dunn et al., 1988, Cullimore and Bennett, 1988; Trepp et al., 1999a; Trepp et al., 1999b; Gregerson et al., 1994, Hirel et al., 1987; Colebatch et al., 2002a) (Figure 1.3).

1.9. Model legumes

A lot of knowledge about symbiosis was gained by the use of bacterial mutants (e.g. Ardourel et al., 1994; Earl et al., 1987; Gubler and Hennecke, 1988). Several of these rhizobial mutants were identified that lead to the formation of ineffective nodules upon infection of their host legume or are unable to induce nodule development at all. Tagging of mutant genes in rhizobia with transposable elements such as Tn5 led to the isolation of numerous genes with crucial roles in SNF. Similar genetic approaches are much more difficult in legumes. The genome of crop legumes such as pea and soybean, plants that have been used extensively for biochemical experiments for many years, are large, complex and cumbersome for genetic analysis and mutation mapping. In addition, reverse genetic approaches are likewise difficult in these species.

To facilitate both forward and reverse genetics in legume research Handberg and Stougaard suggested the diploid (n=6) legume *Lotus japonicus* as a model legume (Handberg and Stougaard, 1992). The advantages of this species included a relatively small genome (472 Mb) and short generation time of 2-3 months. In addition, it can be genetically transformed stably and transiently with *Agrobacterium tumesfasciens* and *Agrobacterium rhizogenes*, respectively (Morris and Robbins, 1992; Yu and Shao, 1991). Similar reasons were put forward by researches who were in favour of *Medicago truncatula* (Barker et al., 1990; Cook, 1999). One of the main differences between both model legumes is that *Lotus* forms determinate nodules while *Medicago* plants develop indeterminate nodules on their root system.

Several mutagenesis projects have been initiated in the past where collections of mutants have been created that are affected at different stages of nodule development and function. These will be further discussed in section 1.11.

1.10. Transformation of legumes with *Agrobacterium rhizogenes* (hairy root transformation)

It is possible to transform *Lotus japonicus* using an *Agrobacterium tumefasciens* mediated gene transfer in order to obtain stable transformants that can be grown over several generations (Yu and Shao, 1991; Oger et al., 1996; Stiller et al., 1997). Stable

transformation now also seems possible in other legumes like soybean (Olhoft et al., 2003), barrel medic (*Medicago truncatula*; Trieu et al., 2000), and *Trifolium repens* (Larkin et al., 1996).

Legume transformation requires tissue culture that takes up to 6 months before transgenic shoots can be transferred to soil where they have to be grown for seed production. It might be possible to reduce this time down to 4 months using root instead of shoot material for plant regeneration (Lombari et al., 2003). To avoid the long time required for tissue culture, *Agrobacterium rhizogenes* can be used for so called hairy root transformation. While hairy-root transformation does not lead to germ-like transformation, it can be used to alter gene expression in nodules that develop on transformed hairy roots. This system has been extensively tested in legumes such as *Lotus japonicus* (Morris and Robbins, 1992; Webb et al., 1996; Stiller et al., 1997), *Medicago truncatula* (Trieu and Harrison, 1996; Boisson-Dernier et al., 2001), *Sesbania rostrata* (Van de Velde et al., 2003) and soybean (Olhoft et al., 2003) but also in non-legumes such as *Brassica napus* (Downs et al., 1994), tobacco and potato (Schmulling et al., 1993). Recent improvements and developments in legume transformation are reviewed in Somers et al. (2003).

To test the applicability of the hairy root system for the trapping of symbiotic genes, transformation experiments with binary vectors possessing a beta-glucurosidase (GUS) or a luciferase reporter driven by a cauliflower mosaic virus (CaMV) 35S promoter were performed. In this study Stiller and co-workers could detect a frequency of co-transfer of a binary T-DNA with a root-inducing (Ri) T-DNA of about 70% (Stiller et al., 1997). But, transient transformation develops a mosaic root system that makes it difficult to assess a phenotype (Limpens et al., 2004). Therefore this system still requires improvement.

Thus, *Agrobacterium rhizogenes* mediated hairy root transformation might be a powerful tool for relatively fast screening of transgenic roots for nodulation phenotypes when introducing a construct to silence endogenous gene expression. Furthermore, it could be used for other applications like promoter-gus studies.

1.11. Isolation of legume *sym*-mutants reveals the function of several genes involved in bacterial perception and the infection process

Establishing model legumes has led to a real revolution in the field of legume research as it became much easier to use techniques like map-based cloning to identify mutations and investigate the function of genes in these mutants. In recent years, many legume symbiosis (*sym*)-mutants defective in early steps of rhizobium recognition or nodule development have been identified (Figure 1.4; Schauser et al., 1998; Kawaguchi et al., 2002), including mutants impaired in root hair swelling, root hair curling and the formation of infection threads (reviewed in Geurts and Bisseling, 2002; Gresshoff, 2003).

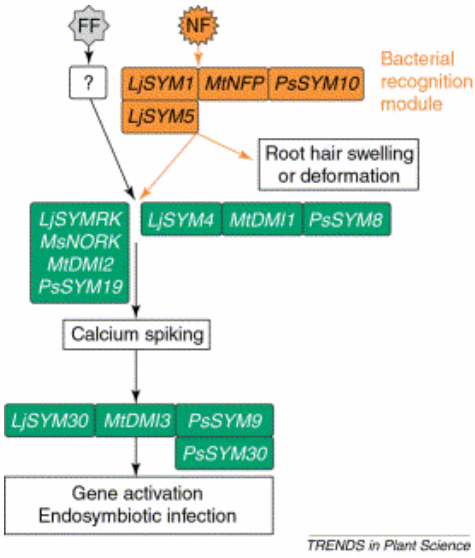

Figure 1. 4: Pathway defined by plant genes required for both bacterial and fungal symbioses.
Genetic pathway required for symbiosis-related gene expression and symbiotic infection. Genes required for both root nodule symbiosis and arbuscular mycorrhiza (AM) define the common SYM pathway (depicted in green) (from: Kistner and Parniske, 2002).

One of the first mutants identified showed an arrest in bacterial recognition (Schauser et al., 1999). It was shown that this mutant, called nodule-interception (*nin*), is blocked at the stage of infection thread formation and it did not exhibit extensive cell division in the cortical cells. Its orthologue (*sym35*) was later identified in pea (Borisov et al., 2003). The coding region of the *nin* gene is in part similar to transcription factors and it contains motifs that confer nitrogen-control on homologues in *Arabidopsis thaliana* (Schauser et al., 1999).

Radutoiu et al. (2003) and Madsen et al. (2003) were the first to clone the putative Nod factor receptors NFR1 and NFR5 in *Lotus japonicus*. Mutants affected in S*ym1* and S*ym5* (Figure 1.4) do not show any responses towards the application of rhizobia and Nod factors. Positional cloning of these genes revealed that they code for LysM-type serine/threonine receptor kinases containing a transmembrane segment that is thought to anchor the NFR1 receptor in the plasma membrane. Furthermore a topology with two extracellular LysM receiver domains and an intracellular kinase is likely. Orthologs of these genes were also identified in *Medicago truncatula* and named LYK3 and LYK4 (Limpens et al., 2003).

Map-based cloning of mutant *sym* genes led to the identification of other genes/proteins that are presumably downstream of the putative Nod factor receptors, including the receptor like kinases like SYMRK from *Lotus japonicus* (Stracke et al., 2002) and its orthologues from *Medicago tuncatula* (NORK) (Figure 1.4; Endre et al., 2002). Calcium-spiking is a plant response downstream of Nod factor perception that is believed to be an integral part of this signalling cascade, which leads to nodule development. Several *sym* mutants that may be defective in calcium signalling downstream of calcium-spiking have been discovered and the defective genes of two of the mutants were identified recently. One of the mutants found in *Medicago truncatula* was named *does not make infections 3* (*dmi3*). The mutated gene of *dmi3* shows strong similarity to a calcium- and calmodulin-dependent protein kinase that can interact with free Ca^{2+} and calcium-bound calmodulin (Levy et al., 2004). Several other mutants have been identified and some of the affected genes were cloned (Schauser et al., 1999).

Another group of legume *sym* mutants are able to develop nodules, but the nodules are ineffective. For instance, the *Medicago truncatula sym1* mutant was reported to form small, round nodules in which the infection aborts in the outer cortical cells of the root. Other nodules developed to the normal elongated stage where bacteria were released but were unable to differentiate into nitrogen fixing bacteroids (Benaben et al., 1995). Two other mutants that are defective in infection are *rit1* and *bit1* both identified in *Medicago truncatula* (Mitra and Long, 2004). In these mutants, infection threads abort in the epidermal or outer cortical cell layers of the roots. Nevertheless, root primordial formation was initiated in these plants as small bumps were observed on the root surface upon infection.

1.12. RNAi technology in legumes

The development of model legumes that were suitable for map-based cloning of genes has accelerated the discovery of key genes for SNF. Importantly, both *Lotus japonicus* and *Medicago truncatula* are also amerable to transformation and therefore, reverse genetics, which should facilitate the functional characterisation of many other genes. Traditionally, reverse genetics has been done using antisense technology (e.g. Temple et al., 1998; Crespi et al., 1994) which leads to post-transcriptional gene silencing (PTGS) (de Carvalho et al., 1992; Waterhouse et al., 1998; Baulcombe, 2000; Matzke et al., 2001).

New findings about the influence of small inhibitory and micro-RNAs on transcriptional regulation of gene expression led to the development of a new method called RNA-interference (RNAi) that can be applied in plants (Waterhouse et al., 1998). As this technique seems to have high potential for efficient PTGS new vectors were created and tested recently (Helliwell and Waterhouse, 2003; Fernando Carrari and Ben Trevaskis, personal communication). They contain two gene specific fragments in reverse orientation that are separated by an intron (Figure 1.5). Expression of these constructs leads to the formation of double stranded hairpin RNA that is targeted for degradation by specific endonucleases called Dicer (Waterhouse et al., 2001a; Waterhouse et al., 2001b).

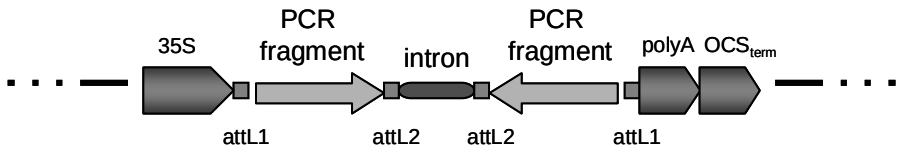

Figure 1. 5: An RNAi cassette that is typically used for this approach.
In this case the flanking regions of the PCR fragment were converted to be usable for GATEWAY cloning. The construct is driven by a CaMV-35S-promoter and terminated by an OCS terminator after polyadenylation.

Dicer produces 20-22 bp long fragments that are used for recognition of endogenous mRNAs that show identity to these short fragments (Metzlaff et al., 1997). Upon detection of the target sense-RNAs these are cleaved and further degraded (reviewed in Waterhouse et al., 2001a; Vaucheret et al., 2001; Vaucheret and Fagard, 2001; Baulcombe, 2004). This technology enables reverse genetic approaches to silence

whole gene families rather than just a single gene of such family. If sequence conservation on nucleotide level is not high enough to identify stretches of 20 bp among different gene family members several small fragments can be cloned behind each other and than used for RNAi.

There were no reports about the functionality of RNAi mediated PTGS available in legumes at the beginning of the thesis. However, for the reasons mentioned above, RNAi technology was tested in *Lotus japonicus* during this project.

1.13. Nodulins

Nodulin genes are those that are specifically induced during nodulation in plants. They are grouped into two classes: The early nodulins (ENODs) are induced within minutes of rhizobial binding and/or Nod factor perception. ENODs are believed to mostly serve a function during nodule development. The second group of nodulins is called late nodulins. These genes encode proteins that are thought to be involved in nodule function and rather than in nodule development *per se*. Their induction can be observed within days after inoculation of the plants with rhizobia.

One of the best characterised early nodulins is the *Enod40* gene, which is induced by Nod factors. Upon Nod factor treatment, expression of *Enod40* is induced first in the pericycle and subsequently in dividing cortical cells and in all differentiating cells of the growing nodule primordium (Crespi et al., 1994; Gamas et al., 1996; Fang and Hirsch, 1998). *Enod40* genes encode highly structured short ORF-mRNAs that seem to be involved in root nodule organogenesis (Campalans et al., 2004).

Two of the earliest Nod factor induced markers are ENOD12 (Scheres et al., 1990) and RIP1 (Peng et al., 1996, Cook et al., 1995). The latter may be involved in the breakdown of ROS during nodulation (Ramu et al., 2002). Both genes are associated with the pre-infection stage and might function in the cell wall modifications, which is observed upon *Rhizobium* infection or Nod factor treatment (Journet et al., 1994, Bauer et al., 1996, Ramu et al., 2002). Promoter-gus studies showed that *Enod12* and *Rip1* are expressed in nodule primordia as well as in root hairs (Terada et al., 2001; Bauer et al., 1997; Peng et al., 1996). However, the physiological function of the *ENOD12* protein, like most nodulins, remains unknown. Furthermore no phenotype has been described that results from silencing of the gene or from plants where the gene was knocked out.

Other examples of early nodulins include proline-rich proteins ENOD2, ENOD5, ENOD10, ENOD11, PRP4 (Munoz et al., 1996), extensins

(ArsenijevicMaksimovic et al., 1997), glycine-rich proteins (GRPs) (Kuster et al., 1995a; Kuster et al., 1995b; Schroder et al., 1997), an apyrase gene from soybean (Day et al., 2000), the clover nodulin *dd23b* (Crockard et al., 2002) and *Nod6* from *Medicago truncatula* (Kapranov et al., 1997). The function of most of them remains still unknown.

One of the major and probably best characterised proteins in nodules, the leghemoglobin protein (see section 1.7), belongs to the class of late nodulin genes. Other late nodulins include a carbonic anhydrase (Kavroulakis et al., 2000), PEPC (Hata et al., 1998), GOGAT (Temple et al., 1998) and sucrose synthase, which was named Nod100 (Kuster et al., 1993; Thummler and Verma, 1987). Those nodulins have known biochemical functions and are obviously involved in C and N metabolism. In contrast, no specific function could so far be assigned to other late nodulins such as *LjNod16* (Kapranov et al., 1997) and *LjNod70* (Szczyglowski et al., 1998).

Over the last three decades hundreds of nodulins have been identified. The first nodulins were found using nodule-specific antibodies (Legocki and Verma, 1980; Strozycki and Legocki, 1988). Nevertheless, this strategy only revealed the existence of a few nodulins. Other methods, such as differential display (Swiderski et al., 2000) and transcriptome analysis are revealing many more nodulins (Colebatch et al., 2002a; Fedorova et al., 2002).

1.14. Legume functional genomics in the postgenomic era

Although some of the tools of functional genomics existed and were applied before the completion of the first bacterial and eukaryotic genome projects, the discipline of functional genomics emerged largely in response to the challenge posed by complete genome sequences. This challenge is to understand the biochemical and physiological function of every gene product, and the complex interplay between them all. Global analyses of various levels of the molecular organisation have been facilitated by remarkable developments in high throughput technologies. These methods and recent developments in this area have recently been reviewed in our group (Colebatch et al., 2002b).

Large scale EST and genome sequencing projects in different legumes provide huge datasets to study genome organisation and transcription in these plants. At the beginning of this thesis project about 36,000 EST sequences from *Lotus japonicus* were deposited in GenBank database (http://www.ncbi.nlm.nih.gov/dbEST/index.html). Upon submission of the thesis (01/05) 111,459 sequences were submitted for *Lotus*. A

similar increase in the amount of DNA sequence can also be seen for each organism represented in the TIGR database.

Until a few years ago, gene expression analysis was confined to one or a few genes at a time, and it was virtually impossible to identify entire sets of genes involved in a common process that are co-ordinately regulated. Increased numbers of publicly available nucleotide sequences together with development of technologies for high-throughput measurement of gene transcript levels have profoundly changed the way in which molecular biologists approach biological questions. Now it is possible to survey the expression level of thousands of genes in parallel, which not only enables identification of novel 'candidate' genes involved in a given biological phenomenon, but also reveals sets of genes and the corresponding biochemical processes that act in concert to achieve a specific biological outcome.

Recently developed technologies for multi-parallel analysis of transcript levels include: massively parallel signature sequencing (MPSS); cDNA-AFLP; and DNA array-based methods (Aharoni and Vorst, 2001).

At the beginning of this project there were only a very few DNA array resources available for legumes world-wide including lupin, soybean, *Medicago* and *Lotus* (Fedorova et al., 2002, Endo et al., 2000; Colebatch et al., 2002a). Transcriptome analysis using DNA arrays enable us to identify nodulins in a more comprehensive way. During this PhD project, the number of publications with transcriptome data and the scale of the arrays used increased markedly (Thibaud-Nissen et al., 2003; Journet et al., 2002; Kuster et al., 2004; Mitra et al., 2004; Colebatch et al., 2004, Kouchi et al., 2004).

In our lab data from a small cDNA array was published at the time the project was started (Colebatch et al., 2002a). Using the 2.3K LjNEST cDNA array, transcripts of 83 different genes were found to be more abundant in nodules than in roots out of which 50 of these had never before been identified as nodule-induced in other plant species. Among those genes some are involved in plant defense responses and in detoxification of reactive oxygen species (ROS) and one may prohibit phytoalexin synthesis. The array experiments also revealed novel nodule specific genes involved in membrane transport (Colebatch et al., 2002a).

EST sequencing and cDNA array projects were also running in other labs including at the Kazusa DNA Research Institute in Japan (KDRI) for *Lotus* and at the Institut National de la Recherche Agronomique (INRA) in Toulouse (*Medicago*). In

order to use the newly released EST sequences from the KDRI in our own lab, our cDNA array facilities needed to be expanded.

1.15. Aim of this work

This work was divided into two major parts. The aim of the first part was to improve resources for *Lotus* transcriptomics and molecular physiology which involved expanding the cDNA array resources and implementing methods for using RNAi technology for reverse genetic approaches. The second part of the project aimed to use methods of functional genomics to investigate the role and physiology of selected candidate genes and proteins inclusing the symbiotic leghemoglobins.

2.0. Materials and Methods

2.1. General Suppliers

AGOWA, Berlin, Germany	DNA sequencing
Amersham, Braunschweig, Germany	Readiprime II DNA labelling system, NAP5 columns, Hybond N^+ membranes for cDNA arrays
Applied Biosystems, Forster City, USA	SYBRGreen reaction mix, Sequence Detection System 7900HT
Beckman Coulter, Krefeld, Germany	LS-6500 Multi-Purpose Scintillation Counter
Biometra, Göttingen, Germany	UNO II PCR machine
BioRad, München, Germany	Smart Spec 3000, BioRad Protein Assay Kit I, equipment for gel electrophoresis
Bio Tek, Winooski, Vermont, USA	Synergy HT microplate reader, KC4 software, HPLC system with components 522, 535, 560
Difco Laboratories, Augsburg, Germany	Bacto-Agar, Bacto-Tryptone, Yeast extract, Peptone
Duchefa, Haarlem, The Netherlands	Gamborg B5 medium, B5 vitamins
Eppendorf, Hamburg, Germany	Microfuges 5417, 5417C, 5417R, electronic and mechanical pipettes
Eurogentec, Seraing, Belgium	Oligonucleotides
Fuji Photo Film, Düsseldorf, Germany	BAS-1800 II phosphor imager
Gibco BRL, Eggenstein, Germany	Geniticin 418
Hartmann, Braunschweig, Germany	Radioisotopes
Heraeus Kulzer, Hanau, Germany	Technovit tissue embedding kit
Invitrogen, Karlsruhe, Germany	Oligonucleotides, Superscript III Reverse Transcriptase, NuPAGE- precast protein gels, -antioxidant, -LDS sample buffer, XCell SureLock Mini-Cell, XCell II Blot Module, Colloidal Coomassie G-250 stain, Protein molecular weight Standard Seeblue, Taq polymerase, Oligonucleotides, RACE-PCR kit, GATEWAY cloning kit
Leica, Bensheim, Germany	Rotation microtome RM2155

Macherey & Nagel, Düren, Germany	Porablot NY amp plus nylon membranes
Merck, Darmstadt, Germany	Standard chemicals
Millipore, Schwalbach, Germany	Membranes for cDNA arrays
New England Biolabs, Frankfurt, Germany	Restriction endonucleases
Olympus, Hamburg, Germany	Systemmicroscope BX41TF
Presens, Regensburg, Germany	MicroxTX2 oxygen microsensor
Promega, Mannheim, Germany	pGEM-Teasy cloning kit, Anti-rabbit alkaline phosphatase F(ab')2 fragment, RNase inhibitor
Qiagen, Hilden, Germany	QIAquick gel extraction kit, RNeasy Plant Extraction Kit, Oligo dT-primer, Nucleotide removal kit, DNA minipreparation kit
Retch, Haan, Germany	Mixer Mill MM300
Roche, Mannheim, Germany	NBT / BCIP tablets, T4 DNA ligase, Restriction endonucleases
Schleicher & Schuell, Einbeck, Germany	Protran nitrocellulose membrane, Filter 0860
Sigma, Deisenhofen, Germany	Standard chemicals, salmon sperm DNA, Ponceau staining for immunoblots, RNase free DNaseI

Manufactor's details of technical equipment that was used for cDNA array production are given in the specific section.

2.2. Growth media and major buffers

(media used for stable transformation of *Lotus japonicus* are described in the corresponding section)

¼ B&D medium (Broughton and Dilworth, 1971)

14 g select agar were autoclaved in 1L water before 125 µl of sterile solutions A, B,C and D (sterile) and 100 µl of sterile 1 M KNO_3 solution were added.

solution	compound	molarity [µM]
A	$CaCl_2$	1000
B	P	500
C	Fe	10
D	Mg	250
	K	1500
	S	500
	Mn	1
	B	2
	Zn	0.5
	Cu	0.2
	Co	0.1
	Mo	0.1

AB medium (filter sterilized) (Cangelosi et al., 1991)

2.5 g sucrose in 450 ml dH_2O

25 ml 20× AB Buffer

25 ml 20× AB Salts

20× AB Buffer (autoclaved)

60.0 g K_2HPO_4

23.0 g NaH_2PO_4-H_2O

dH_2O to 1 L

20× AB Salts (filter sterilized)

20.0 g NH_4Cl

6 g $MgSO_4$-$7H_2O$

3 g KCl

0.26 g $CaCl_2$-$2H_2O$

50 mg $FeSO_4$-$7H_2O$

dH_2O to 1 L (pH 7.0)

LB medium (autoclaved)

10 g Bacto-tryptone

5 g Bacto-yeast extract

10 g sodium chloride (NaCl)

pH was adjusted to 7.5 with 1 M sodium hydroxide (NaOH)

dH_2O to 1 L

SOC medium (autoclaved)

5g Yeast extract

20g tryptone

dH_2O to 1 L

final concentrations of:

10 mM NaCl

2.5 mM KCl

10 mM $MgCl_2$

20 mM $MgSO_4$

20 mM glucose.

TY medium (autoclaved)

5 g tryptone

3 g yeast extract

1 g $CaCl_2$

dH_2O to 1 L

YMB medium (autoclaved)

0.5 g K_2HPO_4

0.1 g NaCl

10 g mannitol

0.4 g yeast extract

0.2 g $MgSO_4$ x $7H_2O$

dH_2O to 1 L

YEB medium (autoclaved)

5 g Bacto-Pepton

1 g Yeast-Extract

5 g Beef-Extract

5 g sucrose

493 mg $MgSO_4$ x $7H_2O$

pH 7.2

dH_2O to 1 L

L0 medium (autoclaved)

3.1 g Gamborg B5 Medium (Duchefa)

pH was adjusted to 5.5 with 0.2 M NaOH

3.5 g Gelrite

dH_2O to 1 L

10 × PCR buffer:

0.5 M	potassium acetate
1%	Tween 20
15 mM	magnesium acetate
0.35 M	TrisBase, pH 10.4
0.15 M	TrisHCl, pH 4.8

final: pH 8.4

20 × SSC

3.0 M	NaCl
0.3 M	sodium citrate

pH 7.0

SSarc buffer

240 ml	Sarcosyl NL30
200 ml	20× SSC
8 ml	0.5 M EDTA, pH 8.0
552 ml	H_2O

Diluted SSarc buffer

100 ml	SSarc
2 ml	0.5 M EDTA, pH 8.0
898 ml	H_2O

Formamide hybridisation buffer:

40 mM	sodium phosphate buffer (pH 6.8)
5 ×	Denhardt Solution (1g/l BSA fraction V, 1g/l Ficoll 400, pH 7.0)
1%	SDS
0.5%	BSA fraction V
10 µg/ml	Herring Sperm (denatured)
50%	Formamide
5 ×	SSC

Alkaline buffer for removing radioactivity:

0.4 M	NaOH
0.6 M	NaCl

Neutralisation buffer:

0.5 M	Tris-HCl (pH 7.5)
1 ×	SSC
0.1 %	SDS

CTAB buffer

16.36 g	NaCl
8 ml	0.5 M EDTA (pH 8.0)
20 ml	1 M Tris-HCl (pH 8.0)
4 g	CTAB

H_2O to 200 ml

Gus-buffer

50 mM	sodium phosphate-buffer pH 7.2
10 mM	EDTA
0.1%	Triton X-100

0.1%	Tween 20
1.05 g/50 ml	$K_4(Fe^{II}(CN_6))$
0.83 g/50 ml	$K_3(Fe^{III}(CN_6))$
0.5 mg/ml	x-Glc

PBS buffer

8 g/l	NaCl
0.2 g/l	KCl
1.44 g/l	Na_2PO_4
0.24 g/l	KH_2PO_4
pH 7.4	

The composition of the different sodium phosphate buffers is described in Sambrook et al. (1989).

2.3. Plant and bacterial growth

Dried *Lotus* seeds were placed in a reaction tube and 2 volumes of 95-97% sulphuric acid were added. After 10 minutes incubation, seeds were carefully washed six times with sterile water before being sterilised in a 2% sodium hypochloride solution for 10-20 minutes. Sterilisation time was dependent on the age of the seeds. Sterilisation was stopped when seed coats were bright brown in colour. Afterwards, seeds were again washed six times in sterile water and then placed onto sterile wet filter paper in a Petridish. Seeds were germinated for at least 3 days at 16/8 hours day/night cycle and 22°C before being transferred onto squared Petridishes containing ¼ B&D (described above) for sterile cultivation or into pots containing soil or quartz sand into the greenhouse. When grown on agar plates, the upper third was removed before the medium was covered with a sterile wet filter paper. Seedlings were placed onto the upper edge of the filter and then grown vertically with the root area being covered with black plastic foil, in a phytotron (16/8 hours day/night cycle, 22°C). Plants were grown for three weeks before being inoculated with *Mesorhizobium loti* (strain NZP2235). The bacterial culture was grown for 2 days at 28°C on a rotary shaker in YMB (containing 6.5% K_2HPO_4) or TY medium prior to application. 2 ml of the bacterial suspension were spun down at 6000 g using a bench top centrifuge and the pellet was resuspended

in liquid ¼ B&D medium. 800 µl of a 1:50 diluted bacterial suspension were applied to the roots of the plants.

For time course experiments nodulated roots were harvested 0, 0.25, 1, 2, 7, 14 and 21 days post inoculation (dpi). Non-inoculated controls were harvested 1, 7, 14 and 21 days after being "inoculated" with water. For experiments where isolated nodules of different ages were used, plants were grown 2 weeks prior to inoculation with *M. loti*. Emerging nodules were labelled 1, 2, 3 and 4 weeks after inoculation by marking them with different colours on the plastic lid of the squared Petridish. Nodules were harvested 4 weeks after inoculation according to their label in separate reaction tubes and frozen in liquid nitrogen immediately.

To obtain tissue for analysis of organ specific expression of target genes, plants were grown for 3 weeks under symbiotic conditions using the vertical plate system. Organs were harvested separately from plants grown on 0.1 mM and on 5.0 mM KNO_3. Control plants (non-inoculated) were grown only on 0.1 mM KNO_3.

The rhizobial mutants, *cgs* and *lpsβ2* as well as the corresponding wild-type strain (Ayac 1 BII) were grown for 2 days in liquid AB medium (see above) containing 30 µg/ml Gentamycin for the mutants. For this experiment plants were grown for two weeks prior to infection.

2.4. cDNA arrays

Two cDNA arrays were constructed. The first one contained PCR amplicons from 11,652 EST-clones (in vector pBluescript) received from the Kazusa DNA Reasearch Institute in Japan (KDRI). The second array contained 9,600 partially redundant EST clones, representing approximately 3,800 genes, from the library created at the Max-Planck-Institute of Plant Molecular Physiology in Golm, which were cloned into pSPORT and pBluescript (LjNEST) (Colebatch et al., 2002a).

2.4.1. PCR amplification of cDNA clones

Lotus cDNA clones were PCR-amplified either from *E. coli* colonies (11.6K LjKDRI clones) or from purified plasmids (9.6K nodule clones). For colony PCR, sets of 384 *E. coli* clones were grown over-night on solid LB-plates under the appropriate antibiotic selection, then inoculated into PCR reactions in 96-well plates. For PCR-amplification from plasmids, purified DNA was diluted in H_2O to approximately 50 ng/µl and one microliter was used as template in the PCR reactions. For pSPORT and

pBlueScript vectors, the following *LacZ* gene primers, which flanked each cDNA insert, were used:

LacZ1: GCTTCCGGCTCGTATGTTGTGTG

LacZ2: AAAGGGGGATGTGCTGCAAGGCG.

PCR was performed in 96 well plates in a reaction volume of 100 µl. A Master Mix of 1× PCR buffer containing 0.2 mM of each dNTP, 10 pmol Primer 1, 10 pmol Primer 2, 1.5 mM MgOAc, 1 unit Taq Polymerase, H_2O to 100 µl) was prepared in appropriate amount and used for the reaction. The amplification programme was 95°C for 5 min; then 35 cycles of [95°C for 1 min, 65°C for 1 min, 72°C for 1.5 min] and finally one cycle of 72°C for 10 min.

Four sets of 96 PCR reactions were combined into one 384 well plate following the pattern indicated in Figure 2.1, using a HYDRA96 Robbins Scientific Robotic system (BioRobotics, England).

2.4.2. Array spotting

The cDNA amplicons were spotted onto Hybond N^+ nylon membranes using a BioGrid robotic system with a 384 gridding tool (BioRobotics, England). The spotting pins had a radius of 0.4 mm and each PCR reaction was transferred 10 times per spot, resulting in a total spotted volume of approximately 0.25 µl. Filters were saturated with 0.5 M NaOH denaturation buffer during spotting, then incubated for at least 5 minutes in 1 M Tris (pH 7.5)/ 1.5 M NaCl neutralisation buffer. Finally, DNA was covalently linked to the membrane using a UV-crosslinker (UV Stratalinker 1800, Stratagene) at 0.120 Joules.

A total of fourty-two 384 well plates (16,128 clones) can be spotted onto a 20 × 20 cm filter using the above robotic system. Each filter (tertiary grid) was divided into six secondary grids, which in turn contain 7 × 384 primary grids. Primary grids consist of a 4 × 4 pattern representing seven clones spotted in duplicates, an empty spot for quantifying the local background (LB), and a human desmin clone (D) used as a control for unspecific binding (Figure 2.1).

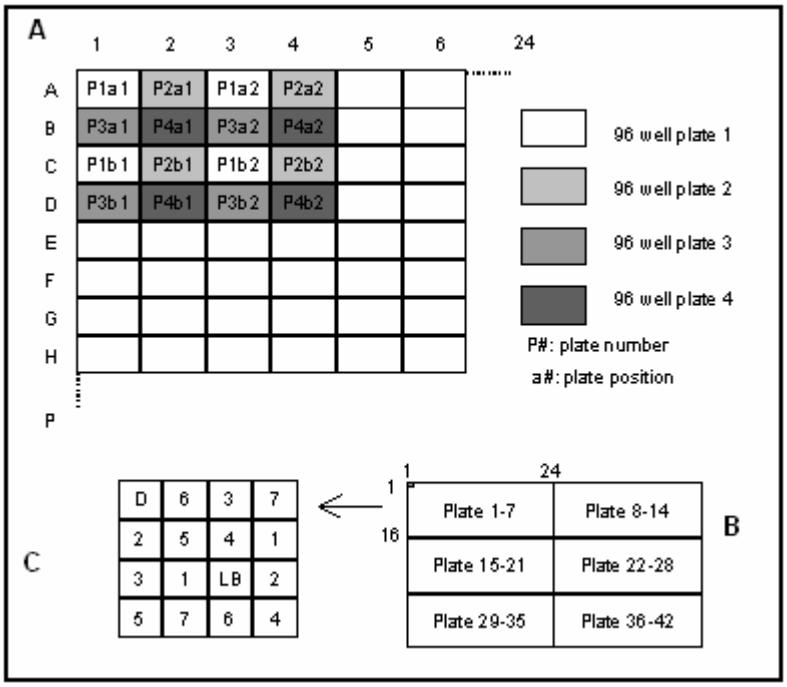

Figure 2. 1: Spotting scheme and clone distribution on the cDNA arrays.

A: Schematic distribution of four 96 well PCR plates after their content has been transferred to one 384 well plate. ***B***: Tertiary grid: The whole filter was subdivided into six secondary grids. Seven 384 well plates were spotted per subarray (primary grid). ***C***: All samples were spotted in duplicates within a 4×4 spot group within the primary grid; D= Desmin, LB= local background.

2.4.3. Probe synthesis and array hybridisation

2.4.3.1. Reference hybridisation

Due to slight variations in PCR amplification and spotting efficiency it was necessary to estimate the amount of DNA applied in each spot. This was achieved by hybridising arrays with a ^{33}P-labelled 13-mer oligonucleotide (5'-TTCCCAGTCACGA-3') complementary to the vector part of each amplified cDNA. The signal obtained for each spot after washing of arrays provides a measure of the amount of DNA in that spot.

Subsequently, each filter was used multiple times (up to 6 times) to measure transcript levels in different biological samples, in so-called complex hybridisations, as described in detail below.

Pre-hybridisation:

Filters were incubated at least 1 hour in 200 ml (1-2 filters) SSarc (see above) at 5°C.

Probe labelling and hybridisation (for 1-2 filters):

Reactions contained the following components:

60 pmol	13-mer oligonucleotide
3 µl	10 × T4 buffer (Roche)
50 µCi	γ^{33}P-dATP
20 units	T4 polynucleotide kinase
H_2O to 30 µl	

Labelling reactions were carried out at 37°C for 30 min, then mixed with 10 ml SSarc before being added to pre-hybridised filters in 200 ml SSarc, and incubated at 5°C overnight.

Filter Washing:

Filters were washed at 5°C for 30 min in 200 ml (1-2 filters) SSarc buffer.

Data capture:

Each filter was exposed to a BioImager screen over-night and scanned the following day in a phosphoimager with a resolution of 50 µM × 50 µM and 16 bits per pixel. Evaluation of data is described below.

Removal of radioactivity:

Bound radioactive probe was removed from filters by incubating them twice in an alkaline buffer at 42°C for 30 min each time. Filters were then neutralised for 30 min at room temperature in neutralisation buffer (see above). Complete removal of radioactivity was confirmed by exposing filters overnight to a BioImager screen. An older procedure that was used during tests involved incubation of the filter for 2 times for 1 hour in 0.1 % SDS and 5 mM Na_2PO_4 (pH 7.2) at 95°C. Due to the strong thermal strain of that treatment that procedure was dropped.

2.4.3.2. Complex hybridisation

Total RNA was used for the preparation of complex radioactive probes for array hybridisation. The radioactive signal associated with each spot on the array was used to

calculate relative transcript abundance, after normalisation for DNA amount in each spot.

Pre-hybridisation:

Different buffer systems were tested: Church buffer (0.25 M Na_2HPO_4, pH 7.2, 5% SDS, 1 mM EDTA (Sambrook et al., 1989)), a commercial hybridisation buffer (Ambion) and a formamide based buffer system (included in the list of buffers at the beginning of this chapter). All filters were pre-hybridised for 4 hours at 65°C (Church buffer) and 42°C (Ambion and formamide buffer).

Labelling of cDNA:

Radioactive cDNA probes were prepared from total RNA by reverse transcription, as follows. A solution of 10-25 µg of total RNA and 1.5 µg of oligo$(dT)_{12-18}$ primer in 12.5 µl DEPC-treated H_2O was heated at 70°C for 10 min to denature the RNA, then cooled on ice for 5 min. Subsequently, 16 µl of cold probe labelling solution (see below) were added and the sample was incubated for a further 10 min at 4°C. The mixture was then incubated at 42°C for 5 min before adding 1 µl of SuperScript III reverse transcriptase (200 units/µl; Invitrogen). The ensuing reaction was allowed to proceed for 1 hour at 42°C, before addition of 0.5 µl of 25 mM unlabelled dCTP, and further incubation at 42°C for 30 min. Reverse transcription was terminated *via* inactivation of the enzyme by heating at 70°C for 15 min.

Probe labelling solution:

Total volume 16 µl:

6 µl	5 × RT buffer (Invitrogen)
2.5 µl	0.1 M DTT (final conc. 8.3 mM)
0.5 µl	25 mM mix of dGTP, dATP, dTTP (final conc. 0.42 mM)
1 µl	RNase inhibitor (40 units/µl)
6 µl	α^{33}P-dCTP (10 µCi/µl)

RNA template was finally hydrolysed by adding of 10 µl of 1 N NaOH and incubating the resulting solution at room temperature for 10 min, followed by 15 min at 50°C. The probe solution was then neutralised by adding 10 µl of 1 N HCl and 2 µl of 1 M sodium phosphate buffer (pH 7.2) and incubated at room temperature for 10 min.

Unincorporated radioactive nucleotides were removed by applying the probe to a silica column (nucleotide removal kit) and eluted in 200 µl elution buffer, following the protocol provided with the kit (QIAGEN).

Labelling efficiency was determined by measuring the ^{33}P radioactivity of 1 µl probe in a LS6500 Scintillation counter (Beckman Coulter).

Hybridisation:

Between 5-15 million cpm of labelled cDNA was added to arrays to the pre-hybridisation solution after being denatured at 95°C for 10 minutes and stored on ice for 5 minutes afterwards. The filters were then incubated at 42°C for approximately 24 hours (formamide buffer and Ambion buffer). Hybridisation temperature for Church buffer was 65°C.

Washing:

Non-specifically bound probe was removed by washing filters using the following procedure. Filters were first washed for

20 min in 100 ml 1 × SSC, 0.1% SDS, 4 mM sodium phosphate pH 7.2 at 65°C, then for

20 min in 100 ml 0.2 × SSC, 0.1% SDS, 4 mM sodium phosphate pH 7.2 at 65°C, and

20 min in 100 ml 0.1 × SSC, 0.1% SDS, 4 mM sodium phosphate pH 7.2 at 65°C.

Data capture:

Each filter was exposed to a BioImager screen over-night and scanned the following day in a BAS-1800 II phosphor imager (Fuji) with a resolution of 50 µM × 50 µM per pixel (16 bits). Evaluation of data was performed as described below.

Removal of radioactivity:

Removal of radioactivity from the filters was carried out as described above (section 2.4.4.1)

2.4.4. Array image analysis and data evaluation

After scanning imaging screens, images were imported into AIS (InterFocus), a commercially available program and analysed using a customised evaluation protocol.

Spot intensity values were exported into HARUSPEX (MPI-MOPP) and statistical analysis using the student T-test was carried out in this database.

2.5. RNA extraction, cDNA synthesis and RealTime RT-PCR

Plant organs were harvested and immediately frozen in liquid nitrogen in a 2 ml reaction tube. Two clean metal balls were added into every tube and frozen again. Plant material was then ground using a Retsch® mixer mill for 2 minutes. RNA was extracted from 100-200 mg ground tissue using an RNeasy extraction kit. 1 µl of the eluted RNA was run on a 1% agarose gel to check for degradation, and quantity was determined spectrophotometrically at 260 nm. 1 µg of total RNA was used for subsequent cDNA synthesis. Total RNA was mixed with 1 µl 10 × DNase reaction buffer and 1 µl DNaseI (1 U/µl) in a total volume of 10 µl and then incubated for 30 minutes at room temperature. After inactivation of the enzyme with 1 µl of 50 mM EDTA, 1 µl RNA was run on a 1% agarose gel again in order to check for RNA degradation. In addition Real-Time RT-PCR was performed on each sample to test for successful DNA removal using an intron- and an ubiquitin10-specific primer pair:

har1intr2f: 5'- CCTGAAATGCCTATTCGTTGAG-3',

har1intr2r: 5'- CACAGCTTCTTCTGCATGCG-3',

LjUbi1f: 5'- TTCACCTTGTGCTCCGTCTTC-3',

LjUbi1r: 5'- AACAACAGCACACACAGCCAATCC-3'.

Each PCR reaction was carried in out in a total volume of 10 µl containing 1 µl DNase treated RNA, 5 µl 5 × SYBR Green Reaction Mix and 4 µl primer mix (0.5 µM of each primer) using a 384-well Real-Time RT-PCR machine.

After confirmation of successful DNA degradation, cDNA synthesis was performed using SuperScriptIII reverse transcriptase, following the protocol of the supplier (Invitrogen). All RT-PCR steps and calculations of relative transcript amounts were described previously (Czechowski et al., 2004).

In order to detect bacterial transcripts, 1 µl of 10 pM of FeNif1R and MlsigAr1 oligonucleotides were added in addition to oligo dT-primer during cDNA synthesis.
Sequences of these and all other primers used for quantitative Real-Time RT-PCR (qRT-PCR) can be found in the appendix (Table 8.1).

2.6. RACE-PCR

To obtain full-length cDNA sequence of *Aox1* 5'-RACE was performed. Total RNA was extracted from 3-week old nodules using an RNeasy kit and cDNA synthesis was performed with SuperscriptIII and the *LjAox1*-specific primer, LjAOXrace1r.

Amplification of the 5'end of *LjAox* cDNA was performed with the 5' RACE PCR kit from Invitrogen following the manufacturer's instructions. The first round of PCR was performed with the abridged anchor primer from the kit and a first *LjAox1*-specific primer. Nested PCR was then performed with the universal primer and a second *LjAox1*-specific primer, LjAOXrace2r. The PCR program used was: 2 min 95 °C; 35 cycles of 95 °C for 15 sec, 58 °C for 30 sec, 70 °C for 1 min; and finally 70 °C for 10 min. The resulting single PCR product was cloned into the pGEM-T-easy vector follwing the manusfactor's protocol and sequenced.

LjAOXrace1r: 5'- GACATTATTAATGGCATACATAGTGCG -3'.

LjAOXrace2r: 5'- GTAATCATCCCATTGAGGTGTGATAG-3'.

2.7. DNA extraction

200-300 mg of plant material was ground in liquid nitrogen before 300 µl of CTAB buffer (described above) were added. Samples were incubated for 30 minutes at 60°C and mixed once during incubation. 300 µl chloroform:isoamylalcohol (24:1) were then added and the sample carefully mixed followed by 10 minutes centrifugation at 6,000 g at room temperature. The upper phase was transferred to a new tube, 10 mg RNase per ml were added and incubated at 37°C for 30 min. Afterwards, samples were stored on ice for 5 minutes before 0.6 volumes of isopropanol were added and DNA was precipitated 1 hour to overnight at 20°C. The DNA was pelleted by centrifugation at 10.600 g for 10 min at 4°C, the supernatant removed, and the pellet washed with 70% EtOH. After 10 minutes centrifugation at 4°C supernatant was removed and DNA pellets were air dried at room temperature. DNA was resuspended in 50 µl TE buffer and stored at –20°C for further analysis.

2.8. Promoter:gus-fusion analysis

After *in silico* identification of the coding sequence of ascorbate oxidase a putative promoter region of 1046 bp was PCR-amplified using the primers:

AOXprom1000fwd 5'-AAGCTTCTTGCTAGTTGGCTAATTTGC-3' and

AOX prom-rev 5'-GGATCCGTTGTTGCTTTTACTTGAAGA-3'.

The forward primer contained a HindIII restriction site while a BamHI site was introduced into the reverse primer. After PCR amplification of the promoter from genomic DNA and HindIII and BamHI restriction, the product was cloned into pBI101 containing the gus-reporter gene 3' of the multiple cloning site. After obtaining a correctly cloned promoter the construct was transformed into *Agrobacterium rhizogenes* which was used for hairy root transformation of *Lotus japonicus* (see below).

2.9. Gus-staining

Plant tissue was placed in an appropriate vessel and covered with Gus-buffer (described above). Samples were then placed in an vacuum apparatus and a vacuum was applied three times for 10 minutes each time. Afterwards, samples were incubated at 37°C for 12-24 hours in the dark before being destained stepwise using 30%, 50%, and 70% ethanol for 10 minutes per step. Tissue was then stored in 70% ethanol at room-temperature.

2.10. RNAi constructs and *Agrobacterium* transformation

To create an RNAi construct for silencing the symbiotic leghemoglobins a 401 bp long fragment was PCR amplified from EST clone LjNEST2H4 (accession number: BI416374) using the following primers:

LjLgEntryF

5'-GGGGACAAGTTTGTACAAAAAAGCAGGCTGGGTTTCACTGCACAGCAAG-3'

LjLgEntryR

5'-GGGGACCACTTTGTACAAGAAAGCTGGGTCATAGGCTACTCCCCAAGCA-3'.

The PCR amplicon contained several conserved regions of the symbiotic hemoglobin genes of appropriate length for induction of post-transcriptional gene silencing (PTGS). Therefore, PTGS of the other members of the symbiotic hemoglobin gene family was expected. The longest stretch of sequence identity with non-symbiotic hemoglobin genes was 16 bp, which were expected to be too short to induce PTGS of these genes.

To produce an empty vector control, a 447 bp long fragment of the β-lactamase gene from the bacterial cloning vector pGEM-T-Easy was used for recombination:

GW-bLACT1f

GGGGACAAGTTTGTACAAAAAAGCAGGCTCGTCGTGTAGATAACTACGATACGG;

GW-bLACT1r

GGGGACCACTTTGTACAAGAAAGCTGGGTCAACTTACTTCTGACAACGATCGG.

In all cases, primers contained the recombination sites AttB1 and AttB2 for GATEWAY cloning. After PCR amplification using taq-polymerase, the fragment was gel-purified and 150 ng were used for the GATEWAY BP reaction to recombine the fragment into the entry vector pDONR207 containing a Gentamycin resistance in the plasmid backbone. The recombination reaction was transformed into the *E. coli* strain DH5α and grown at 37°C on LB plates containing 25 ng/ml Gentamycin over night. Positive clones were selected on the basis of a colony-PCR reaction as well as after restriction analysis of the purified plasmid using a plasmid minipreparation procedure. One selected entry-clone was sequenced before used for further reactions. For the subsequent LR reaction, 150 ng of the entry clone and 150 ng of pBINAR-RNAi (pBIN19 backbone with a converted GATEWAY cassette from pJawohl8) were used. After growing transformed *E.coli* strain DH5α at 37°C over-night on solid LB plates containing 50 ng/ml kanamycin, positive clones were selected by colony PCR as well as by PCR on isolated plasmids after mini-preparation. Universal primers were designed for this reaction that can be used for any insert in pBINAR-RNAi. Both recombination cassettes (forward and reverse; see Figure 1.5) can be amplified with the following primer combinations: forward cassette (CaMV35Sf and RNAi-intronF) and reverse cassette (RNAi-intronR and OCS-termR).

CaMV35Sf : 5’-CCACGTCTTCAAAGCAAGTG-3’

RNAi-intronF: 5’-CTCTTTGAAACCGTTGACCCAT-3’

RNAi-intronR: 5’-GGTCAACGGTTTCAAAGAGAGAGA-3’

OCS-termR: 5’-TGCACAACAGAATTGAAAGC-3’

After successful confirmation by PCR and restriction analysis of the plasmid, the destination clone was transformed into either *Agrobacterium tumefasciens* (strain LBA4404) for stable plant transformation or into *Agrobacterium rhizogenes* (strain AR10) in case of a hairy root transformation (described below).

1 µg of plasmid suspended in sterile water was mixed with ice-cold, electrocompetent *Agrobacterium tumefasciens* or *Agrobacterium rhizogenes* and placed into a electroporation cuvette (width: 0.1 cm). After application of an electric pulse (1.8 kW), bacteria were immediately mixed with 1 ml YEB (*Agrobacterium tumefasciens*) or SOC (*Agrobacterium rhizogenes*) medium and grown for four hours at 28°C on a rotary shaker before 100 µl of the bacterial culture was spread on solid YEB plates, containing 50 ng/ml Kanamycin and 50 ng/ml Rifampicin. For growing *Agrobacterium rhizogenes* 100 µg/ml histidine was also added to the medium. Positive transformants

were selected by picking single colonies for further growth and for colony PCR. Bacterial colonies were resuspended in 10 µl of a 20 mM NaOH solution and incubated for 5 minutes at 37°C prior to PCR reaction. 2 µl of this suspension was used for a 20 µl PCR reaction.

2.11. Stable transformation of *Lotus japonicus*

Stable transformation of *Lotus japonicus* (Gifu) was performed as described previously (Thykjaer et al., 1997), with slight modifications. Seeds were sterilised as described above and placed in 0.15% agarose after washing. This mixture was spread on 0.6% agar and incubated for 5 days in the dark at room temperature. Vessels containing the germinated seeds were transferred to 26°C and continuous light for one day. Afterwards, hypocotyls of at least 140 seedlings were separated from roots and shoots, placed in an over-night culture of *Agrobacterium tumefasciens*, and cut into about 4 pieces while immersed in that culture. Sections were then placed on co-cultivation medium (sterile 1/10 B5 medium; 50 mM MES, pH 5.2 (sterile filtered); 1.2 mg/l kinetin; 1.2 mg/l dichlorophenoxyacetic acid (2,4-D), 0.1× B5 vitamins and 25 mg/l Geniticin (G-418)) that was covered with sterile filter paper. Control hypocotyls were sliced, incubated in sterile YEB medium, and placed on co-cultivation medium without antibiotic selection. Plates were sealed with parafilm and incubated for 7 days in the dark at 21°C before developing calli were transferred to selective callus medium (L0 medium; 3 mg/l kinetin; 3 mg/l 2,4-D; 300 mg/l Claforan; 1× B5 vitamins; 2 % sucrose and 25 mg/l G-418). Callus formation proceeded for 20 weeks in continuous light at 26°C before calli were removed from the remaining hypocotyls and placed on selective callus medium for another 7 weeks at 21°C and 16/8 hours light/dark rhythm. Next, calli were placed on shoot induction medium (L0 medium containing 10 mM NH_4^+; 0.2 mg/l BAP; 25 mg/l G-418; 1× B5 vitamins and 2 % sucrose) for 10 weeks before being transferred for at least 2 weeks onto shoot growth medium (L0 medium containing 0.2 mg/l BAP, 25 mg/l G-418, 1× B5 vitamins and 2 % sucrose). Finally, calli with shoots were placed on shoot elongation medium (L0 medium containing 1× vitamins and 2 % sucrose) for 1-2 weeks before three outgrown shoots were cut off the callus, transferred into soil and grown for seed production.

2.12. Hairy root transformation of *Lotus japonicus*

Seeds were sterilised and germinated as described above (section 2.3). 13-15 seedlings were placed in a square Petridish containing ½ B5 medium (½ B5 macro-and micronutrients; ½ B5 vitamins; 8 g/l Gelrite; pH 5.2) tilted in a slope way when they reached a length of 0.2-0.5 cm. The root was inserted into the medium in order to anchor the plant. Plants were grown for 3 days at 21°C before being transformed. *Agrobacterium rhizogenes* was injected into the stem of the plant using a fine needle. Bacteria were pre-grown on plates as described above (section 2.3) and resuspended in 4 ml YEB medium to obtain a milky suspension. Infected plants were grown for two weeks before plants with visible hairy roots emerging from the injection site were placed in quartz sand and transferred to a phytotron at 21°C at 16/8 hours light dark rhythm for 3-4 weeks. Plants were inoculated with *M. loti* about 4 days after being transferred into quartz sand.

When antibiotic selection was applied to the plants, wild-type roots were removed from plants two weeks after infection with *Agrobacterium rhizogenes* and plants were grown for a further 14 days on the ½ B5 medium (described above) containing 25 µg/ml G-418 before being transferred to quartz sand. Further growth was as described above.

2.13. Immunoblotting

20 mg of infected root or isolated nodule material were homogenised in liquid nitrogen and proteins were extracted in an ice-cold buffer containing 10 mM Tris (pH 8.0), 14 mM NaCl, 5 mM EDTA, 1% Triton X-100, 1 mM PMSF and 1 mM DTT. After centrifugation at 20,800 g for 15 minutes in a microfuge, protein concentrations of the supernatants were determined using the Bradford Protein assay by following the suppliers protocol (Biorad). 10-20 µg total protein was loaded onto a commercial 10 % Bis-Tris SDS polyacrylamide gel and separated at 100 V for 1.5 hours in 1× MES buffer. Proteins were blotted onto a PROTRAN membrane using the XCellII Blot Module (Invitrogen). The blot was performed in a 1× transfer buffer (25 mM Tris-Base (pH 8.0); 190 mM Glycine) for 2.5 hours at 400 mA and 4°C. Equal loading of the lanes and the quality of transfer were checked by using Ponceau Staining of the membrane.

The membrane was blocked with PBS buffer (described above) containing 2 % w/v BSA for at least one hour at room temperature before primary antibody was added. Hybridisation was carried out overnight at 4°C. Before adding the secondary anti-rat

antibody with an IgG-AP conjugate, membranes were washed for 10 minutes in PBS buffer with 0.1 % Tween 20 and then in PBS buffer containing 0.1 % Tween and 1 M NaCl. After incubation of the membranes for 1-2 hours with the secondary antibody, membranes were washed as follows:

10 minutes in PBS, 0.1 % Tween20
10 minutes in PBS, 0.1 % Tween20, 1 M NaCl
10 minutes in PBS, 0.1 % Tween20
5 minutes in PBS
10 minutes in 100 mM Tris-Base, pH 9.0

Staining was carried out by using NBT-BCIP (3 tablets in 30 ml water) for 5-30 minutes. The reaction was stopped by placing the membranes in PBS buffer.

Antisera against soybean leghemoglobin was kindly provided by N. Suganuma (Aichi University of Education, Japan) and the antiserum against component I of the nitrogenase protein was generously provided by T. Bisseling (University of Wageningen, The Netherlands). Both primary antibodies were diluted 1:10.000 and the secondary anti-rabbit antibody (1 mg/ml) was diluted 1:5000 in blocking solution prior to application.

2.14. Oxygen measurements

Oxygen concentrations were measured in intact, 3-week old nodules using a needle-type fiber-optic oxygen microsensor with a tip diameter of less than 50 µm. The location of the tip within the nodule was derived from the scaling of the micromanipulator with which the sensor was pierced through the tissue. The entire procedure was performed under a binocular microscope.

2.15. Tissue fixation, sectioning and microscopy

Nodules were fixed using Technovit 7100 following the protocol provided with the chemicals after stepwise dehydration of the material in 50%, 70%, 90%, 95%, 100% ethanol. Embedded plant material was cut to a thickness of 5-15 µm using a RM2155 microtome (Leica). Dried sections were stained in 1% Toloudine Blue solution for 2 minutes and rinsed with water afterwards. Starch granules were detected by staining the sections in Lugol solution (13 g/l iodide; 20 g/l potassium iodide) for 5 minutes before being washed with water.

2.16. Adenylate Measurements

ATP and ADP were measured using a cycling assay, as described previously (Gibon et al., 2002). To measure ATP-concentrations, aliquots of extracts (5 µl) or standards (0-50 pmol) were dispensed directly into a microtiter plate, followed by 95 µl of 100 mM Tricine/KOH buffer (pH 8.0) containing 10 mM $MgCl_2$, 2 units glycerol-3-phosphate oxidase (Gly3POX), 130 units catalase, 0.4 units glycerol-3-phosphate dehydrogenase (Gly3PDH), 0.05 units triose-phosphate isomerase, 1.3 mM NADH and 2 mM 3-PGA. The sample was mixed and absorbance was measured at 340 nm for 20 min until V_1 was stabilised. This was followed by addition of 0.05 units of Glyceraldehyde-3-phosphate-dehydrogenase and 0.05 units of phosphoglyceraldehyde kinase. The sample was mixed and absorbance was measured at 340 nm for 20 min until V_2 was stabilised.

ADP-concentrations were determined in a 200 µl reaction containing 60 µl Tricine/KOH buffer (pH 8.0), 0.1 units pyruvate phosphate dikinase and 0.05 unit pyrophosphatase. 1 µmol inorganic phosphate and 2 µmol pyruvate were added to 20 µl of extract aliquots or the ADP standard (0-50 pmol). Mixtures were incubated for 50 min at 30°C before being heated for 5 min at 95°C. Samples were put on ice to cool and collected using a microcentrifuge. Supernatants were transferred to a microtiter plate, and 20 µl of 200 mM Tricine/KOH buffer (pH 7.8) containing 0.05 units glycerokinase, 2 units Gly3POX, 0.4 unit Gly3PDH, 130 units catalase, 0.12 µmol NADH, 0.25 µmol glycerol and 50 pmol ADP were added. Absorbance was read for 20 min at 340 nm until V_1 stabilised, then 2 units myokinase (in 100 mM Tricine buffer) were added. Absorbance was monitored for further 20 min at 340 nm until V_2 stabilised.

2.17. Determination of amino acids

20 mg fresh weight of nodule tissue was ground in liquid nitrogen and extracted with 250 µl 80 % ethanol for 20 minutes at 80°C. After centrifugation at 20.800 g the supernatant was removed and kept and the pellet was extracted again with 250 µl 50 % ethanol for 20 minutes at 80°C followed by a second centrifugation. 150 µl of 80% ethanol was added to the remaining pellet and incubated for further 20 minutes at 80°C after the supernatant was transferred into a fresh tube. The supernatants were combined and later used for HPLC analysis of the amino acids after 2 mM HEPES (pH 7.5) was added to the total sample.

For derivatisation 35 µl of sample were transferred in 300 µl sample vials (closed with SnapCaps, to prevent evaporation due to the high temperature in the HPLC

room). 35 µl of o-phthalic acid di-aldeyde (OPA) reagent was added to each sample. After 1.5 min the mixture was injected into the HPLC. Preparation of the OPA reagent was as follows: 25 mg OPA were dissolved in 500 µl methanolto which were added 4.5 ml 0.8 M borate buffer, pH 10.4 (12.37 g boric acid solved in 250 ml water, adjusted with about 4 g KOH to pH 10.4) and 50 µl 3-mercaptopropionic acid.

Analytical conditions:

Wavelengths of fluorescence: excitation 330 nm; emission 450 nm

Standard: 10/20 µM and 20/40 µM amino acid mixture

Calibration: external standard

Column: Hypersil-ODS (C-18) 3µm; Rent-a-column (Knauer B118Y164)

Pre column: Hypersil-3µm, self filled

Flow rate: 0.8 ml/min

Injection volume: 20-50 µl

Buffer A: 1000 ml (8 mM Na_2HPO_4 pH 6.8 (with 40% H_3PO_4) + 4 ml tetrahydrofurane)

Buffer B: 250 ml (46.73%) 40 mM Na_2HPO_4 pH 6.8 (with 40% H_3PO_4); 150 ml (32.71%) Methanol; 110 ml (20.56%) Acetonitrile

Gradient program (OPA_July2003)

0 min	95 % Buffer A
4.3 min	95 % Buffer A
16.25 min	85 % Buffer A
26.3 min	50 % Buffer A
38.3 min	40 % Buffer A
43 min	30 % Buffer A
47 min	0 % Buffer A
52 min	0 % Buffer A
53.5 min	95 % Buffer A
62 min	95 % Buffer A

Short program for major aa

0 min	100 % Buffer A
16min	87 % Buffer A
17.25 min	85 % Buffer A
19.5 min	0 % Buffer A
25.5 min	0 % Buffer A
27 min	100 % Buffer A
35 min	100 % Buffer A

3.0. Results

A significant part of this PhD project was devoted to resource and methods development for functional genomics of *Lotus japonicus*, which is described in the first section of this chapter. These tools were used subsequently to characterise in detail a nodule-induced ascorbate oxidase, and three symbiotic leghemoglobins. The results of this work are presented in sections 3.7 and 3.8, respectively.

3.1. Extension of *Lotus* cDNA arrays

At the start of this project, two sets of partially redundant cDNA arrays had been produced by Gillian Colebatch, which led to the identification of a large number of nodule-induced genes in *Lotus* (Colebatch et al., 2002a). However, neither of these arrays incorporated all the available nodule cDNAs that had been sequenced as part of the EST-project in our group, or the large number of other clones from EST-projects elsewhere. To make full use of these resources, Lene Krusell and I produced nylon arrays containing all 9,600 *Lotus* nodule cDNAs from our EST collection, and a second set of arrays containing a non-redundant set of 11,652 clones obtained from the Japanese EST program. Because of intermittent problems with removing radioactive probes from hybridised filters, a more robust method was developed to enable 'stripping' and re-use of the filters (Ott et al., 2005; *in press*). Finally, to accelerate data mining from these arrays, considerable effort was also put into creating a local database in which all clones were annotated.

3.1.1. Creation of large-scale LjNEST and LjKDRI cDNA arrays

cDNA-clones in the MPI-MP EST-collection were present in either pBluescript or pSPORT. Of the 100 × 96 clones sequenced from these two libraries, 8,554 yielded in high-quality sequences, which were deposited in GenBank, and later incorporated in the *Lotus* database at TIGR (version 3.0). Our EST-collection was maintained as both glycerol stocks of *E. coli* and as solutions of purified plasmid, each in 96-well format. The latter was used as template for PCR to produce sufficient amounts of dsDNA for robotic-spotting onto nylon membranes (see Material and Methods). A small aliquot (5 µl) of each 100 µl PCR reaction was run on an agarose gel to monitor PCR efficiency before each reaction was concentrated to approximately 30 µl by evaporation. On average, 93% of all reactions yielded a substantial amount of product. The remaining reactions failed to produce product.

A non-redundant collection of 11,652 EST clones (31 × 384 clones) was obtained from the Kazusa DNA Research Institute (KDRI) in Japan as bacterial cultures. Colony PCR (see Material and Methods) was performed directly from the liquid bacterial stock or after overnight growth of colonies spotted onto solid LB medium containing 50 µg/ml Ampicillin. PCR reactions were performed in 384-well plates, repeated three times and pooled prior to spotting onto the membranes. PCR amplification efficiency from bacterial clones of the LjKDRI library was about 75% which was less than that obtained using purified plasmids (LjNEST) as template, presumably due to inhibitory effects of bacterial cell debris. In addition, not all clones from the KDRI library grew and could not be amplified.

PCR amplicons were spotted onto nylon membranes without any further purification as described in Material and Methods.

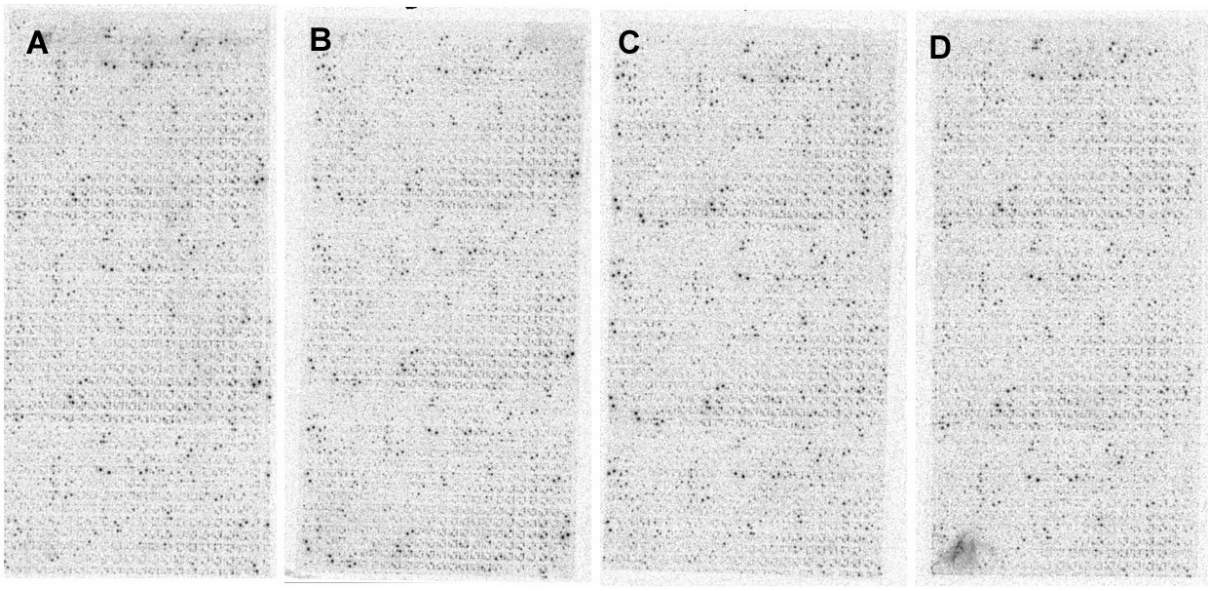

Figure 3.1. 1: Different membranes were tested for hybridisation efficiency.
A: Porablot, B: Millipore, C: Hybond XL, D: Hybond N^+; RNA from potato tubers (8µg) was used to hybridise the filters containing tomato ESTs; 8 million cpm probes were added to the filters for hybridisation.

At the time the arrays were produced there was a general problem in our institute of removing labelled probes from hybridised arrays. Therefore, a substantial amount of time was invested in identifying optimal hybridisation buffers and washing conditions for use of the new *Lotus* arrays. After comparing the initial Church buffer hybridisation system (Sambrook et al., 1989) with a commercial system (Ambion) and a

formamide-based hybridisation system combined with an alkaline washing treatment (see Material and Methods), the latter system was chosen. This system yielded good signal intensity, higher specificity, and low background. It also allowed efficient stripping of probes after hybridisation.

Testing different nylon membranes like Hybond N^+ (Amersham), Hybond XL (Amersham), Millipore and Porablot did not result in differences in signal intensity or stripping ability (Figure 3.1.1). The current optimised protocol for hybridising and stripping cDNA arrays is now in press (Ott et al., 2005, *in press*).

3.2. Mining and computational analysis of cDNA array data

Data processing and mining is a crucial aspect of cDNA array analysis (Figure 3.2.1), and one of the objectives of this project was to improve data mining capabilities for *Lotus* transcriptomics. This was achieved by:

1. *Improving gene annotations*

   In collaboration with Peter Krüger (MPI-MP) a script was developed that enables us to regularly compare the *Lotus* sequences to others deposited in GenBank by using the BLAST algorithm. The first two BLAST hits together with their gene accession number and the e-value of the hit were downloaded and automatically formatted for database use.

2. *Assigning groups of genes represented on both the partially redundant LjNEST array and the non-redundant LjKDRI array*

   Gene annotations obtained from step1 were manually classified into functional categories. All 11,652 KDRI-EST clones were annotated manually using information from BLAST searches and classified into MIPS functional categories (http://mips.gsf.de/projects/funcat) with modifications. Functional categories used were: metabolism (M), signalling and stress (S), transcription (R), protein synthesis and processing (P), intracellular transport (I), transport (T), cellular biogenesis and organisation (B), cell growth, division and DNA synthesis (C), no homology (N), unknown function (U), hits to non-plant genes (X). In total only 26.7% of the KDRI clones could be classified into one of the known functional categories, while 17.8% gave hits to proteins of unknown function and 55.5% showed no homology to any sequences deposited at the NCBI. This almost certainly reflects the fact that these clones were largely sequenced from the 3' untranslated end, which contains less protein coding

information. In contrast only 11% and 25% of the LjNEST clones, which were sequenced from the 5' end, were classified as 'no homology' and 'unknown function', respectively.

A schematic representation of these groups within both sets of arrays can be found in Figure 3.2.2.

3. *Identification of clones representing the same gene on the LjNEST arrays to make use of redundancy to verify 'by consensus' data for each gene*

   The TIGR database was used to identify LjNEST sequences that belonged to a single Tentative Consensus sequence (TC), which likely represented a single gene. In collaboration with Maren Wandrey (MPI-MP) all available *Lotus* TCs and singleton sequences were downloaded from the TIGR database and a list was generated that consisted of all LjNEST clones and their corresponding TC number or singleton designation. This enabled sorting of LjNEST hybridisation data according to the TC number and immediate identification of the redundant clones on the filters. It also facilitated cross-checking of hybridisation data for many genes.

   Of the 9,600 clones that were spotted onto the LjNEST filters, 8,554 were represented by high quality sequences in NCBI of which 8,383 sequences were incorporated into the TIGR update (*Lotus* version 3.0). These 8,383 clones represent 1,197 individual singletons and 2,641 different TCs or approximately 3,800 genes. Thus, on average each gene was represented by 2-3 EST clones on the array. At the time of submission of this thesis, similar data were not available for the LjKDRI library, yet.

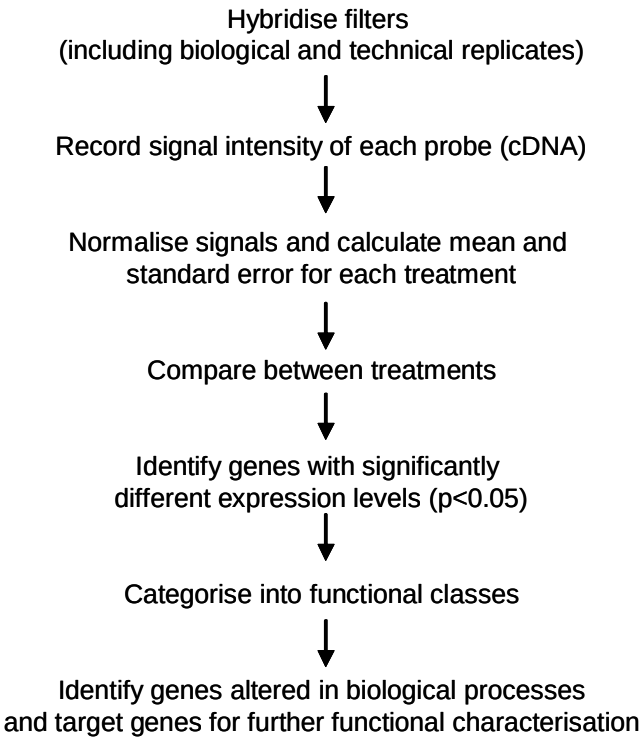

Figure 3.2. 1: Flow chart of the evaluation of a cDNA array experiment.

The measurement of signal intensities was done using AIS software. Raw data were imported into the local HARUSPEX database at MPI-MP and normalised against the reference hybridisation. Student's-T-tests were performed on groups of biological and technical replicates. Categorisation according to the MIPS database was done for all clones.

MAPMAN, a tool to visualize gene expression data, was developed initially for *Arabidopsis thaliana* (Thimm et al., 2004). In order to display cDNA array data from *Lotus japonicus* with MAPMAN, all *Lotus* sequences were compared to the entire *Arabidopsis* genome sequence using the BLAST algorithm. This step enabled us to associate an *Arabidopsis* gene identifier with each LjNEST clone and to adopt pre-defined MAPMAN annotations (codes) for each LjNEST clone. As not all BLAST hits to the Arabidopsis genome gave comparable results to that obtained from the entire NCBI database, the *Arabidopsis* results had to be re-evaluated manually. This analysis was ongoing at the time of submission of this thesis.

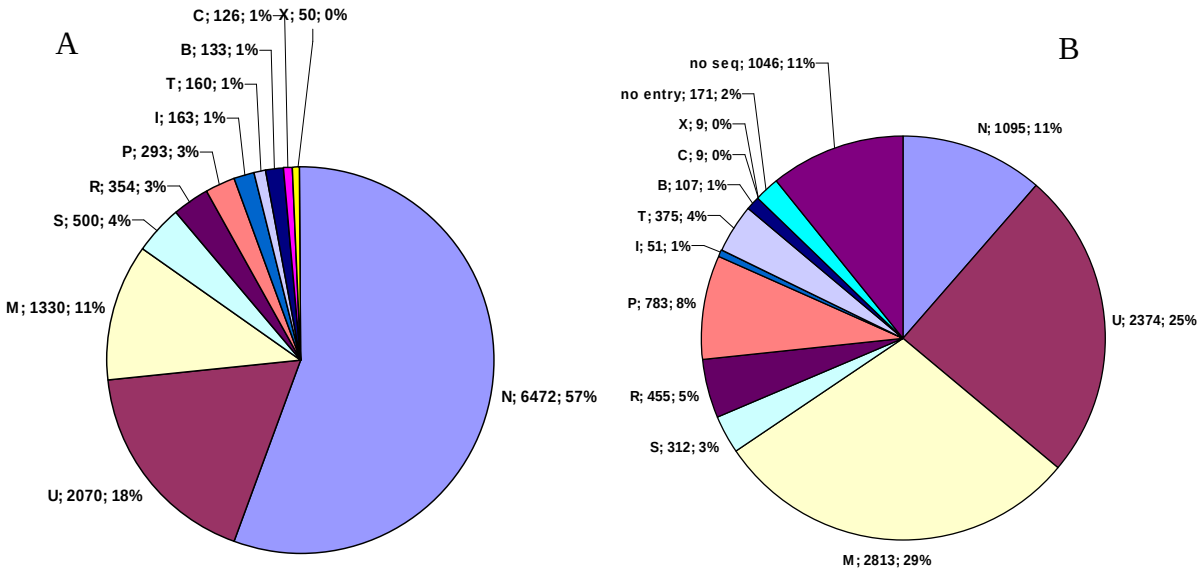

Figure 3.2. 2: Functional categories of the EST clones from the LjKDRI (A) and LjNEST (B) filters. All EST clones from both libraries were manually annotated to one of the functional categories (MIPS) according to their closest hit using the BLAST algorithm. N= no homology; U= unknown function; M= metabolism; S= signalling and stress; R= transcription; P= protein synthesis and processing; I= intracellular transport; T= transport; B= cellular biogenesis and organisation; C= cell growth, division and DNA synthesis; X= hit to non-plant genes.

3.3. International collaborations using our cDNA arrays

After producing the 9.6K LjNEST and the 11.6K KDRI arrays and refining protocols for their use, different experiments were carried out in collaboration with visiting scientists.

3.3.1. Transcript profiling of *Lotus* inoculated with rhizobial mutants

In collaboration with Alejandra D'Antuono and Viviana Lepek (UNSAM-INTECH, Buenos Aires, Argentina) the effects of mutations in the *M. loti cgs* and *lpsβ2* genes of *M. loti* on plant gene expression during nodulation were investigated. The *cgs* mutant carries a Tn5 insertion in a gene coding for cyclic glucan synthase, a component of the bacterial cell wall. When inoculated on *Lotus tenuis* the *cgs* mutant forms white and empty nodules and does not make infection threads. Inoculation of *Lotus japonicus* led to the formation of a larger number of smaller nodules than those observed on *L. tenuis*. The *lps* genes encode lipopolysaccharide synthases and the *lpsβ2* mutant cannot produce the LPS O-antigen domain of lipopolysaccharides. Cell wall analysis of the

mutant showed very low amounts of LPS with a rhamnose:glucose relation of 0.5, in contrast to the wild-type strain with a ratio of 7.

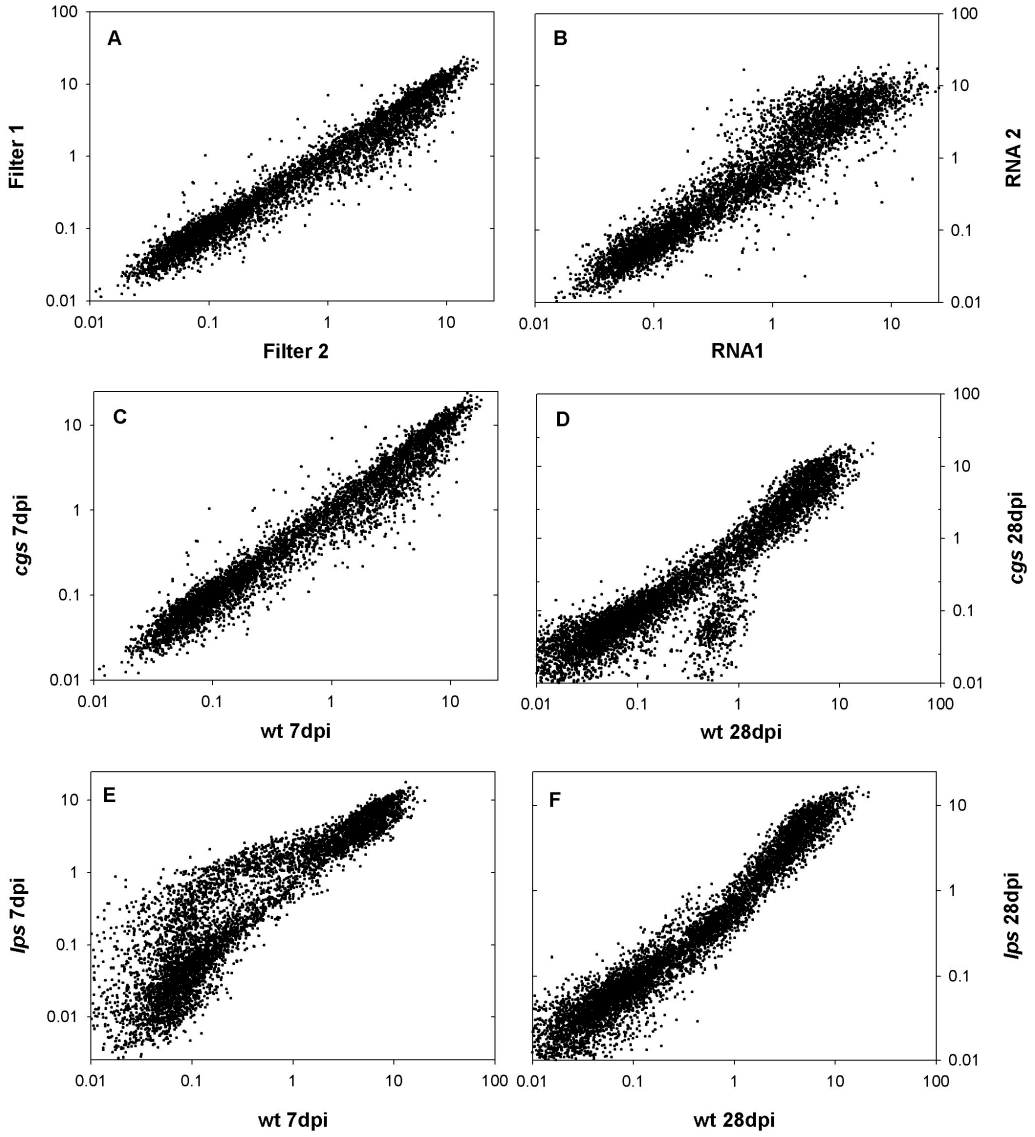

Figure 3.3. 1: Results from array hybridisation with different rhizobial mutants.

Values of normalised data are plotted in all panels. A: technical variability when the same RNA was hybridised to different membranes; B: variance between biological samples; C-D: differential expression of genes at 7 and 28 dpi in wild-type compared to the *cgs* mutant; E-F: differential expression of genes at 7 and 28 dpi in wild-type compared to the *lps* mutant from two biological and two technical replicates.

Inoculation of *Lotus tenuis* and *Lotus japonicus* with the mutant strain apparently led to normal nodule development and numbers (Alejandra D'Antuono and Viviana Lepek, *personal communication*). *Lotus* gene expression was determined in roots inoculated with wild-type *M. loti*, the *cgs* mutant and the *lps* mutant, using the LjNEST arrays.

Technical and biological variability was observed within the treatments (Figure 3.3.1). In the case of the technical replicates about 26% and in case of the biological replicates about 33% of all clones showed a difference greater than +/- 2-fold when comparing the replicates with each other (Figure 3.3.1., panel A and B). Nonetheless, significant changes in gene expression were found in plants inoculated with either the *cgs* or *lps* mutant compared to those inoculated with wild-type *M. loti* both at 7 and 28 dpi (Figure 3.3.1).

When comparing wild-type with the *cgs* mutant 7 and 28 dpi, 1,984 and 1,423 clones, gave significantly different signal intensities ($p<0.05$), respectively. Among those genes differentially expressed at 7 dpi were homologues of the nodulins *Enod36A* (*Glycine max*), *Nlj21* (*Lotus japonicus*), *Enod18* (*Vicia faba*), *Nlj16* (*Lotus japonicus*), uricase (*Lotus japonicus*), genes involved in sugar metabolism, glycolysis and amino acid metabolism, some transcription factors of the MYB and WRKY family, several transporters, and genes involved in flavonoid synthesis and plant defense. Similar genes were identified when comparing wild-type and the *lps* mutant at 7 dpi. After infecting wt plants with the *lps* mutant more clones (3,406) showed significantly different signal intensities compared to wild-type 7 dpi than after infection with the *cgs* mutant. This was due to both, a high variability of the biological samples and a delayed development of nodules induced by the *lps* mutant.

A large number of genes were expressed at lower level in the *cgs* mutant compared to the wild-type at 28 dpi. Among these were genes from carbon metabolism, including genes encoding late nodulins such as trehalose-6-phosphate phosphatases, fructose-bisphosphate aldolase, and glyceraldehyde 3-phosphate dehydrogenase as well as genes coding for key enzymes in nitrogen metabolism like glutamine synthetase and aspartate aminotransferase. On the other hand, no major differences in expression levels could be detected in comparisons of the wild-type and the *lps* mutant. These results were consistent with the phenotypes observed for these mutants as the *lps* mutants form wild-type-like nodules on *Lotus japonicus* whereas only nodule-like structures that do not contain bacteria can be found on roots after inoculation with the *cgs* mutant.

This data-set was also used to compare nodulated roots inoculated with wild-type *M. loti* 7 and 28 dpi as major physiological changes were expected to occur due to functional SNF at 28 dpi. Genes corresponding to 1,558 spotted ESTs were differentially expressed at these developmental stages of which 1,383 could be further

processed in the database. 1,162 of these belonged to existing TCs, 182 were singletons and no entry could be found in the TIGR database for 29 of the ESTs.

3.3.2. Transcript profiling of *Lotus* responses to cadmium

A second collaboration was established with Loreto Naya and Manuel Becana (University of Zaragoza, Spain) to study transcriptional responses of *Lotus japonicus* roots to different concentrations of the toxic metal cadmium. The experiments were carried out using the LjKDRI arrays. Labelled cDNA from RNA of roots that were exposed to 100 µM Cd for 1 and 4 days was hybridised to the arrays. Roots exposed to Cd for 1 day showed 21 up-regulated genes (ratio > 2; $P \leq 0.05$) and 95 down-regulated genes (ratio < 0.5; $P \leq 0.05$). After 4 days of Cd exposure, 79 genes showed significant up-regulation and 81 down-regulation. Searching the TIGR database (http://www.tigr.org/tdb/tgi/plant.shtml) for the 79 genes that were up-regulated after 4 days revealed 17 genes (22%) that are involved in metabolism, 4 genes (5%) in transcription, 3 genes (4%) in protein synthesis, 3 genes (4%) in transport, 1 gene (1%) in signalling, and 1 gene (1%) in cell biogenesis. Also, 1 gene (1%) encodes a possible vacuolar enzyme, 20 genes (25%) encode hypothetical proteins or have unknown function, and 29 genes (37%) have no homology with sequences deposited in public databases. 10 genes that were strongly up-regulated (3.5 < ratio < 18.8) in both Cd treatments were selected for further analysis. These are genes encoding a putative AG-motif binding protein and a serine/threonine protein kinase, genes implicated in metabolism, and a gene responsive to abiotic stress. cDNA array data of the most interesting genes (transcription and signalling) were confirmed by quantitative RealTime RT-PCR (qRT-PCR) of RNA isolated from roots of at least four series of plants grown independently.

3.3.3. Transcript profiling of *Lotus* mutants inoculated with wt rhizobia

Several international guests used our cDNA array facilities for profiling different *Lotus* mutants, including *nin* (Schauser et al., 1999; hybridisations done by Niels Jørgensen from University of Aarhus), the *snf1, 2, 3, 4* mutants that show spontaneous nodulation (hybridisations done by Leila Tirichine from University of Aarhus) and the recently published *nfr1* and *nfr5* mutants (Madsen et al., 2003; Radutoiu et al., 2003; hybridisations done by Mette Grönlund, University of Aarhus). Transcript profiles for the *Lotus* mutants *sym6*, *sym13*, *sym43* and *sym11* were obtained by Vera Voroshilova

in our group. All of these mutants show defects in either nodule development or function. RNA was extracted from roots 3, 7, 14 and 21 dpi. Wild-type plants grown under the same conditions were used as controls. For all of these experiments data mining and evaluation is currently in progress so that no summary of this work can be presented at this stage.

3.4. Identification of interesting candidate genes from array experiments

By using array hybridisations many interesting genes were identified as differentially-expressed during nodule development in wild-type or mutant plants inoculated with wild-type or mutant rhizobia. Earlier work revealed higher expression levels of a sulphate transporter and a putative potassium transporter in nodules compared to uninfected roots (Colebatch et al., 2002a). These transporters were studied in more detail by qRT-PCR as described in section 3.5.2. Another gene that was chosen for further study, because of my interest in nodule redox metabolism, encodes a putative ascorbate oxidase (*LjAox1*). This gene was 3.7-fold (*p*-value: 0.037) induced in the roots (4 wpi) compared to roots harvested 1 wpi with *M. loti* (see section 3.7).

3.5. Validation of cDNA array data by qRT-PCR

A partially-redundant cDNA array containing 5,376 LjNEST clones, representing about 2,500 genes was constructed and used to compare gene transcript levels in nodules to those in uninfected roots from 7-week-old *Lotus* plants. Partial redundancy amongst clones on the array enabled cross-checking of expression data for many genes. Although a majority of the genes represented on the array were not differentially expressed in nodules compared with roots, approximately 860 genes were induced significantly in nodules (nodule/root ratio >2, $p < 0.05$). Over 70% of these had a p-value of less than 0.01 (Colebatch et al., 2004). Compared with the number of nodule-induced genes discovered, relatively few genes were found to be expressed at a lower level in nodules than in roots, a bias that can be explained by the fact that the arrays were created with nodule cDNA clones.

Approximately one-third of all nodule-induced genes encoded proteins involved in metabolism or transport (28 and 5%, respectively). 8% of nodule-induced genes were predicted to be involved in transcription and its control, while an additional 5% are likely to be involved in signalling. Genes involved in protein synthesis (8%), cell biogenesis (3%), cell division (2%), and intracellular transport processes (2%) were also

induced in nodules compared with roots. Approximately one-quarter (26%) of the genes induced in nodules encode proteins that have homologs of unknown function in other species, while the remainder have no known homologs (Colebatch et al., 2004).

EST/TC	Annotation	Array Nod. Sig.	Array Nod./Root	RT-PCR Nod./Root	SE ($n = 3$)
LjNEST44C3/TC2403	DNA-binding protein	0.03	3.00	2.01	0.04
LjNEST50D8/TC881	DNA-binding protein	0.04	3.20	1.38	0.23
LjNEST42C12/TC3685	Zinc-finger protein	0.06	2.90	0.54	0.05
LjNEST6F1/TC1391	bZIP transcription factor	0.06	3.40	1.26	0.06
LjNEST10E7/TC3007	Homeobox RRM-containing protein	0.07	2.30	0.83	0.06
LjNEST14B3/TC1629	KH domain/zinc finger protein	0.08	2.40	0.75	0.01
LjNEST42B1	Zinc-finger protein	0.08	2.70	0.96	0.19
LjNEST6A3/TC902	CCAAT-box-binding transcription factor	0.09	3.60	>8.33	0.81
LjNEST53C8/TC1468	Zinc-finger protein	0.09	2.90	0.51	0.01
LjNEST12E3/TC2417	DNA-binding protein	0.10	4.90	1.38	0.08
LjNEST24D8/TC1447	WRKY family transcription factor	0.10	4.00	0.50	0.05
LjNEST6B9	Transcription factor	0.11	2.50	2.05	0.04
LjNEST54F12/TC2072	DNA-binding protein	0.11	2.40	0.84	0.01
LjNEST16G12/TC1091	MYB family transcription factor	0.12	2.30	0.95	0.05
LjNEST46H8/TC3654	MADS-box protein	0.16	4.20	>168.85	3.48
LjNEST49H11/TC2380	Negative regulator of URS2	0.18	5.00	0.91	0.04
LjNEST53C2	Transcription factor	0.18	3.10	1.65	0.04
LjNEST55C5	PHD-type zinc finger protein	0.18	3.40	>267.44	16.58
LjNEST40D9/TC367	MYB family transcription factor	0.19	11.60	73.82	1.73
LjNEST11A11/TC3269	Zinc-finger protein	0.19	4.60	1.28	0.04
LjNEST25D11/TC507	Carbonic anhydrase	0.34	11.90	15.40	0.04
LjNEST3E1/TC2283	Carbonic anhydrase	0.73	84.20	41.78	0.28
LjNEST15A11/TC2173	Isoliquiritigenin 2′-O-methyltransferase	0.74	17.30	260.46	4.75
LjNEST12H12/TC2109	Nodulin, Nlj21	0.87	24.30	21.29	0.23
LjNEST12C4	Sulphate transporter	1.13	33.70	313.94	8.33
LjNEST16B9	GA 2-oxidase	1.37	39.50	48.66	0.37
LjNEST22F11/TC5829	Leghaemoglobin	21.40	214.60	623.99	10.51

Figure 3.4. 1: Nodule/root gene transcript ratios determined by Real-time RT-PCR.

The first 20 genes encode putative transcription factors, each with relative transcript level in nodules <0.2, as determined by cDNA array analysis (Array Nod. Sig.). The remaining seven genes were expressed at higher levels (Array Nod. Sig. >0.2). Nodule/Root transcript ratios obtained from cDNA array and RT-PCR analysis are shown, togetherwith the standard error (SE) associated with the qRT-PCR analysis. Transcripts of several genes were detected only in nodules by qRT-PCR; nodule/root ratios for these genes are given as the theoretical minimum ratio (>), assuming the root value was at the detection limit (Ct=40).

To validate cDNA array results for some of these genes, qRT-PCR was employed.

In general, there was good qualitative agreement between qRT-PCR results and cDNA array data (Figure 3.4.1). Genes from different pathways that were found to be induced on the arrays were confirmed by qRT-PCR. A more detailed analysis can be found in Colebatch et al., 2004).

qRT-PCR was also used to validate cDNA-array data for a number of previously identified symbiosis-induced genes (Colebatch et al., 2002a) including *LjSst1* and

LjKup, and *LjAox1*, encoding an ascorbate oxidase, which was identified amongst the hundreds of differentially expressed genes described above.

3.5.1. Generation of different cDNA pools

To facilitate further quantitative analysis of expression of these and other genes during nodule development, cDNA was prepared from root and nodule material harvested at multiple time points after inoculation as well as from various plant organs.

Three cDNA pools were created for use by myself and our various collaborators to confirm expression of target genes:

1. *Nodulation time course- infected roots*

   A series of cDNA pools derived from infected and uninfected roots (controls) harvested 0, 0.25, 1, 2, 7, 14 and 21 dpi was produced to monitor induction and repression of target genes in roots and nodules over time.

2. *Nodulation time course- nodules only*

   A series of cDNA pools derived from nodule material harvested at 7, 14, 21 and 28 dpi was produced to validate and extend data obtained from array experiments using nodule tissue.

3. *Organ specificity*

   Pools of cDNAs were synthesised from different organs like nodules, roots (inoculated and uninoculated), leaves, and stems of plants grown under symbiotic and non-symbiotic conditions in order to test for organ-specific expression of selected target genes.

3.5.2. Developmental regulation of *LjSst1* and *LjKup*

Amongst the genes studied in detail by qRT-PCR were *LjSst1* and *LjKup*, which encode a sulphate transporter and a potassium transporter, respectively. In both cases, transcript levels in inoculated roots remained relatively low for the first 7 dpi, but increased substantially afterwards. This coincided with a period of rapid organ growth, indicating that the transporters may be required for resource supply (e.g. *LjSst1*) during rapid cell growth. My data for *LjKup* (Figure 3.5.1) were included in a publication from our group (Desbrosses et al., 2004). The data on *LjSst1* were included in a submitted manuscript describing the map-based cloning of *LjSst1* using the *Lotus sym13*/*sym81* mutant, which are defective in symbiotic nitrogen fixation (Figure 3.5.1).

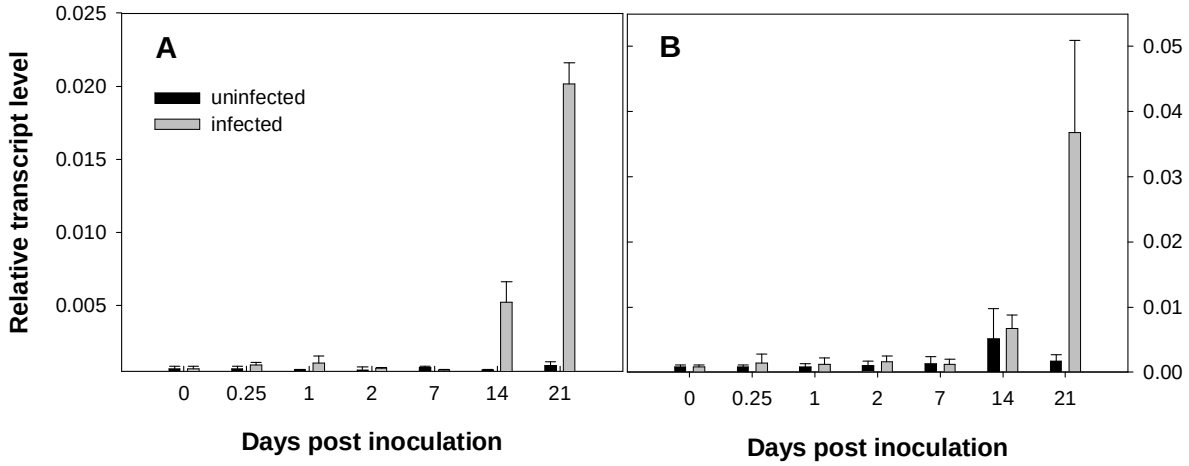

Figure 3.5. 1: Induction of *LjKup* and *LjSst1* expression during nodule development.

Transcript levels for *LjKup* (A) and *LjSst1* (B) were determined in inoculated roots including nodules and uninoculated roots (controls) of *Lotus japonicus* using qRT-PCR. Tissue was harvested at the time points between 0 and 21 days post inoculation (dpi). 8-10 plants were pooled prior to RNA extraction and 3 technical replicates were measured per time point; error bars represent standard deviation of three biological replicates. Expression levels of *LjSst1* and *LjKup* are expressed relative to ubiquitin transcript levels in the same sample.

3.6. *Agrobacterium rhizogenes*-mediated hairy root transformation for rapid phenotypical analysis of nodule expressed genes

To facilitate 'rapid' phenotypical screening of potentially interesting nodule-expressed genes, I combined a procedure for transformation of roots based on the use of *Agrobacterium rhizogenes* (Morris and Robbins, 1992; Webb et al., 1996; Stiller et al., 1997) with a GATEWAY® vector system for RNA interference (RNAi). In a pilot study to test the efficacy of this approach, an RNAi construct that targeted three leghemoglobin (Lb) genes was produced (Figure 3.6.1) and transformed into root cells using *Agrobacterium rhizogenes*.

Nodules that developed on transformed roots, following inoculation with *M. loti* were typically white, rather than leghemoglobin-pink (Figure 3.6.2). Western blot analysis confirmed the absence of the Lb protein in the majority of these nodules (Figure 3.6.2).

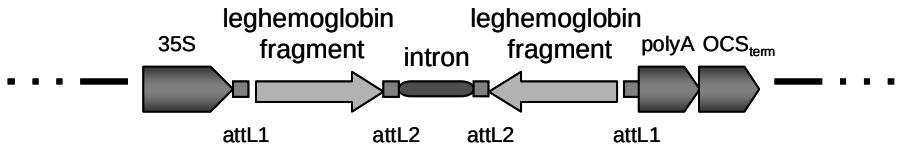

Figure 3.6. 1: Schematic representation of the GATEWAY® cassette used for RNAi.
Two 401 bp PCR-fragments of *LjLb2*, cloned in opposite direction were separated by an intron. Transcription was driven by the CaMV-35S promoter and terminated by an OCS terminator. The GATEWAY cassette was taken from the vector pJawohl8 (provided by Imre Somssich, MPI-ZF, Cologne) and was cloned into the multiple cloning site of the pBIN19 vector, containing a gene that encodes a neomycin phosphotransferase II. That confers kanamycin resistance on transformants.

Thus, although hemoglobins are the most abundant proteins in mature nodules, they are not required for nodule development *per se*. On the other hand, leghemoglobins are important for nodule function, a point that is taken up in more detail later in this chapter (section 3.8).

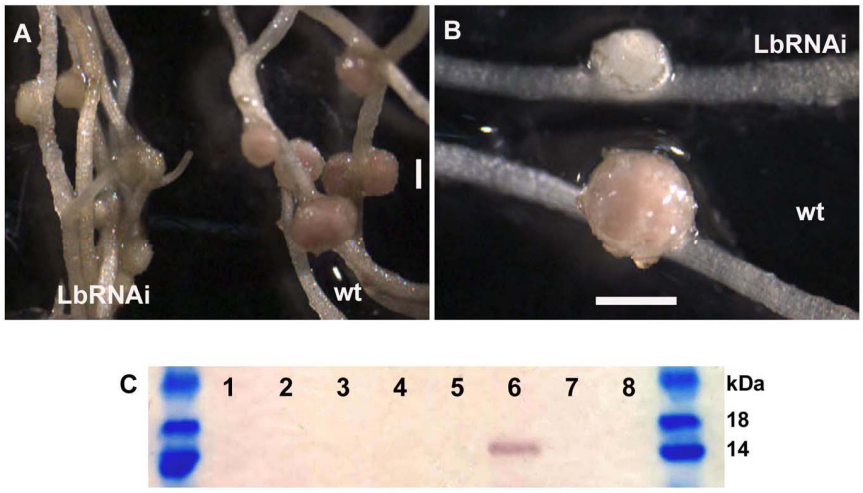

Figure 3.6. 2: Hairy root transformation using an LbRNAi construct.
A: Hairy root transformation using an RNAi construct to silence expression of symbiotic leghemoglobins led to formation of white nodules on transgenic roots while pink nodules developed on wild-type control roots (panel A). **B:** closer view of the transgenic (upper) and wild-type nodules (lower) also revealed a size difference between 4 wpi old nodules. Scale bars indicate 2 mm. **C:** Western Blot analysis of nodules following hairy root transformation. White nodules (lanes 1-5) and wild-type nodules (lane 6) as well as root material from wild-type (lane 7) and transgenic tissue (lane 8) was harvested from the plants. 10 µg total protein was loaded per lane and seperated by SDS-PAGE, blotted onto nitrocellulose membrane and probed with anti-body to soybean leghemoglobin.

Thus, the *Agrobacterium rhizogenes*-RNAi system proved to be effective in eliminating endogenous gene expression in *Lotus* nodules. This system is now being used by myself and others in the group to identify genes with important developmental or other functional roles in nodules. In addition, hairy root transformation can be used to study gene expression using promoter-Gus constructs, an application that is also described below (section 3.7.3).

3.7. Molecular, cellular, and physiological characterisation of ascorbate oxidase in nodules

After method establishment and testing its functionality and applicability hairy root transformation was used during several biological approaches.

3.7.1. Identification of a symbiosis-induced *Aox* using cDNA arrays and *in silico* analysis

The apoplastic enzyme, ascorbate oxidase (*AOX*) regulates the reduction/oxidation (redox) state of the apoplastic ascorbate pool (Pignocchi and Foyer, 2003). Because of the perceived importance of the apoplastic redox state on extracellular signal perception by plant cells and the involvement of ascorbate in plant development, it was interesting to find that an *Aox* gene represented on the LjNEST array was one of the genes induced during nodule development (see section 3.4).

There are currently 6 tentative consensus sequences available for *Aox* in the *Lotus* TIGR database. None of these is regarded as full-length by automatic annotation. Comparing the predicted protein sequences, they can be grouped into 3 distinct classes with TC18839 and TC19920 forming group 1; TC12917, TC14506, and TC11125 belonging to group 2; and TC15779 as a member of group 3 (Figure 3.7.1). The clone LjNEST98c11 that was found to be induced during nodule development belongs to TC11125 (= *LjAox1*).

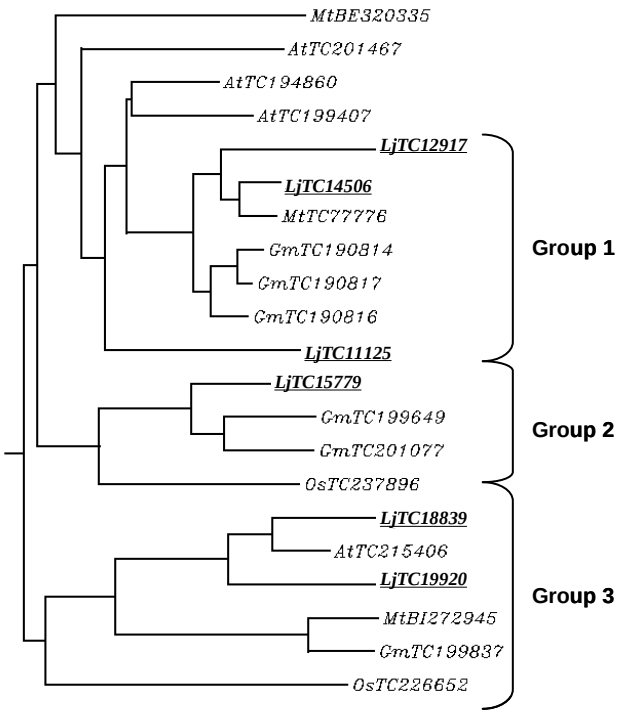

Figure 3.7. 1: Phylogenetic tree of *AOX* protein sequences from different plant species.
Results are presented as a dendogram. Lj= *Lotus japonicus*, Mt= *Medicago truncatula*, Gm= *Glycine max*, At= *Arabidopsis thaliana*, Os= *Oryza sativa*. Sequence information of tentative consensus sequences was obtained from TIGR database.

Based on the EST abundance in different libraries two of the genes represented by TC11125 and TC12917 seem to be exclusively expressed in nodules, while other Aox genes are expressed more strongly in flowers, flower buds and pods (Table 3.7.2)..

TC number	Total no. of ESTs	Whole seedling	Nodules	Roots	Flower/ flower bud	Pods
TC11125	3	0	3	0	0	0
TC12917	2	0	2	0	0	0
TC14506	23	1	0	1	13	8
TC15779	7	1	0	0	2	4
TC18839	2	0	0	0	2	0
TC19920	2	0	0	0	2	0

Table 3.7. 2: EST representation in cDNA libraries derived from different plant organs.
The numbers given in the table represent the numbers of EST clones in the individual libraries. Data were obtained from the TIGR database. (http://www.tigr.org/tigr-scripts/tgi/T_index.cgi?species=l_japonicus; *Lotus* version 3.0).

However, the genes expressed in nodules (TC11125 and TC12917) are not closely related based on phylogenetic analysis (Figure 3.7.1) but fall into the same group

3.7.2. *LjAox1* is specifically expressed in nodules and induced during nodulation

LjAox1 transcript levels in roots increased following inoculation to values 850 × higher than in uninoculated controls 21 dpi (Figure 3.7.3).

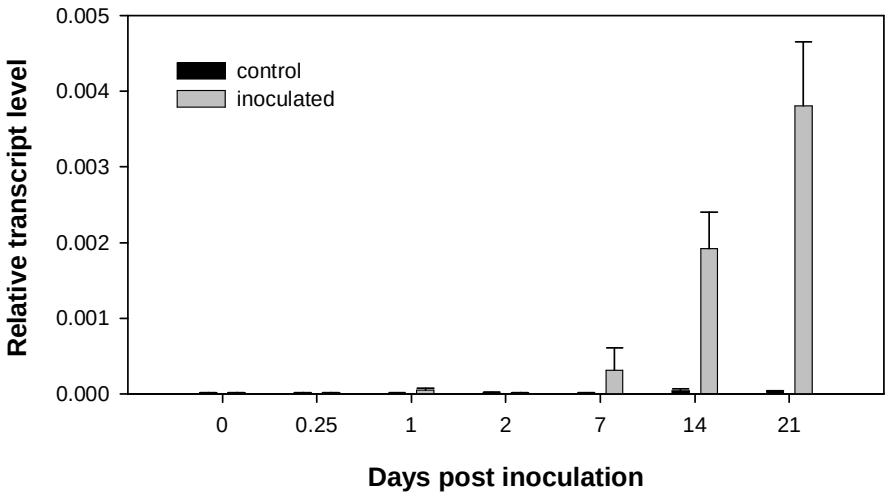

Figure 3.7. 3: Relative transcript levels of *LjAox1* during nodule development.

Relative transcript levels of *LjAox1* were determined for inoculated roots plus nodules and uninoculated roots (controls) of *Lotus japonicus* using qRT-PCR. Tissue was harvested at the time points indicated between 0 and 21 days post inoculation. 8-10 plants were pooled per replicate prior to RNA extraction. Expression levels of *LjAox1* were normalised and expressed relative to ubiquitin. Data from two independent biological replicates are shown. Error bars represent standard deviation of six measurements.

To verify whether the increase of expression derived from developing nodules on roots, the expression of *LjAox1* was tested in various organs (Figure 3.7.4). Transcripts of ascorbate oxidase were more than 200-fold higher in nodules than in any other organ (Figure 3.7.4). Expression levels in infected roots and nodules were higher than in shoot and leaf material harvested from the same plants. Indications that ascorbate oxidase is induced during nitrogen deprivation of plants were obtained as transcript levels were 11-fold higher in roots of uninoculated plants grown for 21 days on 0.1 mM KNO_3 compared to plants of the same age grown on 5.0 mM KNO_3 (Figure 3.7.4).

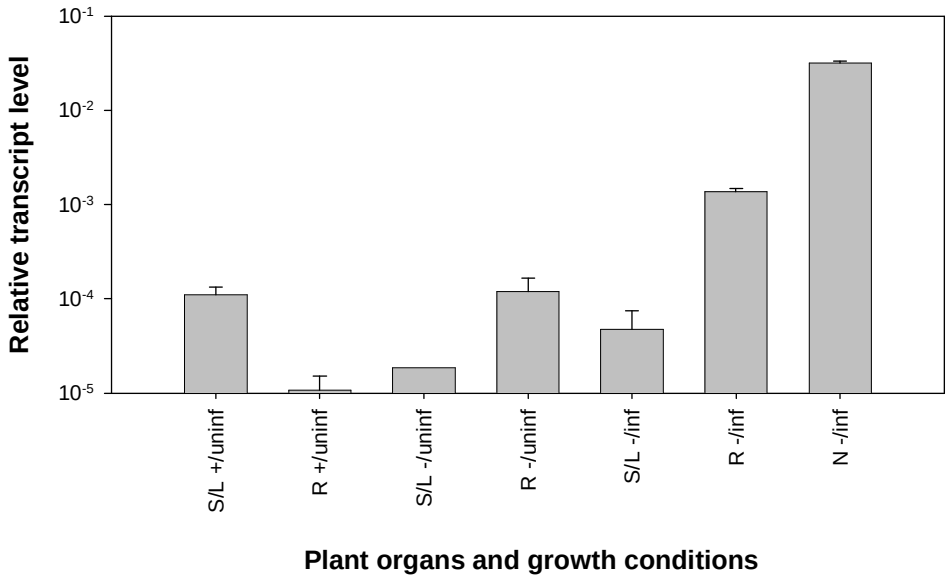

Figure 3.7. 4: Expression of *LjAox1* in different plant organs.

Plants were grown on 5.0 mM (+) and 0.1 mM (-) KNO_3 for three weeks under symbiotic (inf) and non-symbiotic conditions (uninf). Shoots and leaves (S/L), roots (R) and nodules (N) were harvested separately. Material was harvested and pooled from 8-10 individual plants. Three technical replicates were measured per treatment. Error bars indicate standard deviation. Expression levels of *LjAox1* were normalised and expressed relative to ubiquitin.

To obtain more specific information about *Aox1* expression during nodule ontogeny transcript levels of the gene were also determined in isolated nodule tissue 7, 14, 21 and 28 dpi. Expression of *LjAox1* was highest in young, developing nodules and declined in older tissue (Figure 3.7.5). Transcript levels were similar in 7 and 14 days old nodules and dropped by more than 50% at 21 dpi in full-sized nodules. No significant difference in expression was found between 21 and 28 dpi.

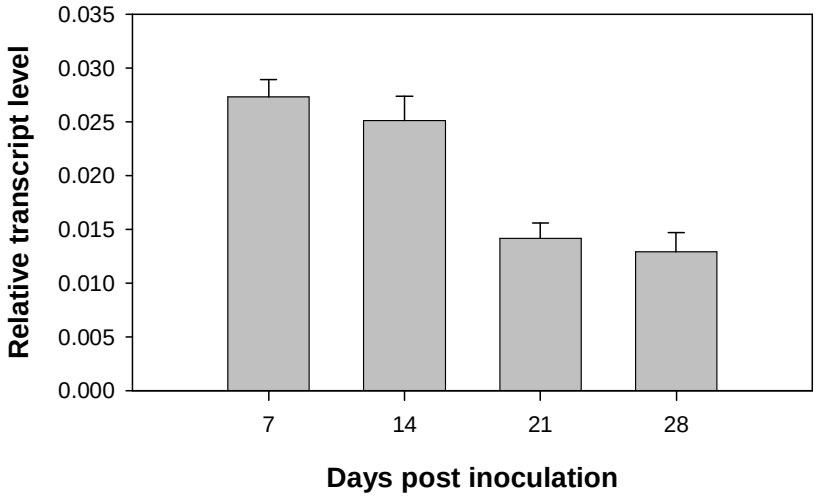

Figure 3.7. 5: *LjAox1* expression in nodules of different age.

Material from 10-30 nodules of at least 15 individual plants were harvested and pooled. Three technical replicates were measured per stage. Error bars indicate standard deviation per sample. Expression levels of *LjAox1* were normalised and expressed relative to ubiquitin.

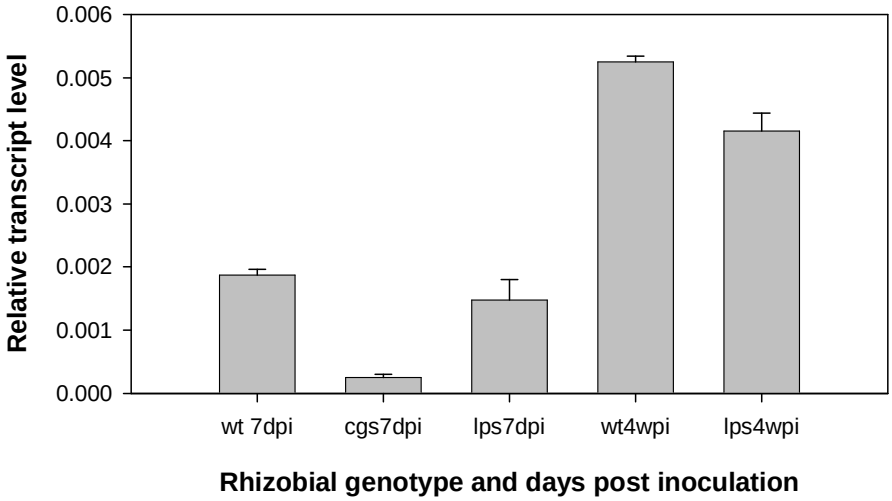

Figure 3.7. 6: *LjAox1* expression requires rhizobial infection.

LjAox1 expression in roots after inoculation with wild-type (wt) rhizobia and two mutants (*cgs* and *lps*). Inoculated plants were grown in the presence of 0.1 mM KNO_3 for 7 and 28 days. Roots were harvested and pooled from 8-10 individual plants. 3 technical replicates were measured per treatment. Error bars indicate standard deviation per sample. Expression levels of *LjAox1* were normalised and expressed relative to ubiquitin.

In seperate experiments *Lotus* seedlings were inoculated with the rhizobial *cgs* and *lpsβ2* mutants (see section 3.4.1). Plants inoculated with the *cgs* mutant showed 7-fold lower levels of *LjAox1* expression in nodulated roots compared to the wild-type

(14% ± 4% of wild-type-level) after one week whereas expression of this gene was similar in plants infected with the mutant *lpsβ2* and wild-type *M. loti* both one and four weeks post inoculation (Figure 3.7.6).

3.7.3. *LjAox1* gene structure and promoter analysis

All EST clones with sequence similarity to ascorbate oxidase genes, which were represented in the LjNEST and LjKDRI libraries were selected for further analysis. Restriction analysis revealed that clone GNf036e07 (LjKDRI library) derived from the same gene as LjNEST98c11 was the longest cDNA representing *LjAox1*. This cDNA was sequenced completely, yielding 948 bp of sequence (Figure 3.7.7). Subsequent 5' RACE-PCR yielded in further 345 bp of cDNA sequence (Figure 3.7.7). A BLAST search of *Lotus* genomic DNA sequence that became available in the meantime located the *LjAox1* gene on TAC clone TM1649. Comparison of the *Lotus LjAox1* gene and protein sequence with that of the closest and full-length homologe from *Medicago truncatula* (MtC20102_GC) led to the identification of a putative start codon (Figure 3.7.7; underlined).

ATGAGCTTCAAAGCTCTTTCCCTTTTGTGTATTTCGTTGGGTTTGTTCTTCCAGATATCATTAGGAGCTG
TGAGACACTACAAGTTTAATGTAGAGTACATGCTTCGCAGACCAGATTGTGAAGAGCACATTGTGATGGG
AATCAATGGCCAGTTTCCTGCCCCCACTATCAGAGCAGAAGTTGGGGATACCCTTGATATTGCACTTACT
AACAAGCTCTTCACGGAAGGAACTGTTCTTCACTGGCATGGAATTACACAGTATGGAACACCTTGGGCAG
ATGGCACTCCTTCCATCTCGCAATGTGCAATAAACCCAGGAGAAACTTTTCACTACAGATTCAAAGTTGA
CAGGCCCGGTACATACATCTACCATGGGCACTATGGTATGCAGAGAGCAGCAGGGTTGTATGGTTCTCTC
ATAGTGGATTTGCCTATGGGACAAAATGAGCCATTCCATTATGATAGTGAGCTCAATCTTTTGCTGAGTG
ATTGGTGGCACACAAGTGCACAAGAGCAACAGGCTCAACTCTCCTCTATACCTAACAGATGGGTTGGTCC
TCCTCAGTCTTTTCTCATTAATGGAAGAGGACAGTACAATTGTTCCTTGGCTGCTAGTCTTATCAACACC
ACCCTGCCCCAATGCAAATTTGAAGGTGGTGAAGAATGTGCACCTCAGATTCTCCATGTTGATCCAAACA
AGACCTACAGGATTAGGATTGCTAGCTCCACTTCCTTAGCTAATCTCAACTTTGCCATTGCCAATCACAA
AATGGTGGTGGTGGAAGCTGATGGAAACTATGAGGAACCATTCATCGTAGATGACTTAGACATATACTCT
GGTGAGACTTATTCTGTTATCATCACCACAAATGAAAACCCAAATCAAAACTACTGGATTTCAGTTGGTT
TTATAGGAGAAAATCTCAAAACCCCACAAGCCCTAACCATACTAAACTACAAAGAAAACAATGCCTCAGT
TTTTCCCACTTCTCCACCCCCTATCACACCTCAATGGGATGATTACAATCGCAGCAAAATATTCTCTCAG
AAAATTCTTGCTCGAAAAGGAACCCCACGCCCTCCAATTTACTATGACCGTAGGCTTCTCCTTCTCAACA
CAGAAAGTTTGGTTGATGGACGCACTATGTATGCCATTAATAATGTCACTTTAATATTACCTTCAACTCC
TTATTTAGTTTCCATTAAGTATAAACTTGATGATGCATTTGACCAAAAAAGCCCCCCTGACAATTTCTCA
TTTGATTATGACATCTACAACTCCCCTGTGTACCCTAATTCAAATACTGGGAGTGGAATCTACATGTTTC
AATTGAACCAAGTGGTTGACGTGGTCCTCCAAAATACCAATATACTGGAGAGGATCAAAAGAAGTGACTT
TCACCCATGGCATTTGCATGGTCATGATTTTTGGATTTTGGGATATGGAGATGGGATGTTCAAACCAGGT
GATGATGAGACCAAATTCAACCTGGAAAACCCACCACTGAGGAACAATGCAGTGCTCTTCCCTTACGGAT
GGACTGCTTTAAGGTTTAAGGCAAATAACCCTGGAGTTTGGGCCTTTCATTGTCACGTTGAGCCTCATTT
GCATATGGGAATGGGTGTGGTTTTTGCGGAGGCTGTTGAAAATGTGGAAGGAATACCTTGGGAAACTCTA
GCATGTGGCCTATTCAGGGGGATTTCA**TGA**AGAAAGAACATAAATGATCAACCTTCTAGCCACTCTTGTA
TTTGCCCAATGTTCGTTTAAGTTAAAATTTCTCTCAAAAAAAAAAA

Figure 3.7. 7: Full-length cDNA sequence of *LjAox1*.

The major part of the sequence derived from clone GNf36e07 (948 bp marked in light grey). A further 345 bp of cDNA sequence were obtained by 5'-RACE-PCR (black) and the remaining 417 bp were identified using the coding sequence of the TAC clone TM1649 (dark grey).

Further analysis of the cDNA and gene sequence revealed the existence of 6 exons, 5 introns, and a coding region of 1,710 bp leading to a protein that consists of 570 amino acids.

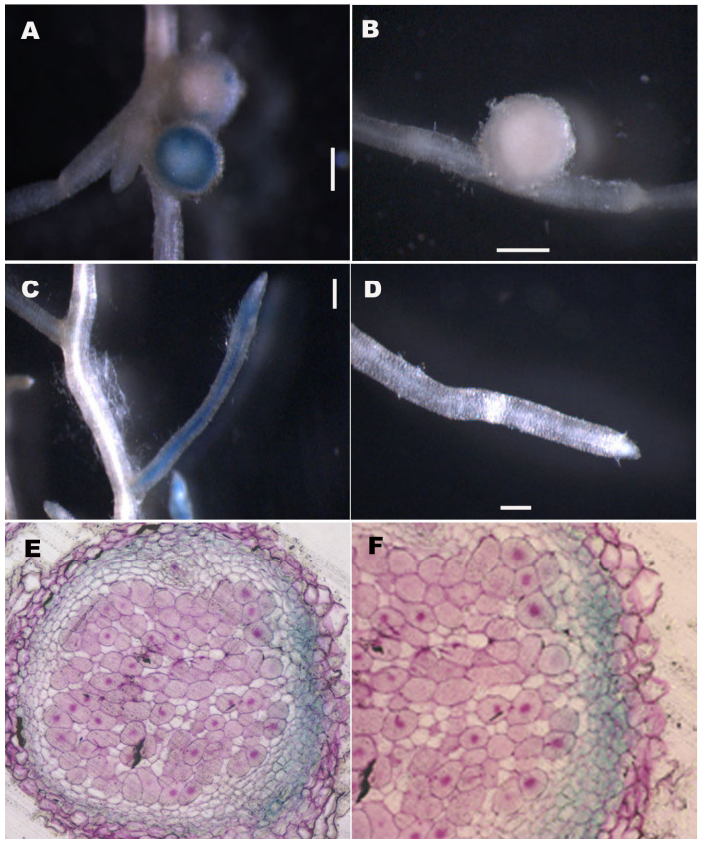

Figure 3.7. 8: Promoter analysis of *LjAox1* using hairy root transformation.
Lotus japonicus was transformed with *Agrobacterium rhizogenes* carrying a 1049 bp long fragment of the *LjAox1* promoter fused to the *Gus* gene. Gus staining was detected in the periphery of transgenic nodules (A) and rarely in secondary roots (C). Controls were transformed with the pBI101 vector alone (panels B and D). E and F: Embedded cross-sections of nodules show Gus-staining in cell layers of the nodule endodermis. Bars indicate 1mm.

Part of the promoter region (1,049 bp upstream of the predicted start codon) was amplified by PCR, fused to the Gus-gene in the cloning vector pBI101 and transformed into *Agrobacterium rhizogenes* for hairy root transformation. Gus-staining of transformed roots revealed reporter gene expression almost exclusively in the nodules and rarely in root tips and the vascular tissue of lateral roots (Figure 3.7.8). Gus-activity was localised to a ring of cells in the periphery of the nodules. This pattern was also evident in sections of embedded material which revealed more clearly expression in the

endodermal and subendodermal cell layers (Figure 3.7.8). Infected and uninfected cells of the inner cortex did not show Gus-staining. Identical results were obtained using *in situ* hybridisation, done in collaboration with Manolis Flementakis, University of Athens (data not shown).

Putative regulatory elements in the cloned (1,049 bp) promoter region were identified using PLACE software (http://www.dna.affrc.go.jp/PLACE/signalscan.html). Several potential regulatory motifs were found, including elements associated with stress responses (MYB1AT, CCAATBOX1), hormone responses (CATATGGMSAUR, DPBFCOREDCDC3) and expression of seed storage proteins in other species (EBOXBNNAPA, RYREPEATLEGUMINBOX, SEF1MOTIF). In addition, several elements were identified that are responsible for tissue specific expression in other systems like AACACOREOSGLUB1, CAATBOX1 and ROOTMOTIFTAPOX1. Furthermore, a DOFCOREZM domain was identified that may serve as a binding site for Dof-transcription factors (Figure 3.7.9) and might regulate *Aox* expression.

Motif name	Motif sequence	Number
AACACOREOSGLUB1	AACAAAC	1
CATATGGMSAUR	CATATG	2
CAATBOX1	CAAT	20
DOFCOREZM	AAAG	12
DPBFCOREDCDC3	ACACNNG	2
EBOXBNNAPA	CANNTG	12
MYB1AT	WAACCA	4
ROOTMOTIFTAPOX1	ATATT	13
RYREPEATBNNAPA	CATGCA	1
SEF1MOTIF	ATATTTAWW	3
CCAATBOX1	CCAAT	4

Figure 3.7. 9: Promoter-motif analysis of *LjAox1* promoter.

A 1,049 bp fragment of the *LjAox1* promoter was analysed using PLACE software. Motif annotation, the characteristic sequence, and the number of times the motif was found in the promoter sequence are shown.

3.8. Leghemoglobin: an essential late nodulin

3.8.1. Characterisation of the leghemoglobin-gene-family in *Lotus*

Despite being the most abundant nodulin in legume root nodules, the physiological role(s) of leghemoglobin proteins has never been fully proofed. Three symbiotic leghemoglobins (Lb) are expressed in *Lotus japonicus* nodules (Uchiumi et al., 2002) Although the TIGR Gene Index (*Lotus* version 3.0) reports 7 symbiotic leghemoglobin tentative consensus sequences (TC 14039, TC14051, TC14052, TC14053, TC14055, TC14063, TC14065) and 2 TCs for non-symbiotic hemoglobins (TC10713 and TC16046) (Table 3.8.1). However, alignments of the TIGR TCs with genomic sequences for the symbiotic hemoglobins confirmed the presence of just three separate genes (Table 3.8.1).

In the following sections the different hemoglobins are named as indicated in the table below:

Name (literature)	LjLb2	LjLb3	LjLb1	LjLb3	LjLb1	LjLb1	LjLb1	LjNSG2	LjNSG1
TIGR annotation	**TC14065**	**TC14039**	**TC14055**	**TC14063**	**TC14051**	**TC14052**	**TC14053**	**TC10713**	**TC16046**
nodule ESTs	315	185	140	6	3	2	2	3	3
seedling ESTs	0	0	0	0	0	0	0	0	5
others	4	3	1	0	0	0	0	0	0
class	symbiotic	symbiotic	symbiotic	symbiotic	symbiotic	symbiotic	symbiotic	non-symbiotic	non-symbiotic
Locus on Chr 5	106906-107895	47052-48461	90151-91118	47052-48461	90151-91118	90151-91118	90151-91118	Other locus	Other locus

Table 3.8. 1: Representation of hemoglobin transcripts in different EST libraries and chromosomal localisation.

Tentative consensus sequences (TCs) and information about different libraries were obtained from the TIGR database. The names *LjLb1*, *LjLb2*, *LjLb3*, *LjNSG1* and *LjNSG2* are according to Uchiumi et al. (2002). The numbers given in the table represent the numbers of EST clones in the individual libraries. Chromosomal positions of the genes are indicated in the panel below. Seven TCs were localised to only three loci on chromosome 5 suggesting the existence of only three leghemoglobin genes.

3.8.2. Leghemoglobins are highly conserved at the nucleotide level

The three symbiotic leghemoglobins show an overall sequence identity of 82% at the nucleotide level when analysed with the CLUSTALW algorithm. cDNA sequence conservation between symbiotic and non-symbiotic hemoglobins is between 34-40% for *LjNsg1* and 52-63% for *LjNsg2* (Figure 3.8.2). As expected, a high degree of sequence conservation is also evident on the protein level with 98% identity between *LjLB1* and *LjLB2* for example. *LjLB3* shows less similarity to *LjLB1* and *LjLB2* with an identity score of 80.5% on amino acid level. The non-symbiotic hemoglobins are as similar to each other (45%) as they are to the symbiotic proteins (*LjNSG1*: 34-37%; *LjNSG2*: 50-57%).

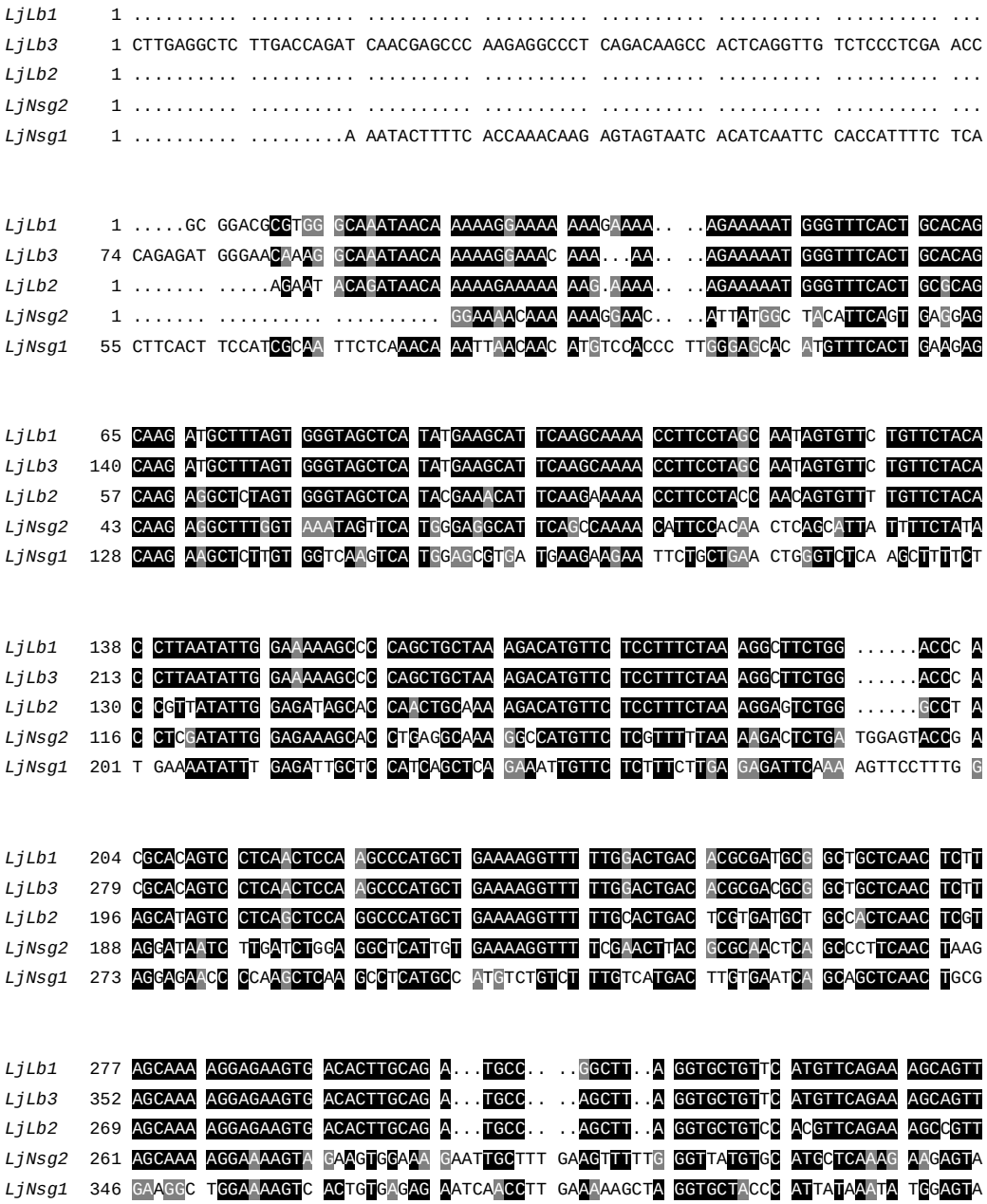

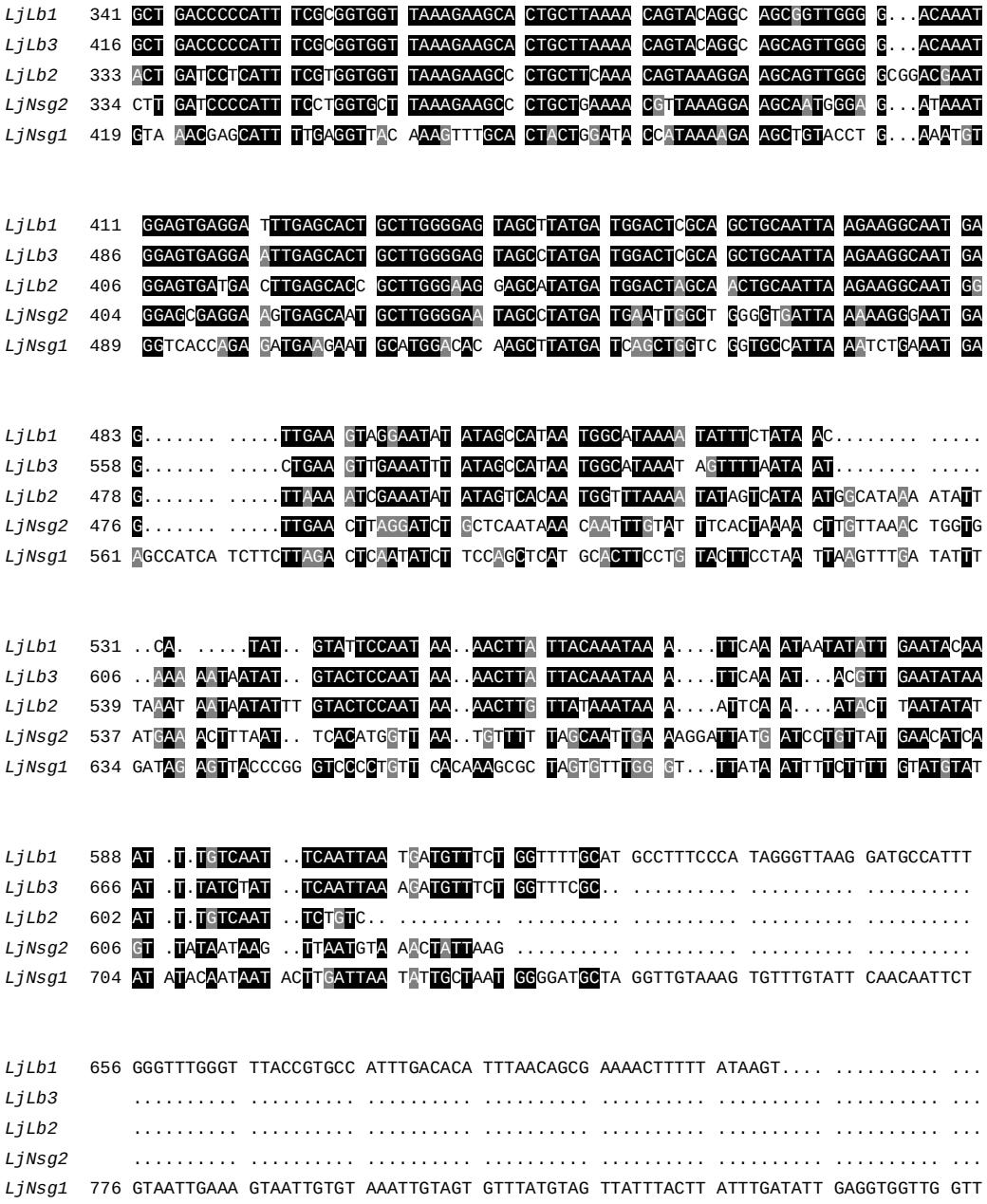

Figure 3.8. 2: Multiple nucleotide sequence alignment of five *Lotus* leghemoglobins.
Nucleotide sequences of the three symbiotic leghemoglobins (*LjLb1*[TC14055], *LjLb2* [TC14065], *LjLb3* [TC14039]) were compared to the non-symbiotic hemoglobin sequences (*LjNsg1* [TC16046] and *LjNsg2* [TC10713]). The alignment was done using the ClustalW algorithm and results were shaded using BOXSHADE software.

Phylogenetic analysis of the hemoglobin sequences from *Lotus japonicus*, *Arabidopsis thaliana*, *Oryza sativa* and *Medicago truncatula* showed that these genes can be divided into symbiotic and non-symbiotic genes (Figure 3.8.3). The symbiotic

hemoglobin sequences of *Medicago* closely cluster with those of *Lotus japonicus* whereas the non-symbiotic hemoglobins of these species group with those of the non-leguminous plants, *Arabidopsis thaliana* and *Oryza sativa*.

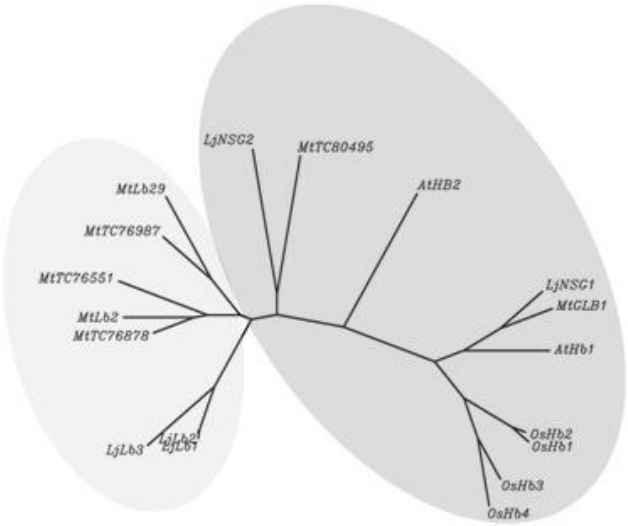

Figure 3.8. 3: Phylogenetic tree of hemoglobins from *Lotus japonicus* and other plant species.
Included in the un-rooted tree are the *Arabidopsis thaliana* hemoglobins, *AtHb1* (TC211680) and *AtHb2* (TC199105); the *Oryza sativa* hemoglobins, *OsHb1* (TC231324), *OsHb2* (TC224250), *OsHb3* (TC229216), *OsHb4* (TC246382); the *Medicago truncatula* hemoglobins *MtLb2* (TC76879), MtTC76878, MtTC76551, MtTC76548, MtLb29 (TC77993), MtTC76987, MtTC80495, *MtGlb1* (TC76971); and the *Lotus japonicus* hemoglobins, *LjLb1* (AB042716), *LjLb2* (AB042717), *LjLb3* (AB008224), *LjNsg1* (TC16046), *LjNsg2* (TC10713). Phylogenetic analysis based on protein sequence was performed using the GenomeNet CLUSTALW server (Koyoto Centre: http://clustalw.genome.jp); the grey shading indicates the two groups of symbiotic (light grey) and non-symbiotic (dark grey) hemoglobins.

3.8.3. Expression patterns of the different hemoglobin genes

To obtain a more accurate measure of transcript levels for the different leghemoglobins in *Lotus*, gene-specific PCR-primers were designed for *LjLb1*, *LjLb2*, *LjLb3*, *LjNsg1* and *LjNsg2*. Symbiotic leghemoglobins were almost exclusively expressed in nodules (Figure 3.8.4). Expression in nodules was between 2,400- and 5,700-fold higher than in roots or leaves. In contrast, although expression of *LjNsg1* was highest in nodules, transcript levels in roots and leaves were only 35- and 5-fold lower, respectively, indicating a more global expression of this gene. The other non-symbiotic hemoglobin, *LjNsg2*, also showed highest expression in nodules. Transcript levels were

622- and 733-fold lower in roots and leaves than in nodules. Transcript levels of the two non-symbiotic hemoglobins were approximately 100-fold lower in nodules than levels of the symbiotic leghemoglobins (Figure 3.8.4).

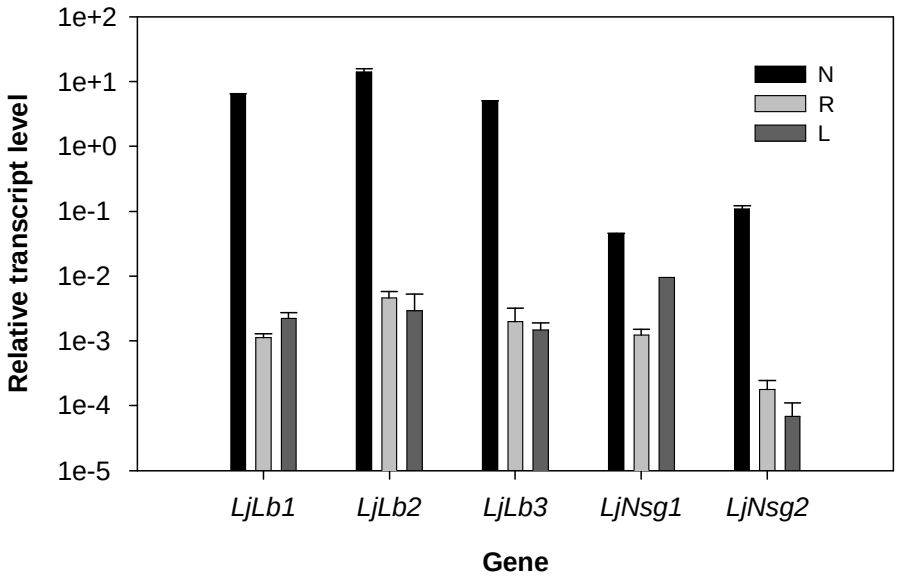

Figure 3.8. 4: Organ-specific expression of different hemoglobin genes in *Lotus japonicus*.
Transcript levels for all symbiotic and non-symbiotic hemoglobins were determined by qRT-PCR. N=nodule (21dpi), R=unioculated roots, L=leaves. Data were normalised and expressed relative to ubiquitin. Error bars indicate standard deviation (n=3).

Induction of hemoglobin gene expression during nodule development was also measured by qRT-PCR. Transcript levels of *LjLb1* increased ten-fold after one day of inoculation with rhizobia and continued to increase for the first two weeks of nodule development (Figure 3.8.5). In contrast, transcript levels of *LjLb2*, *LjLb3* and *LjNsg2* remained low in roots until day two after inoculation, after which levels increased to over 10,000-times higher than in uninoculated roots. The non-symbiotic hemoglobin *LjNsg1* was not strongly induced during nodule development (Figure 3.8.5). Expression of these genes in non-incoulated control roots did not change more than one order of magnitude during the whole experiment.

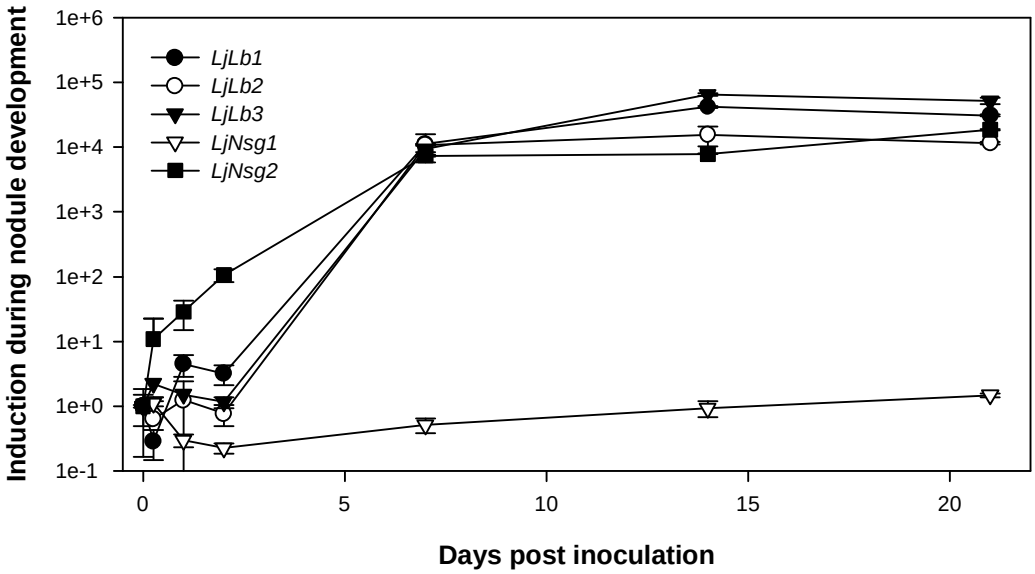

Figure 3.8. 5: Expression of the leghemoglobin and non-symbiotic hemoglobin genes during nodulation.

Relative transcript levels were measured in infected roots, which eventually included nodules and compared to those in uninfected roots by qRT-PCR and plotted on a log-scale. Data were normalised and expressed relative to ubiquitin. Error bars represent the standard deviation of three independent measurements.

3.8.4. Molecular physiology of nodule leghemoglobins

Multiple sequence alignment revealed several stretches of more than 22 base pairs with 100% DNA sequence identity between *LjLb1*, *LjLb2* and *LjLb3*, but no such region of identity was found between the two non-symbiotic hemoglobins and the three symbiotic leghemoglobins (Figure 3.8.2). Thus, an RNAi approach was chosen to investigate the physiological role(s) of the three symbiotic leghemoglobins using *LjLb2* to produce hairpin RNAs (see Materials and Methods).

3.8.4.1. Selection of appropriate transgenic lines showing PTGS of leghemoglobin

After transformation and regeneration, five independent transgenic lines were obtained from which three cuttings of each were grown for seed production (T0). Plants from the segregating T1 generation were analysed phenotypically as a nutrient starvation phenotype was expected due to inefficient SNF. First, the nodules of all lines were visually inspected as it was assumed that the loss of leghemoglobins should lead to the lack of the pinkish colour. This phenotype was observed for lines 2 and 3. Those

plants with white nodules also showed a reduced shoot length when grown under symbiotic conditions (Figure 3.8.6) while no phenotype could be observed when plants were grown in the presence of nitrate-containing fertilizer (Figure 3.8.10). These results indicated a defect in SNF in LbRNAi lines 2 and 3.

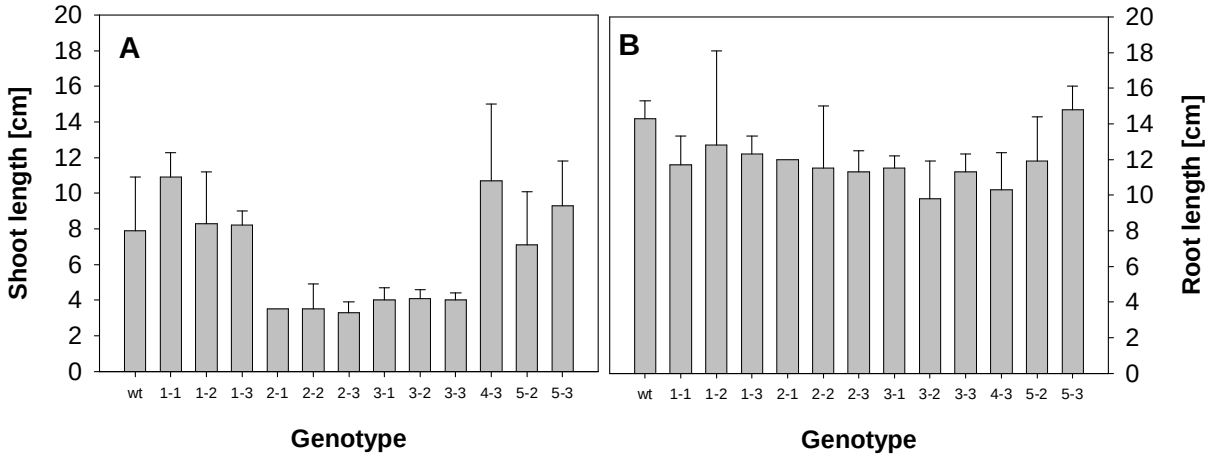

Figure 3.8. 6: Shoot and root length of independent transgenic RNAi-lines.

Shoot (A) and root (B) lengths were determined from plants grown in the greenhouse for 10 weeks under symbiotic conditions. Five independent lines, including sublines, were analysed in the experiment. Error bars indicate the standard deviation of 3-6 individual plants (except #2-1where just one plant could be used for the experiment). In case of lines 2 and 3, plants were pre-selected based on the nodule phenotype.

Transcript levels of total symbiotic leghemoglobins were significantly reduced in lines 2-1, 2-2, 3-2 and 3-3 whereas expression in all sublines of lines 1, 4, 5 as well as in subline 3-1 were higher than in wild-type (Figure 3.8.7). Expression in subline 2-3 could not be measured due to technical problems. T1 plants segregate 1:2:1 (homozygous:hemizygous:null) for the inserted LbRNAi construct in the case that a single T-DNA insertion event occurred during transformation. Thus, one out of four plants in the T1 generation should exhibit wt levels of leghemoglobins. As nodules from more than the plants used for the phenotypical analysis (Figure 3.8.6) were harvested for RNA extraction it is possible that, in case of line 3-1, nodules from a null-plant were included, leading to the high expression level in this line (Figure 3.8.7).

As lines 2-2 and 3-2 showed low expression levels of leghemoglobins and an N-deprivation phenotype under symbiotic conditions, these lines were selected for further experiments.

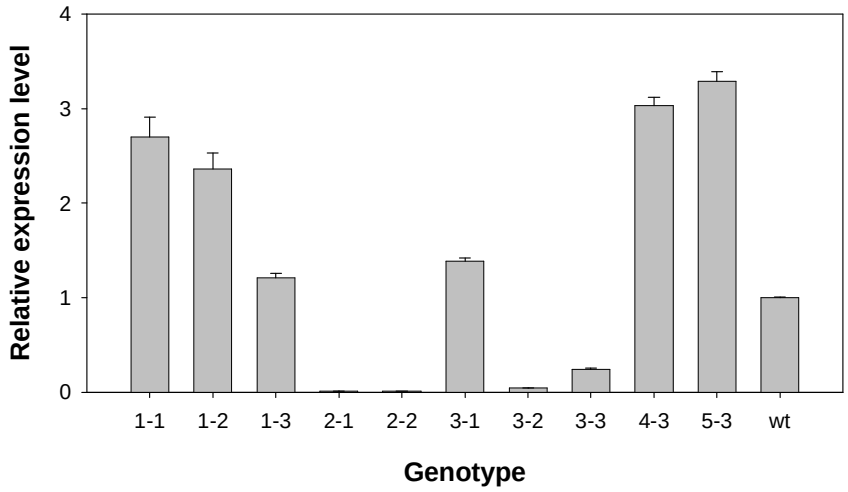

Figure 3.8. 7: Transcript levels of total symbiotic leghemoglobins in all LbRNAi lines obtained after tissue culture.

Nodule tissue was harvested at 28 days post inoculation (dpi). Nodules from 3-4 plants were pooled prior to RNA extraction and 3 technical replicates were measured per line. Error bars represent standard deviation of the sample. Expression levels of leghemoglobins were normalised to ubiquitin and expressed relative to transcript levels of leghemoglobin in the wt.

3.8.4.2. RNAi mediated PTGS of symbiotic leghemoglobins gene expression

Expression of the LbRNAi construct in lines 2-2 and 3-2 led to greater than 97% decrease in transcript levels for all three symbiotic hemoglobin genes (*LjLb1*, *LjLb2* and *LjLb3*, Figure 3.8.8 A) in the T1 generation. In contrast, transcript levels of the non-symbiotic hemoglobins were far less severely reduced in those lines (Figure 3.8.8 A).

3.8.4.3. LbRNAi lines lack leghemoglobin and nitrogenase protein

Western blot analysis was performed to confirm the absence of leghemoglobin protein in LbRNAi lines 2-2 and 3-2. While the leghemoglobin protein was detected in the wild-type plants at 14 dpi using a specific antibody against pea leghemoglobin, no

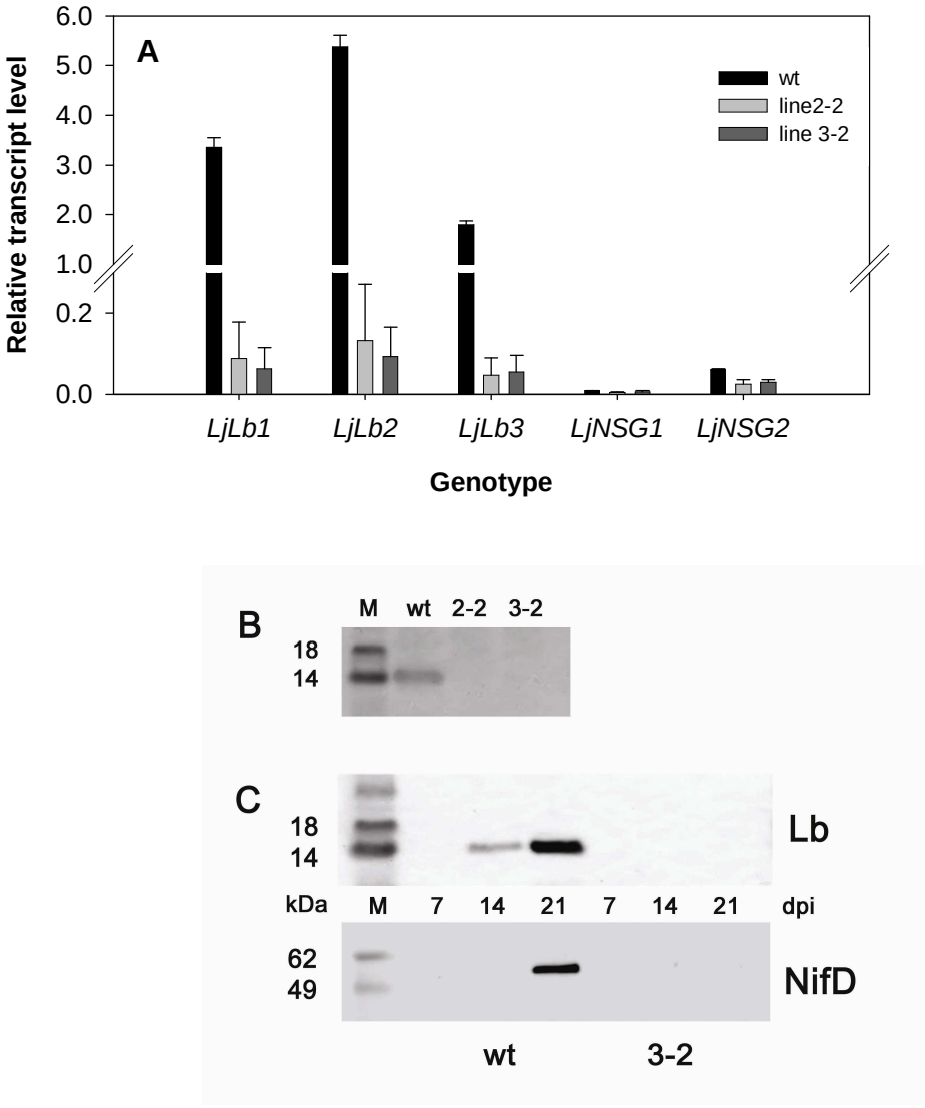

Figure 3.8. 8: Molecular characteristics of LbRNAi lines.

A: Symbiotic and non-symbioitic hemoglobin transcript levels in nodulated roots three weeks after inoculation of wild-type (black) and LbRNAi line 2 (light grey) and 3 (dark grey). Transcript levels were normalised and expressed relative to ubiqutin. **B:** Leghemoglobins were detected by Western Blot analysis in isolated nodules of the wild-type (wt) but not the two LbRNAi lines (2-2 and 3-2). Lane M shows markers of 14 and 18 kDa. **C:** Western blot detection of leghemoglobins (Lb, above) and nitrogenase (NifD, below) in nodulated roots of wild-type (wt) and LbRNAi line 3-2, from 7 to 21 days post-inoculation (dpi). Western blot analyses were performed after SDS-PAGE of 20 µg protein.

leghemoglobin protein was found in nodulated roots (Figure 3.8.8 C) or in isolated nodules of the RNAi-lines (Figure 3.8.8 B). Using an antibody against the nitrogenase *NIFD* subunit, it was found that the *NIFD* protein was absent in inoculated root material of the RNAi-plants, but present in nodulated roots of wild-type plants 21 dpi.

3.8.5. LbRNAi plant phenotypes

3.8.5.1. LbRNAi plants are defective in symbiotic nitrogen fixation

LbRNAi lines 2 and 3 exhibited severely stunted growth compared to the wild-type under symbiotic conditions (Figure 3.8.10). The leaves of the LbRNAi plants grown symbiotically with rhizobia but no external nitrogen were yellowish and chlorotic, a phenotype similar to that of wild-type plants grown in the absence of external nitrogen and without. Other signs of N-deprivation in LbRNAi lines grown under symbiotic conditions were the increase in root/shoot ratio (Figure 3.8.9) and an increased anthocyanin content, manifest as purple pigment in the stems of the plants (Figure 3.8.10). Furthermore LbRNAi plants flowered about 6 weeks later than the wild-type plants under symbiotic conditions.

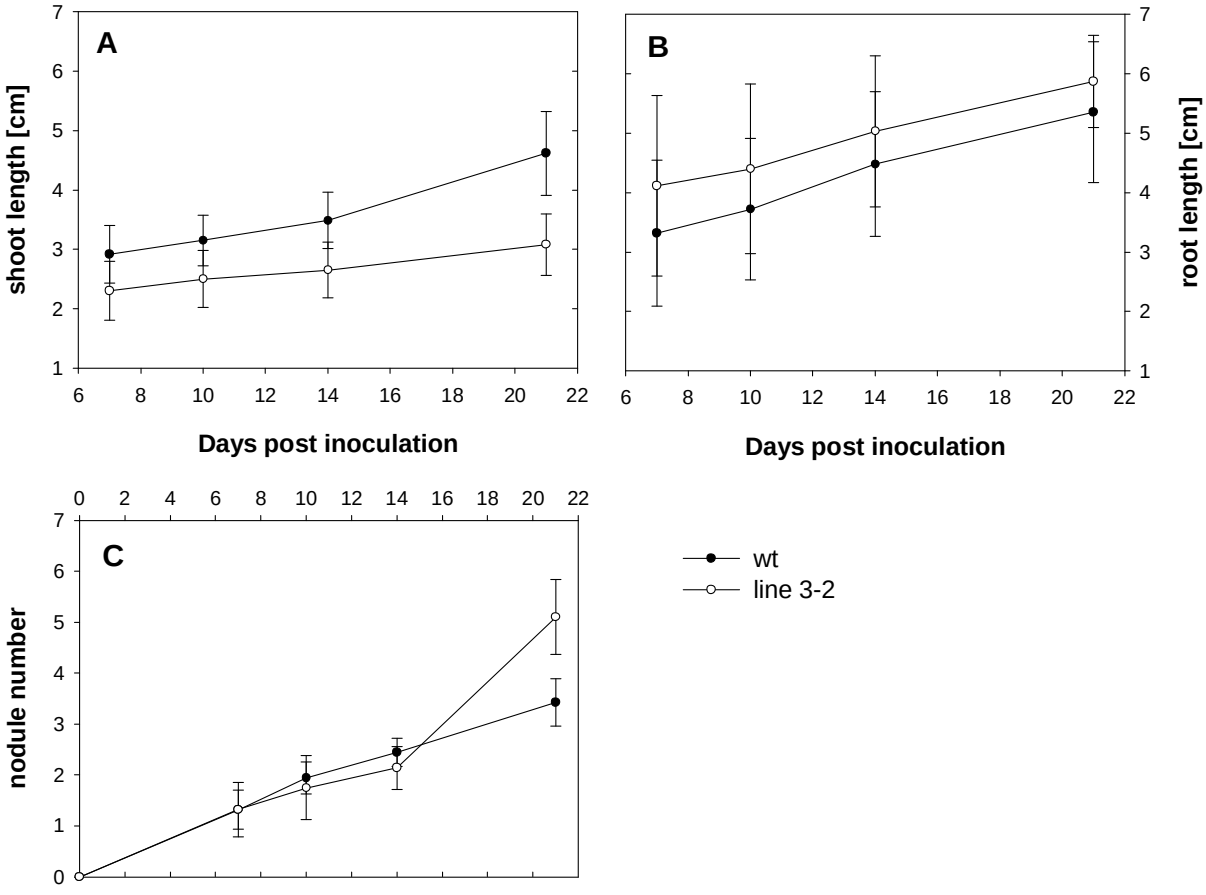

Figure 3.8. 9: Time course of shoot, root and nodule development in LbRNAi-line 3-2 compared to wt.

Shoot (A) and root (B) length as well as nodule number (C) per root were determined 7, 14 and 21dpi. Plants were grown on vertical plates for 2 weeks before being inoculated with *M. loti*.

Another indication of N-deficiency in LbRNAi lines was an increase in nodule number for these plants compared to the wild-type 21 dpi (Figure 3.8.9). Apparently, lack of N-supply from SNF in the LbRNAi lines prohibited feedback inhibition of nodule development in these plants. In contrast, growth of LbRNAi lines on soil with mineral nitrogen added was similar to that of wild-type plants, as was the time to flower (Figure 3.8.10). Thus, the symbiotic growth defect of LbRNAi plants can most easily be explained by a lack of symbiotic nitrogen fixation, a conclusion supported by the observed absence of the nitrogenase protein in nodules of the LbRNAi lines (Figure 3.8.8 C).

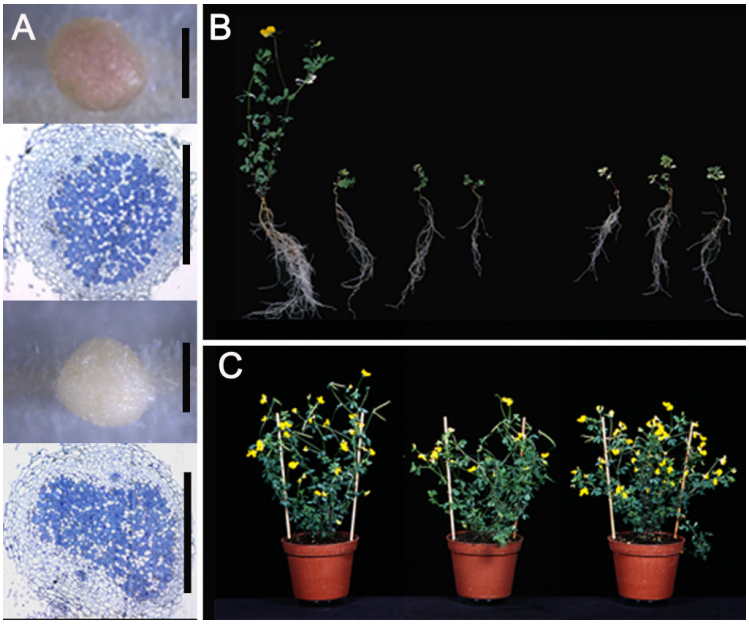

Figure 3.8. 10: Symbiotic and non-symbiotic phenotypes of LbRNAi lines.
A: Typical nodules of wild-type and LbRNAi plants 14 days after inoculation with rhizobia. The top two images show whole and sectioned wild-type nodules, respectively, while the bottom pair depicts the same for LbRNAi line 3-2. Note the absence of leghemoglobin pigmentation in the LbRNAi nodule, but the similar extent of dark-staining, infected cells in the central zone of the nodule section. The scale bars indicate 1 mm. **B:** Ten-week old rhizobia-inoculated plants. Three individuals of two independent LbRNAi lines (2-1, 2-2, 2-3 and 3-1, 3-2, 3-3) are compared with a typical wild-type control. Plants were grown in sand without added mineral nitrogen. **C:** Ten-week old uninoculated plants grown in soil with nitrogen fertiliser. Three LbRNAi individuals are compared to a typical wild-type plant.

Although nodule ontogeny of LbRNAi plants proceeded normally for the first 2-3 weeks post inoculation, nodule expansion ceased 21 dpi, in contrast to wt nodules which continued to expand after this time (Figure 3.8.11). While wild-type nodules

developed prominent lenticels (raised white stripes on the surface of the nodule) these were not evident on the transgenic nodules.

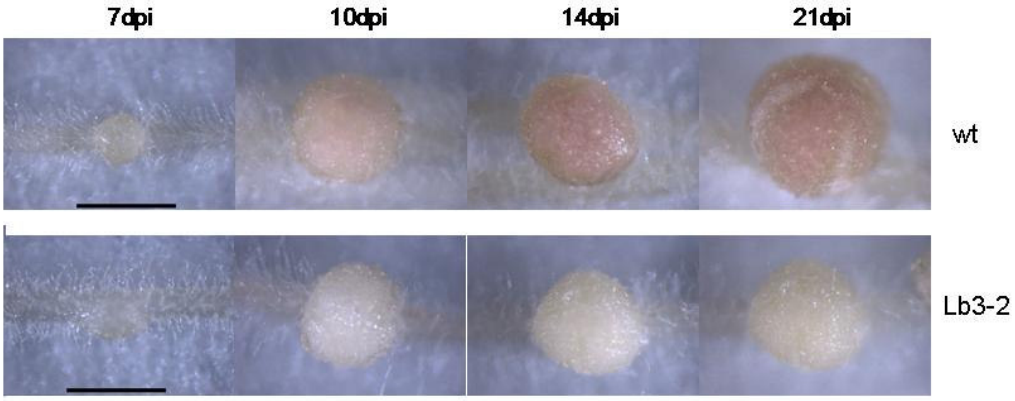

Figure 3.8. 11: Time course of nodule development in wt and LbRNAi plants.

Plants were grown on vertical plates as described in Material and Methods (section 2.3). The nodules depicted are typical of those on wild-type and LbRNAi plants at the times indicated. The scale bar indicates 1mm

3.8.5.2. Microscopical examination of LbRNAi nodules

To determine whether changes in growth rate of LbRNAi nodules 14 dpi was associated with changes in cellular organisation and/or other microscopically visible features, microtome sections of nodules from wild-type and LbRNAi plants were prepared. Microscopical analysis of sections from nodules harvested 14 dpi and 21 dpi showed that wild-type and LbRNAi nodules both had a similar structure and organisation of the infected cells (appearing blue) and uninfected cells (appearing white) (Figure 3.8.12). However, staining with Lugol solution revealed the accumulation of starch granules in uninfected cells of LbRNAi lines. Those granules were found in wild-type nodules only after 21 dpi and starch accumulation was always greater in the LbRNAi lines (Figure 3.8.12).

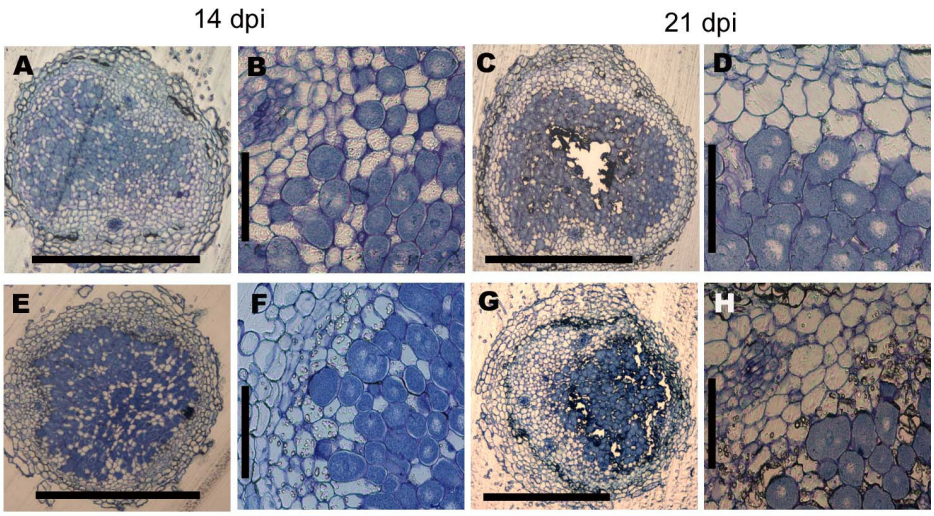

Figure 3.8. 12: Cellular morphology of nodules from wt and LbRNAi plants 14 and 21 dpi.
Nodules were embedded in plastic (Technovit) and cut into sections of 5 µm thickness. A-D: wildtype nodules; E-H LbRNAi nodules. Bars indicate 1 mm (A, C, E, F) and 50 µm (B, D, F, H). The corresponding close-up is located to the right of each nodule cross-section.

3.8.6. Further characterisation of LbRNAi plants

3.8.6.1. LbRNAi lines contain less bacteria inside the nodule

qRT-PCR was used to measure the relative bacterial population size in RNAi and wild-type nodules at 14 and 21 dpi. Population 'size' was determined by measuring the amount of bacterial DNA per unit fresh weight, using PCR primers for the genes *SigA*, *NifH* and *NifD*.

Similar results were obtained for all 3 genes with gene copy number between 0.6-0.8 of wild-type in the RNAi lines tested (Figure 3.8.13). Thus, the bacterial population inside nodules of the RNAi lines was slightly smaller than in wild-type nodules but certainly viable as the increase in expression towards 21 dpi indicates.

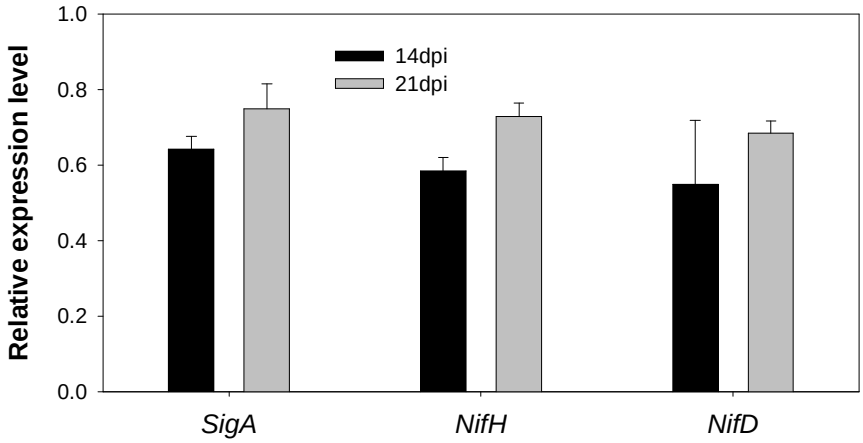

Figure 3.8. 13: Relative bacterial population within wild-type and LbRNAi nodules 14 and 21 dpi. DNA was extracted from isolated nodules and primed with gene specific primers for the bacterial genes *SigA*, *NifH* (Fe protein), and *NifD* (FeMo protein), as well as with oligo-dT for plant genes. Bacterial DNA contents were normalised to plant ubiquitin and expressed relative to wild-type (=1); dpi=days post inoculation. Error bars indicate standard deviation of three replicates.

3.8.6.2. Lack of leghemoglobins leads to increased free oxygen concentrations inside LbRNAi nodules

In view of the proposed physiological roles of leghemoglobins, it was of interest to measure oxygen concentrations in LbRNAi lines. This was done using a needle-type fibre-optic oxygen micro-sensor. Steady-state levels of free-oxygen were higher throughout nodules of LbRNAi lines than for the wild-type controls (Figure 3.8.14). Wild-type nodules exhibited a steep oxygen-gradient from the surface towards the centre of the nodule, with levels of 14.9% (± 5.5%) of ambient oxygen within 0.2 diameters of the surface, and below 1% ambient oxygen for most of the central, infected zone. In contrast, nodules from LbRNAi lines exhibited a shallower oxygen-gradient with 48% (± 5.3%) of ambient oxygen at 0.2 diameters and never less than 4.5% (± 0.7%), even at the center of the nodules (Figure 3.8.14).

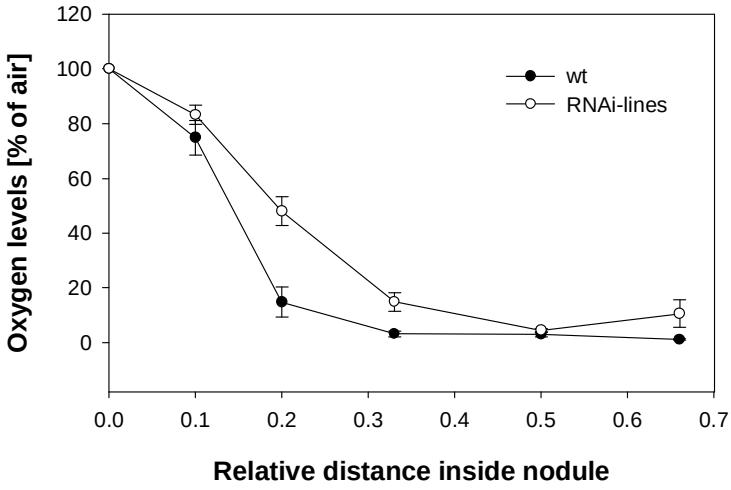

Figure 3.8. 14: Transects of free-oxygen in nodules.

Free oxygen concentrations in nodules from wild-type (filled) and LbRNAi lines (open) are shown and levels are expressed as a percentage of the concentration in air. The surface and center of nodules are indicated on the x-axis by 0.0 and 0.5, respectively. Data points represent the mean (+/- SD) of measurements in 11-13 independent nodules.

3.8.6.3. Loss of leghemoglobins affects the energy status of nodules

To test if changes in oxygen concentrations have an effect on the energy status of the nodules, ATP and ADP concentrations in nodules of wild-type and LbRNAi-plants were measured using a cycling assay.

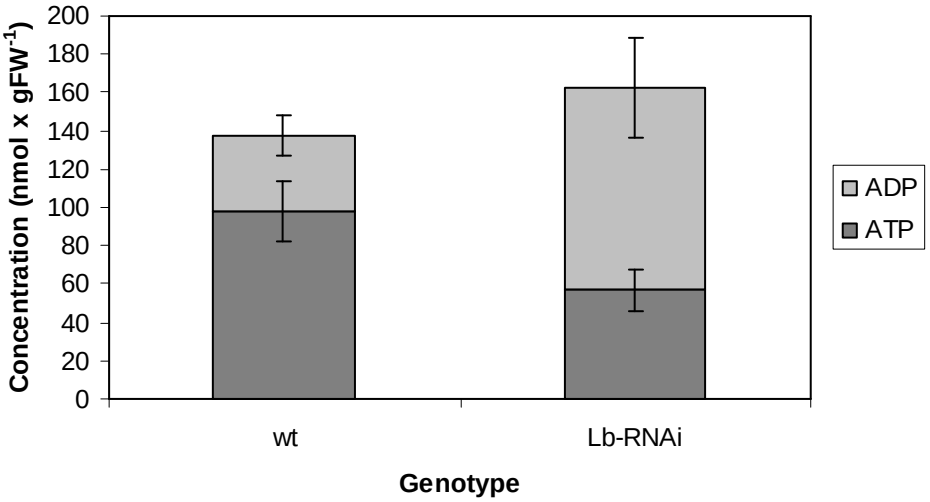

Figure 3.8. 15: Adenylate levels in nodules from wild-type and LbRNAi plants.

ATP (dark grey) and ADP (light grey) concentrations were determined in 21day old nodules using a cycling assay. AMP concentrations could not be measured. Error bars indicate standard deviation of 6 independent measurements on different samples.

In nodules of wild-type plants, an average ATP concentration of 98 nmol × gFW^{-1} (± 16) was measured while in LbRNAi plants the value was 57 nmol × gFW^{-1} (± 11). Concentrations of ADP in nodules of wild-type and LbRNAi plants were 40 nmol × gFW^{-1} (± 10) and 105 nmol × gFW^{-1} (± 26), respectively. Thus, the total amount of ATP+ADP was similar in wild-type and LbRNAi nodules, but the ratio ATP/ADP was 4.5-fold higher in wild-type nodules. In other words, leghemoglobins appeared to be necessary to maintain a higher energy charge in nodules.

3.8.6.4. Concentrations of free amino acids is altered in LbRNAi nodules

HPLC was used to measure the concentrations of free amino acids in nodules of LbRNAi and wild-type plants. Several amino acids were less abundant in the LbRNAi nodules than in the wild-type including glutamate and asparagine, two major amino acids that are exported from nitrogen fixing nodules (Figure 3.8.16). LbRNAi nodules also contained less alanine, argenine, GABA, tyrosine and phenylalanine than wild-type nodules. In contrast, levels of aspartate and glutamine were not significantly changed. Of those amino acids that gave significant p-values, only tryptophan and valine showed increased concentrations in LbRNAi nodules compared to nodules from wild-type plants (Figure 3.8.16).

	wild-type		LbRNAi line 3		
amino acid	**average**	**stdev**	**average**	**stdev**	**p-value**
Aspartic acid	6.69	1.12	5.84	0.95	0.192
Glutamic acid	57.30	8.53	43.04	7.94	0.013
Asparagine	295.11	18.05	60.01	15.08	0.000
Serine	10.37	1.80	12.39	3.20	0.250
Glutamine	5.62	1.02	4.87	1.21	0.300
Glycine	6.07	0.72	6.45	1.83	0.689
Homoserine	0.95	0.31	0.77	0.35	0.397
Threonine	4.59	0.56	6.04	1.55	0.086
Histidine	13.57	2.00	8.49	1.05	0.000
Citrulline	6.20	0.84	5.02	1.20	0.098
ß-Alanine	2.22	0.73	1.35	0.44	0.024
Alanine	83.98	8.77	35.36	10.05	0.000
Arginine	3.28	0.45	2.42	0.41	0.006
GABA	36.65	8.99	12.41	4.57	0.000
Tyrosine	37.35	6.09	21.65	3.20	0.000
Valine	2.77	0.35	3.99	0.92	0.021
Methionine	0.44	0.17	0.60	0.25	0.289
Tryptophan	0.58	0.19	1.63	0.57	0.003
Phenylalanine	4.76	0.70	2.48	0.64	0.000
L-Isoleucine	2.58	0.41	2.48	0.71	0.784
Leucine	6.26	1.07	6.45	1.68	0.832
Ornithine	0.49	0.26	1.07	0.73	0.140
Lysine	3.59	0.61	3.42	0.72	0.690

Figure 3.8. 16: Amino acid concentrations in nodules of wt and LbRNAi plants.

Amino acids were determined by HPLC analysis in isolated nodules at 6 wpi. Concentrations are expressed as [µmol × gFW^{-1}]. Measurements were done on 5 and 10 independent biological samples in the wild-type and LbRNAi line 3, respectively. Variance was tested by one-way ANOVA analysis and expressed as a p-value. All pairs with a p-value of ≤ 0.05 are regarded as being significantly different.

4.0. Discussion

4.1. *Lotus japonicus* cDNA arrays- an important tool for functional genomics

Global transcript profiling in plants has developed rapidly in the last few years and has become an important tool for plant functional genomics. Several technologies have been used to study the transcriptome of different plant species under a variety of different conditions. The complete sequence of species like *Arabidopsis thaliana* led to the development of full-genome arrays such as Affymetrix® chips and other oligonucleotide chips. The first legume Affymetrix® chip was recently developed for *Medicago truncatula* (Mitra et al., 2004) which contains probes for 10K genes. A similar chip for *Lotus japonicus* is currently being produced.

Resources for large scale transcript profiling in *Lotus japonicus* were improved during this PhD project. The LjNEST (9.6K) and LjKDRI (11.6K) arrays, together with an 18K cDNA array described recently (Kouchi et al., 2004), are the largest cDNA arrays currently available for *Lotus japonicus* transcriptome analysis. Optimisation of the hybridisation protocol in combination with improved tools for data mining and evaluation, which were developed in this project, facilitate more rapid transcriptome analysis than ever before in *Lotus japonicus*. This makes our resources a valuable component of *Lotus japonicus* functional genomics (Ott et al., 2005; *in press*). The two different arrays that we have produced complement each other because of the different origin of the cDNAs that were spotted on the filters. The LjNEST arrays were so far used for the identification of genes involved in nodule development and function, e.g. to study the differences between nodules induced by wild-type rhizobia and those derived from rhizobial mutants (*cgs* and *lpsβ2*), or to study gene expression in the spontaneous nodulation mutants *snf1, snf2, snf3, snf4* that form empty, nodule-like structures. In case of transcriptome profiling of the *nfr1* and *nfr5* mutants, which do not form nodules, the LjKDRI arrays (whole plant ESTs) were preferred. The same holds true for the investigation of cadmium stress on roots of *Lotus japonicus*. Several genes that were tested independently by qRT-PCR confirmed the results from the arrays indicating high robustness of the data.

To improve handling of array data, all clones on the arrays were functionally annotated using categories defined in the MIPS database. In the case of the LjNEST arrays, TC numbers for all clones were also acquired which enables the user to evaluate easily the reliability and reproducibility of the results by comparing hybridisation

signals for all clones belonging to the same TC (gene) (TIGR database for *Lotus japonicus* version 3.0). TC numbers have not been attached to LjKDRI clones, as the sequences of these clones were not released to the NCBI and subsequently implemented into the TIGR database until very recently. The same tools and database structure used for LjNEST arrays will soon be developed for the LjKDRI arrays.

Real-Time RT-PCR (qRT-PCR) was used to confirm cDNA array data indicating differential expression of interesting genes, as it was shown to be very accurate even at low expression levels of genes (Czechowski et al., 2004). qRT-PCR was performed on several genes that were found to be induced in nodules compared to uninfected roots including transcription factors, a lysophospholipase, two carbonic anhydrases, an ent-kaurene synthase A, a GA 2-oxidase, *MtN24*, *LjSst1*, *cOMT* and the symbiotic leghemoglobins (Figure 3.4.1). This confirmed differential expression of these genes that was found using the 5.6K NEST arrays (Colebatch et al., 2004). Comparable data were recently published using an 18K cDNA array that was hybridised with labelled ss-cDNAs from nodulated roots of different stages (Kouchi et al., 2004). The authors identified 1076 up-regulated and 277 down-regulated genes. Many of the genes that were found to be induced during nodulation were also identified and confirmed during our experiments.

The gene encoding the potassium transporter LjKUP was identified in the first set of arrays to be highly expressed in nodules (Colebatch et al., 2002a) but lower transcript levels were also found in other plant organs. A more detailed study of the developmental regulation of this gene showed it to be strongly induced 14 and 21 dpi (Figure 3.5.2). The induction kinetics suggests an involvement in nodule function rather than development *per se* as no significant induction of the gene was found one week after inoculation when roots contained immature nodules. *LjKup* was also induced in plants with defective nodules resulting from inoculation with the rhizobial mutant *nifA*$^-$. A similar situation was found when the *Lotus japonicus* mutants *sym11* (fix$^-$) and *har1-1* (fix$^+$) were inoculated with wild-type *M. loti* but transcript levels were not induced in *sym6*, a mutant which only makes small bumps and does not develop mature nodules (Desbrosses et al., 2004). During nodule development, root cortical and pericycle cells undergo substantial expansion (and division), which requires large amounts of K^+, not only to maintain ion homeostasis, but also to provide turgor pressure for cell growth. Massive induction of *LjKup* gene expression during nodulation, and the location of the protein in the plasma membrane indicate that LjKUP may play an important role in cell

expansion during the latter stages of nodule development. Consistent with this idea were observations that KUP homologs in plants are essential for cell and tissue expansion (Elumalai et al., 2002; Rigas et al., 2001). Continued, high expression levels of *LjKup* in mature nodules of *Lotus japonicus*, which because of their determinate nature cease to grow significantly after maturity, indicate that the protein fulfils additional and/or alternative functions during SNF. From these and other data it was concluded that KUPs may play an active role in ionic and osmotic homeostasis in cells of *Lotus japonicus* (Desbrosses et al., 2004). The amenability of *Lotus japonicus* to reverse genetics will enable us test the importance of *LjKup* in nodule development and SNF in the future.

A second nodule-induced transporter, LjSST1, was identified using cDNA arrays (Colebatch et al., 2002a, Kouchi et al., 2004). Map based cloning of the mutations of *sym13* and *sym81* revealed that both mutants were affected in this sulphate transporter gene. *LjSst1* shows a similar expression pattern to *LjKup* (Figure 3.6.2). Nodules of *sym13*/*sym81* are not able to fix nitrogen, which indicates that LjSST1 plays a crucial role in SNF. Data from proteome analysis indicate that this transporter is located on the symbiosome membrane (SM) (Wienkoop and Saalbach, 2003). This suggests that *LjSst1* may be necessary to provide sulphate to the bacteroids. If the localisation data can be confirmed, LjSST1 would be the first transporter of the SM to be found that is essential for SNF. As it is, LjSST1 is the first nodule transporter to be identified that is crucial for SNF.

4.2. Ascorbate and AOX

The function of ascorbic acid (ascorbate; vitamin c) in oxidative stress responses was first described for photosynthetic tissue but in recent years information on the role of vitamin c in non-photosynthetic organs like roots has been gathered (for review see Noctor and Foyer, 1998). The main function of ascorbate in plants is believed to be in detoxification of ROS. However, recently there has been increasing interest in its role in plant development and cell proliferation, processes that are linked to ROS-metabolism (Horemans et al., 2003).

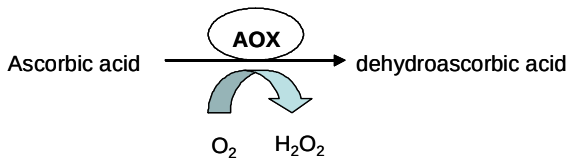

Figure 4.2. 1: The ascobate oxidase reaction.

AOXs (EC-number: 10.1.3.3) catalyse the oxidation of ascorbate to DHA and the two electrons reduction of O_2 to water (Figure 4.2.1). They belong to the family of blue multicopper oxidases that includes laccases, ceruloplasmin and some other less characterised enzymes (Santagostini et al., 2004). Recent reports indicate that the AOX protein is located almost exclusively in the apoplast (Vanacker et al., 1998) where it may play a role in the detoxification of gases like ozone that can induce oxidative stress (Sanmartin et al., 2003). This hypothesis is strengthened by the findings that *Aox* was induced during elicitor treatment and wounding stress, whereas no induction of the gene was found when methyl-jasmonate was applied to the plants (Garcia-Pineda et al., 2004). In addition, induced *Aox* expression upon rhizobial infection was leading it to its designation as nodulin23 (*MtN23*) (Gamas et al., 1996). An early study on crude extracts of soybean nodules reported an ascorbate and oxygen consuming enzyme that was hypothesised to be an ascorbate oxidase (Udvardi et al., 1986). However, detailed studies on AOXs in nodules are yet to be reported.

In non-leguminous plants high expression of *Aox* genes has been reported in roots, stems and flower buds as well as in fruits of melon, pumpkin, cucumber and orange (summarised in Garcia-Pineda et al., 2004). Horemans and co-workers showed in tobacco BY2 cells that ascorbate concentrations are elevated during cell division, while concentrations of DHA decline (Horemans et al., 2003). On the other hand reduced ascorbate levels in the quiescent center of maize roots were correlated with the absence of cell division in an extended G1 phase (Kerk et al., 2000). These data are consistent with a role of ascorbate in the cell cycle. Interestingly addition of ascorbate to roots of *Allium cepa* and *Pisum sativum* accelerated cell proliferation (De Pinto et al., 1999; Cordoba-Pedregosa Mdel et al., 2003; Potters et al., 2000; Del Carmen Cordoba-Pedregosa et al., 2003; De Tullio et al., 1999). So, ascorbate and DHA seem to be involved in cell expansion and cell division.

Cross-linking of the cell wall components is required during development and can be achieved using hydrogen peroxide, a product of the AOX reaction (Figure 4.2.1). This is supported by the finding that ascorbate can serve as a co-factor of cytosolic prolyl-hydroxylase. This enzyme is involved in the biosynthesis of hydroxyproline-rich proteins that have key functions for cell wall structure (De Tullio et al., 1999).

Using the 11.6K LjNEST arrays, an ascorbate oxidase *LjAox1* (LjNEST98c11) was found to be more highly expressed in infected roots 4 wpi compared to 1 wpi. EST analysis suggests the existence of six *Aox* genes in *Lotus japonicus* with two of them

predominantly expressed in nodules (TC11125 and TC12917). Phylogenetic analysis of the sequences showed that these two proteins are more similar to AOX proteins from leguminous plants than non-legumes (Figure 3.7.1). This together with their nodule-induced expression pattern suggests that these *Aox* genes may serve specialised functions during SNF.

It was shown above that *LjAox1* transcript levels are highest in nodules (Figure 3.7.4) and increased constantly over time during nodule development (Figure 3.7.3), but eventually declined as nodules aged (Figure 3.7.5). Similar data were obtained from *in silico* analysis using the *Medicago truncatula* database (http://medicago.toulouse.inra.fr/Mt/EST/ DOC/MtB.html). Clone MtC20102_GC was identified to be the closest homologue of LjNEST98c11, showing 71% identity on nucleotide level. MtC20102_GC was found to be mainly expressed in nodules with the highest value in young nodules (0.41‰ of the total library). This confirms the classification of this gene as an early nodulin (Gamas et al., 1996). Taken together, these results imply that the gene may be involved in nodule development rather than in nodule function *per se*.

In order to address possible functions of *LjAox1* in nodules, spatial expression of the gene was investigated using promoter-gus fusion. Locally defined gus-activity around the endodermis of the nodule was found and implies a specialised function of the gene product in this tissue (Figure 3.7.8) which is believed to contribute to the oxygen diffusion barrier (ODB) in nodules. Using the membrane permeable dye lucifer-yellow it was shown earlier that the endodermis itself might not function as an ODB alone (Brown and Walsh, 1996). Recent findings suggest the apoplastic space, especially when it is filled with water, to maintain oxygen diffusion resistance (Streeter and Salminen, 1993, Witty and Minchin, 1994). Interestingly, AOX enzyme activity was reported to be mainly apoplastic (Vanacker et al., 1998). An active involvement of *LjAox1* in limiting O_2 diffusion at the site of the ODB is very unlikely as this barrier is rather physical than biochemical. Biochemical impact could be supported by AOX activity that leads to the formation of H_2O_2 (Figure 4.2.1) which is known to play a role in cell wall cross-linking. Such cross-linking could enhance physical strength of the endodermal cell layer while it is also needed for normal development.

Its possible apoplastic localisation makes the enzyme also an interesting candidate to be involved in controlling cell cycle by regulating the availability and the redox status of cellular and apoplastic ascorbate pool as shown in tobacco (Horemans et

al., 2000). This is also supported by high expression of *LjAox1* in young, developing nodules (Figure 3.7.5) and its spatial expression around the nodule endodermis (Figure 3.7.8). It is likely that induction of *LjAox1* expression during the time-course experiments (Figure 3.7.3) was observed as, in case of legumes developing determinate nodules, new nodules are continuously formed on the root system. But, when nodule development was impaired using the rhizobial mutant *cgs*, *LjAox1* expression was significantly lower in those nodules compared to nodules that were induced by the corresponding wild-type rhizobial strain (Figure 3.7.6). A correlation of *Aox* expression with plant growth was recently demonstrated in tobacco (Pignocchi et al., 2003). Tobacco plants over-expressing an endogenous *Aox* by 40-times showed enhanced growth and stem elongation compared to the wild-type and a 3.5-fold increase of apoplastic DHA. Furthermore, the authors showed by using different plant hormones, which either enhanced or stopped growth, that expression of this gene correlates with these effects (Pignocchi et al., 2003). To which extent these findings can be applied to nodule development remains to be shown.

Different motifs were identified in the putative promoter region of *LjAox1*. Among them were sequences that were described to be involved in stress (MYB1AT (*Arabidopsis thaliana*), CCAATBOX1 from *Glycine max*) and hormone responses (CATATGGMSAUR (*Arabidopsis thaliana*) and DPBFCOREDCDC3 from *Glycine max*), in tissue specific expression (AACACOREOSGLUB1 from *Oryza sativa* and the CAATBOX1 from *Pisum sativum*) as well as a putative binding domain for Dof-transcription factors (DOFCOREZM) which was identified in *Zea mays*. All these motifs were predicted by the PLACE-software, but so far no experimental approach was taken to investigate roles of these putative motifs *in planta*. It was suggested previously that *Aox* expression and activity in maize may be controlled by the plant hormone auxin (Kerk and Feldman, 1995). Auxin was also described to be important in nodule development (de Billy et al., 2001; Pacios-Bras et al., 2003) so that it may be possible that the putative motifs CATATGGMSAUR and DPBFCOREDCDC3 are involved in hormonal regulation of *LjAox1* in nodules (Figure 3.7.9). The DOFCOREZM-motif could also be a likely candidate for further experimental investigation, as Dof-transcription factors have been recently described to regulate *Aox* expression in pumpkin (Umemura et al., 2004). Two putative Dof-like transcription factors were found in the LjNEST cDNA library (LjNEST13a12 and LjNEST89d2). Interestingly LjNEST13a12 was found to be 2.4-fold ($p = 0.03$) induced in the same experiment in

which the *LjAox1* induction was observed. Further experiments have to reveal a possible functional correlation between these genes.

4.3. Symbiotic leghemoglobins are indispensable for SNF

Large-scale EST sequencing projects and clustering of EST sequences into TCs has provided insights into some of the major players that are involved in SNF in *Lotus japonicus*. This is especially the case for highly transcribed nodulin genes like symbiotic leghemoglobin genes which direct the synthesis of millimolar concentrations of leghemoglobin proteins in root nodules. Leghemoglobins are the most abundant nodulins in legume nodules.

4.3.1. Expression of leghemoglobins

Leghemoglobins are encoded by multi-gene families (Figures 3.8.2 and 3.8.3), and each gene being highly expressed in nodules of *Lotus japonicus* (Figures 3.8.4 and 3.8.5). Expression analysis revealed three symbiotic leghemoglobin (Lb) genes to be predominantly expressed in *Lotus japonicus* (*LjLb1*, *LjLb2* and *LjLb3*) (Figure 3.8.1) (Uchiumi et al., 2002). Symbiotic as well as the two non-symbiotic (*LjNsg1* and *LjNsg2*) hemoglobins were mainly expressed in nodules and induction of these genes (except *LjNsg1*) were observed already 24 hours after inoculation of the roots with *M. loti* (Figure 3.8.5). Expression pattern and accumulation of the protein were shown to be similar to earlier findings (Sato et al., 2001).

4.3.2 Successful PTGS of symbiotic leghemoglobins

A reverse genetic approach was chosen in *Lotus japonicus* nodules to induce post-transcriptional gene silencing (PTGS) of all three leghemoglobin genes. Sequence identity was high between the three symbiotic leghemoglobin genes, with 6 stretches of at least 20 bp with 100% identity, providing the potential to induce PTGS to all three symbiotic hemoglobins using RNAi technology (Figure 3.8.2) (Waterhouse et al., 2001a; Waterhouse et al., 2001b). A 401 bp long PCR fragment derived from *LjLb2* was sufficient to silence transcripts of all three leghemoglobins leading to the lack of leghemoglobin protein in nodules of the transgenic lines (Figures 3.8.8). In contrast, transcript levels of the non-symbiotic hemoglobin genes *LjNsg1* and *LjNsg2* were only slightly reduced in these plants (Figure 3.8.8). Thus, RNAi proved to be a powerful technology to silence simultaneously several members of a gene family with high

transcript levels. Until now the use of RNAi in legumes was restricted to PTGS of lowly transcribed genes (Limpens et al., 2003) or of exogenous transgenes like GFP and GUS (Kumagai and Kouchi, 2003; Limpens et al., 2004). Expression of our LbRNAi construct in hairy roots of *Lotus japonicus* silenced Lb genes in transformed roots but not adjacent non-transformed roots (Figure 3.6.2) indicating that PTGS does not spread systemically within the root system, as found previoulsy (Limpens et al., 2004). Spreading of PTGS to the shoot as reported before (Kumagai and Kouchi, 2003) could not be tested because the Lb genes are not expressed in the shoot.

4.3.3. The LbRNAi phenotype

Silencing of leghemoglobin genes in *Lotus japonicus* nodules enabled us to show for the first time that leghemoglobins are indispensable for SNF in *Lotus japonicus* (Figure 3.8.10).

Transgenic plants lacking symbiotic leghemoglobin proteins showed the typical above-ground symptoms of nitrogen starvation, including anthocyanin accumulation in the stem, chlorotic leaves, reduced shoot growth (reviewed in Fernandes and Rossiello, 1995; Banba et al., 2001) and consequently an increase in root/shoot ratio (Figure 3.8.9). As no phenotypical difference was found when growing LbRNAi plants and wild-type on full N-nutrition (Figure 3.8.10), it can be concluded that the observed phenotype is exclusively derived from the lack of reduced nitrogen-compounds in the plants. Therefore, symbiotic hemoglobins are not essential for non-symbiotic plant growth and development.

Nodules of LbRNAi plants were white and arrested in growth around 14 dpi (Figure 3.8.10 and 3.8.11), a phenotype also observed in other *fix*$^-$ nodules (Banba et al., 2001). In general, legumes react to non-functional nodules by investing no further nutritional resources to those nodules and by induction of new nodules in an attempt to overcome nitrogen deficiency. This was also the case in LbRNAi plants: the increase in nodule number between 14-21 dpi (Figure 3.8.9) correlated with the arrest of nodule growth at the same time (Figure 3.8.11). Although transgenic nodules were smaller than wild-type nodules, there were no major morphological differences between the two types of nodules (Figure 3.8.10). However, the bacterial population within the LbRNAi nodules was reduced by 30% compared to wild-type nodules (Figure 3.8.13). Thus, although rhizobial infection and nodule colonisation appeared to proceed normally in

LbRNAi nodules, restricted resource allocation to non-functional LbRNAi nodules may have limited rhizobial proliferation.

4.3.4. Molecular physiology of symbiotic leghemoglobins

Given the proposed roles of leghemoglobins in oxygen transport and buffering in nodules, based on their biochemical characteristics (Wittenberg et al., 1972; Bergersen and Goodchil, 1973; Wittenberg et al., 1974; Bergersen, 1996) it was important to compare free oxygen concentrations in transgenic and wild-type nodules, as these roles have not been confirmed *in planta* until now. Using an oxygen microsensor it was demonstrated that free oxygen concentrations in the transgenic nodules were elevated compared to the wild-type (Figure 3.8.14). The lack of leghemoglobin in LbRNAi nodules resulted in a shallower oxygen gradient from the epidermis to the center of the nodule, where concentrations reached a minimum compared to wild-type nodules. Unlike wt nodules, which contained a large central region of very low oxygen where SNF occurs, LbRNAi nodules exhibited a much restricted zone of very low free oxygen concentrations (Figure 3.8.14). Gradients in O_2-concentration were shown previously in other tissues of different plant species like in rape and wheat seeds, where almost hypoxic conditions were found (Porterfield et al., 1999; van Dongen et al., 2004). But, here it was demonstrated for the first time *in planta* that free oxygen concentrations are altered when abolishing leghemoglobin protein synthesis.

The findings are in partial agreement with a model that addressed changes in free oxygen concentrations upon nitrate treatment of nodules (Denison and Harter, 1995). The authors calculated that reducing Lb concentrations to 5% of the controls would lead to increased O_2 concentration in intercellular airspaces more than 100×. The model also predicted big increases in the steepness of O_2 gradients within infected cells in the presence of leghemoglobins. Those gradients were also shown by imaging fractional oxygenation of leghemoglobin in yellow sweetclover nodules (Denison and Okano, 2003). However, Denison and Harter assumed uniform O_2 concentrations throughout the intercellular airspaces (in order to save computing time), so the model is silent with respect to the gradients that were observed in wt and LbRNAi nodules in the experiments presented here.

It was also demonstrated that the nitrogenase protein was absent in transgenic nodules (Figure 3.8.8). It is likely that elevated O_2-concentrations found in LbRNAi

nodules, led to inactivation and loss of the oxygen sensitive nitrogenase protein. A strong correlation of leghemoglobin content and nitrogenase activity in nodules was suggested previously (Dakora, 1995).

Facilitation of oxygen delivery to respiring bacteroids is thought to be one of the main functions of leghemoglobin. To test this, the energy status of nodules was determined by measuring concentrations of ATP and ADP. It was shown, that total adenylate levels were similar in transgenic and wild-type nodules while the ATP/ADP ratio was significantly lower in LbRNAi nodules due to higher concentrations of ADP and lower concentrations of ATP (Figure 3.8.15). AMP, which usually makes up only a small proportion of the total adenylate pool, could not be measured in these experiments. These results suggest that respiration was reduced in LbRNAi nodules, although this remains to be confirmed by more direct measurements. The results are consistent with a role for Lb in oxygen delivery to the principal site of respiration, namely the bacteroids. Reduction in the rate of O_2 consumption as a result of loss of leghemoglobins in LbRNAi nodules could account for the increased steady-state O_2 levels measured through these nodules. Thus, leghemoglobins appear to be important not only to enhance oxygen delivery to the sites of respiration, but also to maintain the low oxygen concentrations required for SNF. High flux rates mediated by leghemoglobin in combination with low concentrations of free oxygen are therefore one of the major differences to other plant organs, where low free oxygen leads to inhibition of respiration and a higher ATP/ADP ratio (Geigenberger, 2003).

Using light microscopy it was shown, that the morphology of LbRNAi nodules was largely unchanged. However, starch accumulation was found in uninfected cells of those nodules (Figure 3.8.12). Such accumulation was also observed in other legume mutants like *crinkle* (Tansengco et al., 2003), and *alb1* and *fen1* (Imaizumi-Anraku et al., 1997) in *Lotus japonicus*, and in ineffective mutants of alfalfa (Vance and Johnson, 1983), soybean (Forrest et al., 1991), and pea (Novak et al., 1995). The accumulation of starch in amyloplasts in mutants ineffective in SNF indicates that plant-derived photosynthates, which serve as an energy source for nitrogen fixation, cannot be fully consumed in those nodules (Postma et al., 1990). This is probably due to a lower demand for carbon by the resident rhizobia as it was previously shown that starch also accumulated to higher amounts in soybean nodules hosting the rhizobial mutant LSG184 which lacks alpha-ketoglutarate dehydrogenase and exhibits delayed nitrogen fixation activity (Green and Emerich, 1997). Another possibility is that the TCA cycle,

needed to provide electrons to nitrogenase, is slowed down and resulting in feedback inhibition due to lack of bacterial nitrogenase protein. Consequently sucrose cannot be further metabolised to malate but is deposited as starch in the uninfected cells.
In general starch accumulation is known to occur in non-leguminous plants, when oxygen tension increases and storage metabolism to be inhibited under low oxygen conditions (reviewed in Geigenberger, 2003). This may provide an additional or alternative explanation for the observed increase in starch accumulation in LbRNAi nodules.

4.3.5. Changes amino acid concentrations due to the lack of functional SNF

From the findings discussed above it can be assumed, that central nitrogen metabolism is severely affected in plants lacking leghemoglobins in nodules. Elevated levels of the amino acid asparagine in nodules containing the rhizobial mutant *CFN037* (containing a Tn5mob insertion in the promoter region of the thiCOGE gene cluster involved thiamine biosynthesis) compared to nodules with the resident wild-type strain, were demonstrated previously (Silvente et al., 2003). Infection of *Phaseolus vulgaris* with this strain led to the formation of more effective nodules compared to those obtained after infection with the wild-type strain. This is indirectly in agreement with the changes in amino acids levels presented here (Figure 3.8.16) if assumed that levels of these amino acids are correlated with the effectiveness of the nodules. Our findings of lower concentrations of some major amino acids are also supported by studies on enzymes like NADH-glutamate synthase (GOGAT) which is highly in roots and nodules (Cordovilla et al., 2000). Silencing GOGAT in alfalfa nodules impaired carbon and nitrogen metabolism in the nodules and resulted in a nutritional starvation phenotype with similar symptoms like chlorotic leaves and reduced shoot growth as it was reported for the Lb-RNAi plants here (Cordoba et al., 2003). Therefore, decreased concentrations of amino acids like glutamate and asparagine suggest the absence of SNF in LbRNAi nodules.

5.0. Summary

During this PhD project three technical platforms were either improved or newly established in order to identify interesting genes involved in SNF, validate their expression and functionally characterise them. An existing 5.6K cDNA array (Colebatch et al., 2004) was extended to produce the 9.6K LjNEST array, while a second array, the 11.6K LjKDRI array, was also produced. Furthermore, the protocol for array hybridisation was substantially improved (Ott et al., 2005, *in press*). After functional classification of all clones according to the MIPS database and annotation of their corresponding tentative consensus sequence (TIGR) these cDNA arrays were used by several international collaborators and by our group (Krusell et al., 2005; *in press*). To confirm results obtained from the cDNA array analysis different sets of cDNA pools were generated that facilitate rapid qRT-PCR analysis of candidate gene expression. As stable transformation of *Lotus japonicus* takes several months, an *Agrobacterium rhizogenes* transformation system was established in the lab and growth conditions for screening transformants for symbiotic phenotypes were improved. These platforms enable us to identify genes, validate their expression and functionally characterise them in the minimum of time.

The resources that I helped to establish, were used in collaboration with other people to characterise several genes like the potassium transporter *LjKup* and the sulphate transporter *LjSst1*, that were transcriptionally induced in nodules compared to uninfected roots, in more detail (Desbrosses et al., 2004; Krusell et al., *submitted*). Another gene that was studied in detail was *LjAox1*. This gene was identified during cDNA array experiments and detailed expression analysis revealed a strong and early induction of the gene during nodulation with high expression in young nodules which declines with the age of the nodule. Therefore, *LjAox1* is an early nodulin. Promoter:gus fusions revealed an *LjAox1* expression around the nodule endodermis. The physiological role of *LjAox1* is currently being persued *via* RNAi.

Using RNA interference, the synthesis of all symbiotic leghemoglobins was silenced simultaneously in *Lotus japonicus*. As a result, growth of LbRNAi lines was severely inhibited compared to wild-type plants when plants were grown under symbiotic conditions in the absence of mineral nitrogen. The nodules of these plants were arrested in growth 14 post inoculation and lacked the characteristic pinkish colour. Growing these transgenic plants in conditions where reduced nitrogen is available for the plant led to normal plant growth and development. This demonstrates that

leghemoglobins are not required for plant development *per se*, and proves for the first time that leghemoglobins are indispensable for symbiotic nitrogen fixation. Absence of leghemoglobins in LbRNAi nodules led to significant increases in free-oxygen concentrations throughout the nodules, a decrease in energy status as reflected by the ATP/ADP ratio, and an absence of the bacterial nitrogenase protein. The bacterial population within nodules of LbRNAi plants was slightly reduced. Alterations of plant nitrogen and carbon metabolism in LbRNAi nodules was reflected in changes in amino acid composition and starch deposition (Ott et al., 2005, *accepted in Current Biology*). These data provide strong evidence that nodule leghemoglobins function as oxygen transporters that facilitate high flux rates of oxygen to the sites of respiration at low free oxygen concentrations within the infected cells.

6.0. Outlook

As described above, the cDNA arrays produced here represent a valuable source for *Lotus japonicus* functional genomics. To guarantee easy handling of array data, data mining tools should be further improved. This includes a regular update of the closest homologue sequences identified by using the BLAST algorithm and implementing new TC annotations from TIGR into the database. This latter step still remains to be made for the LjKDRI arrays.

Despite the interesting developmental and spatial expression pattern of *LjAox1* the physiological function of the protein remains still unclear. RNAi technology should help to clarify its role in the future.

To determine whether LjAOX1 is present in the apoplast, as it has been suggested for other plant ascorbate oxidases, a full-length cDNA of *LjAox1* will be fused to either an HA-tag or to the green fluorescent protein (GFP) and expressed in transformed hairy roots prior to immuno- or fluorescence localisation. Data on the localisation of the AOX protein in nodules will help us to interpret any phenotypical changes resulting from LjAOX1-RNAi experiments.

Further work will be done on LbRNAi plants to explore the role of leghemoglobins in plant and bacteroid differentiation during nodule development. The LjNEST arrays will be used to identify differences in the transcript profiles between LbRNAi and wild-type nodules at different developmental stages. A focus will be on the time around 14 dpi when nodule development seems to be arrested, as well as after 21 days or 28 days when nitrogen is actively fixed in the wild-type but not in the transgenic plants. The same material will be used for metabolic profiling using GC-MS. These approaches should yield deeper insight into global changes in metabolism and other cellular processes that depend on the presence of leghemoglobins. To determine the role of leghemoglobins in bacteroid differentiation, a variety of *Mesorhizobium loti* reporter lines will be used which contain promoters of marker genes (*FixA*, *FixG*, *FixN*, *FixV*, *NifA2*, *NifH*) coupled to the *lacZ* reporter gene. Expression, or lack of expression of the reporter gene during nodule development will provide *in situ* information on the differentiation state of bacteroids (in collaboration with Clive Ronson, New Zealand). To supplement this work, electron microscopy will be used to determine the bacteroid structure in LbRNAi nodules (in collaboration with Euan James, UK)

7.0. Acknowledgements

Like any other PhD student, I experienced all the “ups” and “downs” of science and tried to find a proper balance of excitement and frustration. Beside the possibility to do research with hardly any technical limitations, this institute of molecular plant physiology opens the unique opportunity of various collaborations with other people which is one part of research that has made me so excited during the last three years. There are numerous people that helped me with all the methods, gave advice and a few who were always there when facing one of the “downs” of science. Many thanks to Michael Udvardi for supervising the thesis and giving me the opportunity to work on projects that really excited me. There were hard and controversial discussions about many things but, I guess, this is part of the business and so far, we were always able to find ways through these phases and that is most important. Beside the scientific content of the projects I would like to thank Michael for the various possibilities of all the international collaborations. That experience alone was worth the three years. As every PhD student I went through the whole process of learning, which is so much easier when experienced Post-docs are available in the lab. Special thanks to Guilhem Desbrosses who taught me many lessons especially in the beginning and later Lene Krusell. And Lene, thanks for so much more later on! If I would have the chance to work with you again, I would not hesitate a minute to do it. But beside these three people of the group all the others contributed in one way or the other to this work. Special thanks goes to Tomasz Czechowski for the advice with qRT-PCR, to Maren Wandrey for the bioinformatics, to Vivien Bock, Susanne Freund, Katrin Piepenburg and Diana Sahid for technical assistance and to Armin and Zuza for proofreading. It was a pleasure to work together will all of the members of the AG Udvardi. When the leghemoglobin project went into its “hot” phase, Cathrin Günther joined as student helper but in fact, the enthusiasm she put into the project practically and the phone-calls in the late evening when she had an idea, were much more than one could ever expect from a student helper. That definitively makes her an important author on the paper. Many more people were involved in my project and I would especially thank Joost van Dongen, Helene Vigeolas, Natalia Palacios, Regina Feil, Yves Gibon, Peter Krüger and Joachim Selbig for their various contributions including methods, discussion, and the one or other goal on the kicker. Also many thanks to the people running infrastructure in the institute like the IT service and the gardeners. They made my life much easier. Norio Suganuma (University of Aichi, Japan) and Ton Bisseling (University of

Wageningen, The Netherlands) provided the antibodies. As Ton said on a conference after presenting the LbRNAi results: “Seems that the stuff worked pretty good!” I agree. Satoshi Tabata and Shusei Sato (both Kazusa DNA Research Iinstitute, Japan) provided the TAC clones and are the endless source for genomic information of *Lotus japonicus*. That was of much help and accelerated some experiments very much. My three evaluators, maybe I should them call them “terminators” when looking back into the past, Mark Stitt, Joachim Kopka and Arnd Heyer deserve special thanks as well. Thanks for keeping me out of more trouble! Scientifically last but by far from least I would like to thank Alejandra D’Antuono and Viviana Lepek (INTECH-UNSAM Buenos Aires, Argentina) for the collaboration on the bacterial mutants and cDNA arrays. Beside interesting data, I definitively don’t want to miss the experience of yerba mate, dulce de leche, havanetas and all the nice people in the lab during my visit of the lab in Buenos Aires in the Argentinian summer of 2004.

Mathias Wegner, I would say, the man who reserved the word “extreme” for himself (from the jacket via the stickleback and science), always reminded me during our numerous discussions and activities of the “proper work-life-balance”. You are completely right and thanks for that. There are four more people who deserve special thanks with respect to the “life” part of the balance. Thanks Johanna, Anja, Olaf and Zuza! I don’t want to miss any moment with them during the last three years and one even longer. Beside all the nice people inside and outside work (not to forget my flat mates), it was mainly them who gave me the energy to go happily through all that.

I think here has to be some space left for a great thanks to my parents and Henning, who, in the end, made all this possible. I will now finally be number four out of four, soon …

And one last comment after the intensive phase of writing up the thesis: Michael, you see, I have written a novel again. But I think, it’s o.k. for this part of the thesis… ☺.

8.0 Literature

Aharoni, A. and Vorst, O. (2001) DNA microarrays for functional plant genomics. *Plant Mol Biol*, **48**, 99-118.

Albrecht, C., Geurts, R. and Bisseling, T. (1999) Legume nodulation and mycorrhizae formation; two extremes in host specificity meet. *Embo J*, **18**, 281-288.

Appleby, C.A. (1984) Leghemoglobin and Rhizobium Respiration. *Annual Review of Plant Physiology and Plant Molecular Biology*, **35**, 443-478.

Ardourel, M., Demont, N., Debelle, F., Maillet, F., de Billy, F., Prome, J.C., Denarie, J. and Truchet, G. (1994) Rhizobium meliloti Lipooligosaccharide Nodulation Factors: Different Structural Requirements for Bacterial Entry into Target Root Hair Cells and Induction of Plant Symbiotic Developmental Responses. *The Plant Cell*, **6**, 1357-1374.

ArsenijevicMaksimovic, I., Broughton, W.J. and Krause, A. (1997) Rhizobia modulate root-hair-specific expression of extensin genes. *Molecular Plant-Microbe Interactions*, **10**, 95-101.

Arwas, R., McKay, I.A., Rowney, F.R.P., Dilworth, M.J. and Glenn, A.R. (1985) Properties of organic-acid utilization mutants of rhiz-obium-leguminosarum strain-300. *J Gen Microbiol*, **131**, 2059-2066.

Banba, M., Siddique, A.B., Kouchi, H., Izui, K. and Hata, S. (2001) Lotus japonicus forms early senescent root nodules with Rhizobium etli. *Mol Plant Microbe Interact*, **14**, 173-180.

Barker, D.G., Bianchi, S., Blondon, F., Dattee, Y., Duc, G., Essad, S., Flament, P., Gallusci, P., Genier, G., Guy, P., Muel, X., Tourneur, J., Denarie, J. and Huguet, T. (1990) Medicago truncatula, a model plant for studying the molecular genetics of the Rhizobium-legume symbiosis. *Plant Mol Biol*, **Rep 8**, 40-49.

Bauer, P., Poirier, S., Ratet, P. and Kondorosi, A. (1997) MsEnod12A expression is linked to meristematic activity during development of indeterminate and determinate nodules and roots. *Molecular Plant-Microbe Interactions*, **10**, 39-49.

Bauer, P., Ratet, P., Crespi, M.D., Schultze, M. and Kondorosi, A. (1996) Nod factors and cytokinins induce similar cortical cell division, amyloplast deposition and MsEnod12A expression patterns in alfalfa roots. *Plant Journal*, **10**, 91-105.

Baulcombe, D. (2004) RNA silencing in plants. *Nature*, **431**, 356-363.

Baulcombe, D.C. (2000) Molecular biology. Unwinding RNA silencing. *Science*, **290**, 1108-1109.

Becana, M., Dalton, D.A., Moran, J.F., Iturbe-Ormaetxe, I., Matamoros, M.A. and Rubio, M.C. (2000) Reactive oxygen species and antioxidants in legume nodules. *Physiol Plantarum*, **109**, 372-381.

Benaben, V., Duc, G., Lefebvre, V. and Huguet, T. (1995) Te7, an Inefficient Symbiotic Mutant of Medicago-Truncatula Gaertn Cv Jemalong. *Plant Physiology*, **107**, 53-62.

Bergersen, F.J. (1996) Delivery of O2 to bacteroids. *Protoplasma*, **191**, 9-20.

Bergersen, F.J. and Goodchil, D.J. (1973) Aeration Pathways in Soybean Root Nodules. *Australian Journal of Biological Sciences*, **26**, 729-740.

Bergersen, F.J. and Turner, G.L. (1967) Nitrogen Fixation by Bacteroid Fraction of Breis of Soybean Root Nodules. *Biochimica Et Biophysica Acta*, **141**, 507-&.

Bergersen, F.J. and Turner, G.L. (1993) Effects of concentration of substrates supplied to N2-fixing soybean bacteroids in flow chamber experiments. *Proc R Soc Lond B*, **251**, 95-102.

Bogusz, D., Appleby, C.A., Landsmann, J., Dennis, E.S., Trinick, M.J. and Peacock, W.J. (1988) Functioning Hemoglobin Genes in Non-Nodulating Plants. *Nature*, **331**, 178-180.

Boisson-Dernier, A., Chabaud, M., Garcia, F., Becard, G., Rosenberg, C. and Barker, D.G. (2001) Agrobacterium rhizogenes-transformed roots of Medicago truncatula for the study of nitrogen-fixing and endomycorrhizal symbiotic associations. *Mol Plant Microbe Interact*, **14**, 695-700.

Bolton, E., Higgisson, B., Harrington, A. and O'Gara, F. (1986) Dicarboxylic acid transport in Rhizobium meliloti: isolation of mutants and cloning of dicarboxylic acid transport genes. *Arch. Microbiol*, **144**, 142-146.

Borisov, A.Y., Madsen, L.H., Tsyganov, V.E., Umehara, Y., Voroshilova, V.A., Batagov, A.O., Sandal, N., Mortensen, A., Schauser, L., Ellis, N., Tikhonovich, I.A. and Stougaard, J. (2003) The sym35 gene required for root nodule development in pea is an ortholog of nin from Lotus japonicus. *Plant Physiology*, **131**, 1009-1017.

Brewin, N.J. (1991) Development of the Legume Root Nodule. *Annual Review of Cell Biology*, **7**, 191-226.

Broughton, W.J. and Dilworth, M.J. (1971) Control of leghaemoglobin synthesis in snake beans. *Biochem J*, **125**, 1075-1080.

Brown, S.M., Chudek, J.A., Hunter, G., Sprent, J.I., Walsh, K.B. and Wurtz, G. (1997) Proton density and apoplastic domains within soybean nodules in relation to the oxygen diffusion barrier. *Plant Cell and Environment*, **20**, 1019-1029.

Brown, S.M. and Walsh, K.B. (1996) Anatomy of the legume nodule cortex: Species survey of suberisation and intercellular glycoprotein. *Australian Journal of Plant Physiology*, **23**, 211-225.

Brundrett, M.C. (2002) Coevolution of roots and mycorrhizas of land plants. *New Phytol*, **154**, 275-304.

Buikema, W.J., Szeto, W.W., Lemley, P.V., Orme-Johnson, W.H. and Ausubel, F.M. (1985) Nitrogen fixation specific regulatory genes of Klebsiella pneumoniae and Rhizobium meliloti share homology with the general nitrogen regulatory gene ntrC of K. pneumoniae. *Nucleic Acids Res*, **13**, 4539-4555.

Campalans, A., Kondorosi, A. and Crespi, M. (2004) Enod40, a short open reading frame-containing mRNA, induces cytoplasmic localization of a nuclear RNA binding protein in Medicago truncatula. *Plant Cell*, **16**, 1047-1059.

Cangelosi, G.A., Best, E.A., Martinetti, G. and Nester, E.W. (1991) Genetic analysis of Agrobacterium. *Methods Enzymol*, **204**, 384-397.

Catoira, R., Galera, C., de Billy, F., Penmetsa, R.V., Journet, E.P., Maillet, F., Rosenberg, C., Cook, D., Gough, C. and Denarie, J. (2000) Four genes of Medicago truncatula controlling components of a nod factor transduction pathway. *Plant Cell*, **12**, 1647-1665.

Colebatch, G., Desbrosses, G., Ott, T., Krusell, L., Montanari, O., Kloska, S., Kopka, J. and Udvardi, M.K. (2004) Global changes in transcription orchestrate metabolic differentiation during symbiotic nitrogen fixation in Lotus japonicus. *Plant Journal*, **39**, 487-512.

Colebatch, G., Kloska, S., Trevaskis, B., Freund, S., Altmann, T. and Udvardi, M.K. (2002a) Novel aspects of symbiotic nitrogen fixation uncovered by transcript profiling with cDNA arrays. *Mol Plant Microbe Interact*, **15**, 411-420.

Colebatch, G., Trevaskis, B. and Udvardi, M.K. (2002b) Functional genomics: tools of the trade. *New Phytol*, **153**, 27-36.

Cook, D., Dreyer, D., Bonnet, D., Howell, M., Nony, E. and Vandenbosch, K. (1995) Transient Induction of a Peroxidase Gene in Medicago-Truncatula Precedes Infection by Rhizobium-Meliloti. *Plant Cell*, **7**, 43-55.

Cook, D.R. (1999) Medicago truncatula--a model in the making! *Curr Opin Plant Biol*, **2**, 301-304.

Copeland, L., Lee, H.S. and Cowlishaw, N. (1995) Carbon metabolism in chickpea nodules. *Soil Biol. Biochem.*, **27**, 318-385.

Copeland, L., Vella, J. and Hong, Z. (1989) En-zymes of carbohydrate metabolism in soy-bean nodules. *Phytochemistry*, **28**, 57-61.

Cordoba, E., Shishkova, S., Vance, C.P. and Hernandez, G. (2003) Antisense inhibition of NADH glutamate synthase impairs carbon/nitrogen assimilation in nodules of alfalfa (Medicago sativa L.). *Plant J*, **33**, 1037-1049.

Cordoba-Pedregosa Mdel, C., Cordoba, F., Villalba, J.M. and Gonzalez-Reyes, J.A. (2003) Differential distribution of ascorbic acid, peroxidase activity, and hydrogen peroxide along the root axis in Allium cepa L. and its possible relationship with cell growth and differentiation. *Protoplasma*, **221**, 57-65.

Cordovilla, M.D., Perez, J., Ligero, F., Lluch, C. and Valpuesta, V. (2000) Partial purification and characterization of NADH-glutamate synthase from faba bean (Vicia faba) root nodules. *Plant Science*, **150**, 121-128.

Crespi, M.D., Jurkevitch, E., Poiret, M., Daubentoncarafa, Y., Petrovics, G., Kondorosi, E. and Kondorosi, A. (1994) Enod40, a Gene Expressed During Nodule Organogenesis, Codes for a Nontranslatable Rna Involved in Plant-Growth. *Embo Journal*, **13**, 5099-5112.

Crockard, A., Bjourson, J., Dazzo, B. and Cooper, J.E. (2002) A white clover nodulin gene, dd23b, encoding a cysteine cluster protein, is expressed in roots during the very early stages of interaction with Rhizobium leguminosarumbiovar trifolii and after treatment with chitolipooligosaccharide Nod factors. *J Plant Res*, **115**, 439-447.

Cullimore, J.V. and Bennett, M.J. (1988) The Molecular-Biology and Biochemistry of Plant Glutamine-Synthetase from Root-Nodules of Phaseolus-Vulgaris L and Other Legumes. *Journal of Plant Physiology*, **132**, 387-393.

Cullimore, J.V. and Miflin, B.J. (1984) Immunological Studies on Glutamine-Synthetase Using Antisera Raised to the 2 Plant-Forms of the Enzyme from Phaseolus Root-Nodules. *Journal of Experimental Botany*, **35**, 581-587.

Czechowski, T., Bari, R.P., Stitt, M., Scheible, W.R. and Udvardi, M.K. (2004) Real-time RT-PCR profiling of over 1400 Arabidopsis transcription factors: unprecedented sensitivity reveals novel root- and shoot-specific genes. *Plant J*, **38**, 366-379.

Dakora, F.D. (1995) A functional relationship between leghemoglobin and nitrogenase based on novel measurements of the two proteins in legume root nodules. *Annals of Botany*, **75**, 49-54.

Day, R.B., McAlvin, C.B., Loh, J.T., Denny, R.L., Wood, T.C., Young, N.D. and Stacey, G. (2000) Differential expression of two soybean apyrases, one of which is an early nodulin. *Molecular Plant-Microbe Interactions*, **13**, 1053-1070.

de Billy, F., Grosjean, C., May, S., Bennett, M. and Cullimore, J.V. (2001) Expression studies on AUX1-like genes in Medicago truncatula suggest that auxin is required at two steps in early nodule development. *Mol Plant Microbe Interact*, **14**, 267-277.

de Carvalho, F., Gheysen, G., Kushnir, S., Van Montagu, M., Inze, D. and Castresana, C. (1992) Suppression of beta-1,3-glucanase transgene expression in homozygous plants. *Embo J*, **11**, 2595-2602.

De Pinto, M.C., Francis, D. and De Gara, L. (1999) The redox state of ascorbate-dehydroascorbate pair as a specific sensor of cell division in tobacco BY-2 cells. *Protoplasma*, **209**, 90-97.

De Tullio, M.C., Paciolla, C., Dalla Vecchia, F., Rascio, N., D'Emerico, S., De Gara, L., Liso, R. and Arrigoni, O. (1999) Changes in onion root development induced by the inhibition of peptidyl-prolyl hydroxylase and influence of the ascorbate system on cell division and elongation. *Planta*, **209**, 424-434.

Del Carmen Cordoba-Pedregosa, M., Cordoba, F., Villalba, J.M. and Gonzalez-Reyes, J.A. (2003) Zonal changes in ascorbate and hydrogen peroxide contents, peroxidase, and ascorbate-related enzyme activities in onion roots. *Plant Physiol*, **131**, 697-706.

Denison, R.F. (1992) Mathematical-Modeling of Oxygen Diffusion and Respiration in Legume Root-Nodules. *Plant Physiology*, **98**, 901-907.

Denison, R.F. and Harter, B.L. (1995) Nitrate Effects on Nodule Oxygen Permeability and Leghemoglobin (Nodule Oximetry and Computer Modeling). *Plant Physiol*, **107**, 1355-1364.

Denison, R.F. and Layzell, D.B. (1991) Measurement of Legume Nodule Respiration and O2 Permeability by Noninvasive Spectrophotometry of Leghemoglobin. *Plant Physiology*, **96**, 137-143.

Denison, R.F. and Okano, Y. (2003) Leghaemoglobin oxygenation gradients in alfalfa and yellow sweetclover nodules. *Journal of Experimental Botany*, **54**, 1085-1091.

Desbrosses, G., Kopka, C., Ott, T. and Udvardi, M.K. (2004) Lotus japonicus LjKUP is induced late during nodule development and encodes a potassium transporter of the plasma membrane. *Mol Plant Microbe Interact*, **17**, 789-797.

Downie, J.A. (1994) Signalling strategies for nodulation of legumes by rhizobia. *Trends Microbiol*, **2**, 318-324.

Downs, C.G., Christey, M.C., Maddocks, D., Seelye, J.F. and Stevenson, D.G. (1994) Hairy roots of Brassica napus: I. Applied glutamine overcomes the effects of phosphinothricin treatment. *Plant Cell Rep*, **14**, 37-40.

Doyle, J.J. (2001) Leguminosae. In Brenner, S. and Miller, J.H. (eds.), *Enzyclopedia of Genetics*. Academic Press, San Diego, pp. 1081-1085.

Dunn, K., Dickstein, R., Feinbaum, R., Burnett, B.K., Peterman, T.K., Thoidis, G., Goodman, H.M. and Ausubel, F.M. (1988) Developmental regulation of nodule-specific genes in alfalfa root nodules. *Mol Plant Microbe Interact*, **1**, 66-74.

Earl, C.D., Ronson, C.W. and Ausubel, F.M. (1987) Genetic and structural analysis of the Rhizobium meliloti fixA, fixB, fixC, and fixX genes. *J Bacteriol*, **169**, 1127-1136.

Ehrhardt, D.W., Atkinson, E.M. and Long, S.R. (1992) Depolarization of Alfalfa Root Hair Membrane-Potential by Rhizobium-Meliloti Nod Factors. *Science*, **256**, 998-1000.

Ehrhardt, D.W., Wais, R. and Long, S.R. (1996) Calcium spiking in plant root hairs responding to Rhizobium nodulation signals. *Cell*, **85**, 673-681.

Elumalai, R.P., Nagpal, P. and Reed, J.W. (2002) A mutation in the Arabidopsis KT2/KUP2 potassium transporter gene affects shoot cell expansion. *Plant Cell*, **14**, 119-131.

Endo, M., Kokubun, T., Takahata, Y., Higashitani, A., Tabata, S. and Watanabe, M. (2000) Analysis of expressed sequence tags of flower buds in Lotus japonicus. *DNA Res*, **7**, 213-216.

Endre, G., Kereszt, A., Kevei, Z., Mihacea, S., Kalo, P. and Kiss, G.B. (2002) A receptor kinase gene regulating symbiotic nodule development. *Nature*, **417**, 962-966.

Fang, Y.W. and Hirsch, A.M. (1998) Studying early nodulin gene ENOD40 expression and induction by nodulation factor and cytokinin in transgenic alfalfa. *Plant Physiology*, **116**, 53-68.

Fedorova, M., van de Mortel, J., Matsumoto, P.A., Cho, J., Town, C.D., VandenBosch, K.A., Gantt, J.S. and Vance, C.P. (2002) Genome-wide identification of nodule-specific transcripts in the model legume Medicago truncatula. *Plant Physiol*, **130**, 519-537.

Felle, H.H., Kondorosi, E., Kondorosi, A. and Schultze, M. (1995) Nod Signal-Induced Plasma-Membrane Potential Changes in Alfalfa Root Hairs Are Differentially Sensitive to Structural Modifications of the Lipochitooligosaccharide. *Plant Journal*, **7**, 939-947.

Felle, H.H., Kondorosi, E., Kondorosi, A. and Schultze, M. (1998) The role of ion fluxes in Nod factor signalling in Medicago sativa. *Plant Journal*, **13**, 455-463.

Fernandes, M.S. and Rossiello, R.O.P. (1995) Mineral Nitrogen in Plant Physiology and Plant Nutrition. *Critical Reviews in Plant Sciences*, **14**, 111-148.

Finan, T.M., Wood, J.M. and Jordan, D.C. (1983) Symbiotic properties of C4-dicarboxylic acid transport mutants of Rhizobium leguminosarum. *J Bacteriol*, **154**, 1403-1413.

Fischer, H.M. (1994) Genetic regulation of nitrogen fixation in rhizobia. *Microbiol Rev*, **58**, 352-386.

Forrest, S.I., Verma, D.P.S. and Dhindsa, R.S. (1991) Starch content and activities of starch-metabolizing enzymes in effective and ineffective root nodules of soybean. *Canadian Journal of Botany-Revue Canadienne De Botanique*, **69**, 697-701.

Gage, D.J. (2004) Infection and invasion of roots by symbiotic, nitrogen-fixing rhizobia during nodulation of temperate legumes. *Microbiology and Molecular Biology Reviews*, **68**, 280-+.

Gamas, P., Niebel Fde, C., Lescure, N. and Cullimore, J. (1996) Use of a subtractive hybridization approach to identify new Medicago truncatula genes induced during root nodule development. *Mol Plant Microbe Interact*, **9**, 233-242.

Garcia-Pineda, E., Castro-Mercado, E. and Lozoya-Gloria, E. (2004) Gene expression and enzyme activity of pepper (Capsicum annuum L.) ascorbate oxidase during elicitor and wounding stress. *Plant Sci*, **166**, 237-243.

Geigenberger, P. (2003) Response of plant metabolism to too little oxygen. *Curr Opin Plant Biol*, **6**, 247-256.

Geurts, R. and Bisseling, T. (2002) Rhizobium nod factor perception and signalling. *Plant Cell*, **14**, S239-S249.

Gibon, Y., Vigeolas, H., Tiessen, A., Geigenberger, P. and Stitt, M. (2002) Sensitive and high throughput metabolite assays for inorganic pyrophosphate, ADPGlc, nucleotide phosphates, and glycolytic intermediates based on a novel enzymic cycling system. *Plant Journal*, **30**, 221-235.

Green, L.S. and Emerich, D.W. (1997) he formation of nitrogen-fixing bacteroids is delayed but not abolished in soybean infected by an alpha-ketoglutarate dehydrogenase-deficient mutant of Bradyrhizobium japonicum. *Plant Physiol*, **114**, 1359-1368.

Gregerson, R.G., Miller, S.S., Petrowski, M., Gantt, J.S. and Vance, C.P. (1994) Genomic Structure, Expression and Evolution of the Alfalfa Aspartate-Aminotransferase Genes. *Plant Molecular Biology*, **25**, 387-399.

Gresshoff, P.M. (2003) Post-genomic insights into plant nodulation symbioses. *Genome Biology*, **4**, 201.

Gualtieri, G. and Bisseling, T. (2000) The evolution of nodulation. *Plant Mol Biol*, **42**, 181-194.

Gubler, M. and Hennecke, H. (1988) Regulation of the fixA gene and fixBC operon in Bradyrhizobium japonicum. *J Bacteriol*, **170**, 1205-1214.

Handberg, K. and Stougaard, J. (1992) Lotus japonicus, an autogamous, diploid legume species for classical and molecular genetics. *Plant J*, **2**, 487-496.

Hargrove, P.W., Vanin, E.F., Kurtzman, G.J. and Nienhuis, A.W. (1997) High-level globin gene expression mediated by a recombinant adeno-associated virus genome that contains the 3' gamma globin gene regulatory element and integrates as tandem copies in erythroid cells. *Blood*, **89**, 2167-2175.

Hata, S., Izui, K. and Kouchi, H. (1998) Expression of a soybean nodule-enhanced phosphoenolpyruvate carboxylase gene that shows striking similarity to another gene for a house-keeping isoform. *Plant J*, **13**, 267-273.

Helliwell, C. and Waterhouse, P. (2003) Constructs and methods for high-throughput gene silencing in plants. *Methods*, **30**, 289-295.

Hellriegel, H. and Wilfarth, H. (1888) Untersuchungen über die Stickstoffnahrung der Gramineon und Leguminosen. *Ztschr. Ver. Rübenzucker-Industrie Deutschen Reichs*.

Herendeen, P.S., Magallon-Puebla, S., Lupia, R., Crane, P.R. and Kobylinska, J. (1999) A preliminary conspectus of the Allon flora from the Late Cretaceous (Late Santonian) of central Georgia, USA. *ANNALS OF THE MISSOURI BOTANICAL GARDEN*, **86**, 407-471.

Hirel, B., Bouet, C., King, B., Layzell, D., Jacobs, F. and Verma, D.P.S. (1987) Glutamine-Synthetase Genes Are Regulated by Ammonia Provided Externally or by Symbiotic Nitrogen-Fixation. *Embo Journal*, **6**, 1167-1171.

Hirsch, A.M. (1992) Developmental Biology of Legume Nodulation. *New Phytologist*, **122**, 211-237.

Hohnjec, N., Becker, J.D., Puhler, A., Perlick, A.M. and Kuster, H. (1999) Genomic organization and expression properties of the MtSucS1 gene, which encodes a nodule-enhanced sucrose synthase in the model legume Medicago truncatula. *Molecular and General Genetics*, **261**, 514-522.

Horemans, N., Foyer, C.H. and Asard, H. (2000) Transport and action of ascorbate at the plant plasma membrane. *Trends Plant Sci*, **5**, 263-267.

Horemans, N., Potters, G., De Wilde, L. and Caubergs, R.J. (2003) Dehydroascorbate uptake activity correlates with cell growth and cell division of tobacco bright yellow-2 cell cultures. *Plant Physiol*, **133**, 361-367.

Hunt, S. and Layzell, D.B. (1993) Gas-Exchange of Legume Nodules and the Regulation of Nitrogenase Activity. *Annual Review of Plant Physiology and Plant Molecular Biology*, **44**, 483-511.

Imaizumi-Anraku, H., Kawaguchi, M., Koiwa, H., Akao, S. and Syono, K. (1997) Two ineffective-nodulating mutants of Lotus japonicus: different phenotypes caused by the blockage of endocytotic bacterial release and nodule maturation. *Plant Cell Physiol*, **38**, 871-881.

Journet, E.P., Pichon, M., Dedieu, A., Debilly, F., Truchet, G. and Barker, D.G. (1994) Rhizobium-Meliloti Nod Factors Elicit Cell-Specific Transcription of the Enod12 Gene in Transgenic Alfalfa. *Plant Journal*, **6**, 241-249.

Journet, E.P., van Tuinen, D., Gouzy, J., Crespeau, H., Carreau, V., Farmer, M.J., Niebel, A., Schiex, T., Jaillon, O., Chatagnier, O., Godiard, L., Micheli, F., Kahn, D., Gianinazzi-Pearson, V. and Gamas, P. (2002) Exploring root symbiotic programs in the model legume Medicago truncatula using EST analysis. *Nucleic Acids Res*, **30**, 5579-5592.

Kapranov, P., deBruijn, F.J. and Szczyglowski, K. (1997) Novel, highly expressed late nodulin gene (LjNOD16) from Lotus japonicus. *Plant Physiology*, **113**, 1081-1090.

Kavroulakis, N., Flemetakis, E., Aivalakis, G. and Katinakis, P. (2000) Carbon metabolism in developing soybean root nodules: the role of carbonic anhydrase. *Mol Plant Microbe Interact*, **13**, 14-22.

Kawaguchi, M., Imaizumi-Anraku, H., Koiwa, H., Niwa, S., Ikuta, A., Syono, K. and Akao, S. (2002) Root, root hair, and symbiotic mutants of the model legume Lotus japonicus. *Mol Plant Microbe Interact*, **15**, 17-26.

Kerk, N.M. and Feldman, L.J. (1995) A biochemical model for the initiation and maintenance of the quiescent center: implications for organization of root meristems. *Development*, **121**, 2855-2833.

Kerk, N.M., Jiang, K. and Feldman, L.J. (2000) Auxin metabolism in the root apical meristem. *Plant Physiol*, **122**, 925-932.

Kistner, C. and Parniske, M. (2002) Evolution of signal transduction in intracellular symbiosis. *Trends in Plant Science*, **7**, 511-518.

Kouchi, H., Shimomura, K., Hata, S., Hirota, A., Wu, G.J., Kumagai, H., Tajima, S., Suganuma, N., Suzuki, A., Aoki, T., Hayashi, M., Yokoyama, T., Ohyama, T., Asamizu, E., Kuwata, C., Shibata, D. and Tabata, S. (2004) Large-scale analysis of gene expression profiles during early stages of root nodlule formation in a model legume, Lotus japonicus. *DNA Res*, **11**, 263-274.

Kubo, H. (1939) Über das Hämoprotein aus den Wurzelknöllchen von Leguminosen. *Acta Phytochimica (Tokyo)*, **11**, 195-200.

Kumagai, H. and Kouchi, H. (2003) Gene silencing by expression of hairpin RNA in Lotus japonicus roots and root nodules. *Mol Plant Microbe Interact*, **16**, 663-668.

Kurkdjian, A.C. (1995) Role of the Differentiation of Root Epidermal Cells in Nod Factor (from Rhizobium meliloti)-Induced Root-Hair Depolarization of Medicago sativa. *Plant Physiol*, **107**, 783-790.

Kurz, W.G.W. and Larue, T.A. (1977) Citric-Acid Cycle Enzymes and Nitrogenase in Nodules of Pisum-Sativum. *Canadian Journal of Microbiology*, **23**, 1197-1200.

Kuster, H., Fruhling, M., Perlick, A.M. and Puhler, A. (1993) The Sucrose Synthase Gene Is Predominantly Expressed in the Root-Nodule Tissue of Vicia-Faba. *Molecular Plant-Microbe Interactions*, **6**, 507-514.

Kuster, H., Hohnjec, N., Krajinski, F., El Yahyaoui, F., Manthey, K., Gouzy, J., Dondrup, M., Meyer, F., Kalinowski, J., Brechenmacher, L., van Tuinen, D., Gianinazzi-Pearson, V., Puhler, A., Gamas, P. and Becker, A. (2004) Construction and validation of cDNA-based Mt6k-RIT macro- and microarrays to explore root endosymbioses in the model legume Medicago truncatula. *Journal of Biotechnology*, **108**, 95-113.

Kuster, H., Quandt, H.J., Broer, I., Perlick, A.M. and Puhler, A. (1995a) The promoter of the Vicia faba L. VfENOD-GRP3 gene encoding a glycine-rich early nodulin mediates a predominant gene expression in the interzone II-III region of transgenic Vicia hirsuta root nodules. *Plant Mol Biol*, **29**, 759-772.

Kuster, H., Schroder, G., Fruhling, M., Pich, U., Rieping, M., Schubert, I., Perlick, A.M. and Puhler, A. (1995b) The nodule-specific VfENOD-GRP3 gene

encoding a glycine-rich early nodulin is located on chromosome I of Vicia faba L. and is predominantly expressed in the interzone II-III of root nodules. *Plant Mol Biol*, **28**, 405-421.

Kuzma, M.M., Hunt, S. and Layzell, D.B. (1993) Role of Oxygen in the Limitation and Inhibition of Nitrogenase Activity and Respiration Rate in Individual Soybean Nodules. *Plant Physiology*, **101**, 161-169.

Larkin, P.J., Gibson, J.M., Mathesius, U., Weinman, J.J., Gartner, E., Hall, E., Tanner, G.J., Rolfe, B.G. and Djordjevic, M.A. (1996) Transgenic white clover. Studies with the auxin-responsive promoter, GH3, in root gravitropism and lateral root development. *Transgenic Res*, **5**, 325-335.

Layzell, D.B., Gaito, S.T. and Hunt, S. (1988) Model of Gas-Exchange and Diffusion in Legume Nodules .1. Calculation of Gas-Exchange Rates and the Energy-Cost of N2 Fixation. *Planta*, **173**, 117-127.

Legocki, R.P. and Verma, D.P. (1980) Identification of "nodule-specific" host proteins (nodulins) involved in the development of rhizobium-legume symbiosis. *Cell*, **20**, 153-163.

Levy, J., Bres, C., Geurts, R., Chalhoub, B., Kulikova, O., Duc, G., Journet, E.P., Ane, J.M., Lauber, E., Bisseling, T., Denarie, J., Rosenberg, C. and Debelle, F. (2004) A putative Ca2+ and calmodulin-dependent protein kinase required for bacterial and fungal symbioses. *Science*, **303**, 1361-1364.

Limpens, E., Franken, C., Smit, P., Willemse, J., Bisseling, T. and Geurts, R. (2003) LysM domain receptor kinases regulating rhizobial Nod factor-induced infection. *Science*, **302**, 630-633.

Limpens, E., Ramos, J., Franken, C., Raz, V., Compaan, B., Franssen, H., Bisseling, T. and Geurts, R. (2004) RNA interference in Agrobacterium rhizogenes-transformed roots of Arabidopsis and Medicago truncatula. *Journal of Experimental Botany*, **55**, 983-992.

Lombari, P., Ercolano, E., El Alaoui, H. and Chiurazzi, M. (2003) A new transformation-regeneration procedure in the model legume Lotus japonicus: root explants as a source of large numbers of cells susceptible to Agrobacterium-mediated transformation. *Plant Cell Rep*, **21**, 771-777.

Madsen, E.B., Madsen, L.H., Radutoiu, S., Olbryt, M., Rakwalska, M., Szczyglowski, K., Sato, S., Kaneko, T., Tabata, S., Sandal, N. and Stougaard, J. (2003) A receptor kinase gene of the LysM type is involved in legume perception of rhizobial signals. *Nature*, **425**, 637-640.

Matzke, M.A., Matzke, A.J.M., Pruss, G.J. and Vance, V.B. (2001) RNA-based silencing strategies in plants. *Current Opinion in Genetics & Development*, **11**, 221-227.

Metzlaff, M., O'Dell, M., Cluster, P.D. and Flavell, R.B. (1997) RNA-mediated RNA degradation and chalcone synthase A silencing in petunia. *Cell*, **88**, 845-854.

Mitra, R.M. and Long, S.R. (2004) Plant and bacterial symbiotic mutants define three transcriptionally distinct stages in the development of the Medicago truncatula/Sinorhizobium meliloti symbiosis. *Plant Physiol*, **134**, 595-604.

Mitra, R.M., Shaw, S.L. and Long, S.R. (2004) Six nonnodulating plant mutants defective for Nod factor-induced transcriptional changes associated with the legume-rhizobia symbiosis. *Proceedings of the National Academy of Sciences of the United States of America*, **101**, 10217-10222.

Moloney, A.H. and Layzell, D.B. (1993) A Model of the Regulation of Nitrogenase Electron Allocation in Legume Nodules .1. The Diffusion Barrier and H-2 Inhibition of N2 Fixation. *Plant Physiology*, **103**, 421-428.

Morris, P. and Robbins, M.P. (1992) Condensed tannin formation by Agrobacterium rhizogenes transformed root and shoot organ cultures of Lotus corniculatus. *J Exp Bot*, **43**, 221-231.

Munoz, J.A., Palomares, A.J. and Ratet, P. (1996) Plant genes induced in the Rhizobium legume symbiosis. *World Journal of Microbiology & Biotechnology*, **12**, 189-202.

Noctor, G. and Foyer, C.H. (1998) ASCORBATE AND GLUTATHIONE: Keeping Active Oxygen Under Control. *Annu Rev Plant Physiol Plant Mol Biol*, **49**, 249-279.

Novak, K., Pesina, K., Nebesarova, J., Skrdleta, V., Lisa, L. and Nasinec, V. (1995) Symbiotic tissue degradation pattern in the ineffective nodules of three nodulation mutants of pea (Pisum sativum L.). *Annals of Botany*, **76**, 303-313.

Oger, P., Petit, A. and Dessaux, Y. (1996) A simple technique for direct transformation and regeneration of the diploid legume species Lotus japonicus. *Plant Sci*, **116**, 159-168.

Olhoft, P.M., Flagel, L.E., Donovan, C.M. and Somers, D.A. (2003) Efficient soybean transformation using hygromycin B selection in the cotyledonary-node method. *Planta*, **216**, 723-735.

Pacios-Bras, C., Schlaman, H.R., Boot, K., Admiraal, P., Langerak, J.M., Stougaard, J. and Spaink, H.P. (2003) Auxin distribution in Lotus japonicus during root nodule development. *Plant Mol Biol*, **52**, 1169-1180.

Panter, S., Thomson, R., de Bruxelles, G., Laver, D., Trevaskis, B. and Udvardi, M. (2000) Identification with proteomics of novel proteins associated with the peribacteroid membrane of soybean root nodules. *Molecular Plant-Microbe Interactions*, **13**, 325-333.

Peng, H.M., Dreyer, D.A., VandenBosch, K.A. and Cook, D. (1996) Gene structure and differential regulation of the Rhizobium-induced peroxidase gene rip1. *Plant Physiology*, **112**, 1437-1446.

Phillips, D.A. and Streit, W.R. (1996) Legume signals to rhizobial symbionts: a new approach for defining rhizosphere colonization. In Stacey, G. and Keen, N.T. (eds.), *Plant Microbe Interactions*. Chapman and Hall, New York, pp. 236-271.

Pignocchi, C., Fletcher, J.M., Wilkinson, J.E., Barnes, J.D. and Foyer, C.H. (2003) The function of ascorbate oxidase in tobacco. *Plant Physiol*, **132**, 1631-1641.

Pignocchi, C. and Foyer, C.H. (2003) Apoplastic ascorbate metabolism and its role in the regulation of cell signalling. *Curr Opin Plant Biol*, **6**, 379-389.

Porterfield, D.M., Kuang, A., Smith, P.J., Crispi, M.L. and Musgrave, M.E. (1999) Oxygen-depleted zones inside reproductive structures of Brassicaceae: implications for oxygen control of seed development. *Can J Bot*, **77**, 1439-1446.

Postma, J.G., Jager, D., Jacobsen, E. and Feenstra, W.J. (1990) Studies on a non-fixing mutant of pea (Pisum sativum L.): I. Phenotypical description and bacteroid activity. *Plant Sci*, **69**, 151-161.

Potters, G., Horemans, N., Caubergs, R.J. and Asard, H. (2000) Ascorbate and dehydroascorbate influence cell cycle progression in a tobacco cell suspension. *Plant Physiol*, **124**, 17-20.

Preisig, O., Zufferey, R., ThonyMeyer, L., Appleby, C.A. and Hennecke, H. (1996) A high-affinity cbb(3)-type cytochrome oxidase terminates the symbiosis-specific respiratory chain of Bradyrhizobium japonicum. *Journal of Bacteriology*, **178**, 1532-1538.

Pueppke, S.G. and Broughton, W.J. (1999) Rhizobium sp. strain NGR234 and R-fredii USDA257 share exceptionally broad, nested host ranges. *Molecular Plant-Microbe Interactions*, **12**, 293-318.

Radutoiu, S., Madsen, L.H., Madsen, E.B., Felle, H.H., Umehara, Y., Gronlund, M., Sato, S., Nakamura, Y., Tabata, S., Sandal, N. and Stougaard, J. (2003) Plant recognition of symbiotic bacteria requires two LysM receptor-like kinases. *Nature*, **425**, 585-592.

Ramu, S.K., Peng, H.M. and Cook, D.R. (2002) Nod factor induction of reactive oxygen species production is correlated with expression of the early nodulin gene rip1 in Medicago truncatula. *Mol Plant Microbe Interact*, **15**, 522-528.

Rigas, S., Debrosses, G., Haralampidis, K., Vicente-Agullo, F., Feldmann, K.A., Grabov, A., Dolan, L. and Hatzopoulos, P. (2001) TRH1 encodes a potassium transporter required for tip growth in Arabidopsis root hairs. *Plant Cell*, **13**, 139-151.

Rolfe, B.G. and Gresshoff, P.M. (1988) Genetic-Analysis of Legume Nodule Initiation. *Annual Review of Plant Physiology and Plant Molecular Biology*, **39**, 297-319.

Ronson, C.W., Lyttleton, P. and Robertson, J.G. (1981) C4-dicarb-oxylate transport mutants of Rhizobium trifolii form ineffective nodules on Trifolium repens. *Proc Natl Acad Sci U S A*, **78**, 4284-4288.

Saalbach, G., Erik, P. and Wienkoop, S. (2002) Characterisation by proteomics of peribacteroid space and peribacteroid membrane preparations from pea (Pisum sativum) symbiosomes. *Proteomics*, **2**, 325-337.

Sambrook, J., Fritsch, E.F. and Maniatis, T. (1989) *Molecular Cloning*. Cold Spring Harbor Laboratory Press, Cold Spring Harbor.

Sanmartin, M., Drogoudi, P.A., Lyons, T., Pateraki, I., Barnes, J. and Kanellis, A.A. (2003) Over-expression of ascorbate oxidase in the apoplast of transgenic tobacco results in altered ascorbate and glutathione redox states and increased sensitivity to ozone. *Planta*, **216**, 918-928.

Santagostini, L., Gullotti, M., De Gioia, L., Fantucci, P., Franzini, E., Marchesini, A., Monzani, E. and Casella, L. (2004) Probing the location of the substrate binding site of ascorbate oxidase near type 1 copper: an investigation through spectroscopic, inhibition and docking studies. *Int J Biochem Cell Biol*, **36**, 881-892.

Santana, M.A., Pihakaski-Maunsbach, K., Sandal, N., Marcker, K.A. and Smith, A.G. (1998) Evidence that the plant host synthesizes the heme moiety of leghemoglobin in root nodules. *Plant Physiology*, **116**, 1259-1269.

Sato, T., Onoma, N., Sueyoshi, K. and Ohyama, T. (2001) Changes in four leghemoglobin components in nodules of hypernodulating soybean (Glycine max [L] Merr.) mutant and its parent in the early nodule developmental stage. *Plant and Soil*, **237**, 129-135.

Schauser, L., Handberg, K., Sandal, N., Stiller, J., Thykjaer, T., Pajuelo, E., Nielsen, A. and Stougaard, J. (1998) Symbiotic mutants deficient in nodule establishment identified after T-DNA transformation of Lotus japonicus. *Mol Gen Genet*, **259**, 414-423.

Schauser, L., Roussis, A., Stiller, J. and Stougaard, J. (1999) A plant regulator controlling development of symbiotic root nodules. *Nature*, **402**, 191-195.

Scheres, B., Vandewiel, C., Zalensky, A., Horvath, B., Spaink, H., Vaneck, H., Zwartkruis, F., Wolters, A.M., Gloudemans, T., Vankammen, A. and Bisseling, T. (1990) The Enod12 Gene-Product Is Involved in the Infection Process During the Pea Rhizobium Interaction. *Cell*, **60**, 281-294.

Schmulling, T., Rohrig, H., Pilz, S., Walden, R. and Schell, J. (1993) Restoration of fertility by antisense RNA in genetically engineered male sterile tobacco plants. *Mol Gen Genet*, **37**, 385-394.

Schroder, G., Fruhling, M., Puhler, A. and Perlick, A.M. (1997) The temporal and spatial transcription pattern in root nodules of Vicia faba nodulin genes encoding glycine-rich proteins. *Plant Molecular Biology*, **33**, 113-123.

Sheehy, J.E., Minchin, F.R. and Witty, J.F. (1985) Control of Nitrogen-Fixation in a Legume Nodule - an Analysis of the Role of Oxygen Diffusion in Relation to Nodule Structure. *Annals of Botany*, **55**, 549-562.

Silvente, S., Camas, A. and Lara, M. (2003) Molecular cloning of the cDNA encoding aspartate aminotransferase from bean root nodules and determination of its role in nodule nitrogen metabolism. *Journal of Experimental Botany*, **54**, 1545-1551.

Soltis, P.S., Soltis, D.E., Savolainen, V., Crane, P.R. and Barraclough, T.G. (2002) Rate heterogeneity among lineages of tracheophytes: integration of molecular and fossil data and evidence for molecular living fossils. *Proc Natl Acad Sci U S A*, **99**, 4430-4435.

Somers, D.A., Samac, D.A. and Olhoft, P.M. (2003) Recent advances in legume transformation. *Plant Physiol*, **131**, 892-899.

Spaink, H.P. (2000) Root nodulation and infection factors produced by rhizobial bacteria. *Annu Rev Microbiol*, **54**, 257-288.

Stiller, J., Martirani, L., Tuppale, S., Chian, R.-J., Chiurazzi, M. and Gresshoff, P.M. (1997) High frequency transformation and regeneration of transgenic plants in the model legume Lotus japonicus. *J Exp Bot*, **48**, 1357-1365.

Stowers, M.D. and Elkan, G.H. (1983) The Transport and Metabolism of Glucose in Cowpea Rhizobia. *Canadian Journal of Microbiology*, **29**, 398-406.

Stracke, S., Kistner, C., Yoshida, S., Mulder, L., Sato, S., Kaneko, T., Tabata, S., Sandal, N., Stougaard, J., Szczyglowski, K. and Parniske, M. (2002) A plant receptor-like kinase required for both bacterial and fungal symbiosis. *Nature*, **417**, 959-962.

Streeter, J.G. and Salminen, S.O. (1993) Alterations in Apoplastic and Total Solute Concentrations in Soybean Nodules Resulting from Treatments Known to Affect Gas-Diffusion. *Journal of Experimental Botany*, **44**, 821-828.

Strozycki, P. and Legocki, A.B. (1988) Isolation and characterization of root nodule proteins from lupin. *Acta Biochim Pol*, **35**, 39-50.

Swiderski, M.R., Zaborowska, Z. and Legocki, A.B. (2000) Identification of new nodulin cDNAs from yellow lupine by differential display. *Plant Science*, **151**, 75-83.

Szczyglowski, K., Shaw, R.S., Wopereis, J., Copeland, S., Hamburger, D., Kasiborski, B., Dazzo, F.B. and De Bruijn, F.J. (1998) Nodule Organogenesis and Symbiotic Mutants of the Model Legume Lotus japonicus. *MPMI*, **11**, 684-697.

Tansengco, M.L., Hayashi, M., Kawaguchi, M., Imaizumi-Anraku, H. and Murooka, Y. (2003) crinkle, a novel symbiotic mutant that affects the infection thread growth and alters the root hair, trichome, and seed development in Lotus japonicus. *Plant Physiol*, **131**, 1054-1063.

Temple, S.J., Bagga, S. and Sengupta-Gopalan, C. (1998) Down-regulation of specific members of the glutamine synthetase gene family in alfalfa by antisense RNA technology. *Plant Mol Biol*, **37**, 535-547.

Terada, R., Ignacimuthu, S., Bauer, P., Kondorosi, E., Schultze, M., Kondorosi, A., Potrykus, I. and Sautter, C. (2001) Expression of early nodulin promoter gene in transgenic rice. *Current Science*, **81**, 270-276.

Thibaud-Nissen, F.O., Shealy, R.T., Khanna, A. and Vodkin, L.O. (2003) Clustering of microarray data reveals transcript patterns associated with somatic embryogenesis in soybean. *Plant Physiology*, **132**, 118-136.

Thimm, O., Blasing, O., Gibon, Y., Nagel, A., Meyer, S., Kruger, P., Selbig, J., Muller, L.A., Rhee, S.Y. and Stitt, M. (2004) MAPMAN: a user-driven tool to display genomics data sets onto diagrams of metabolic pathways and other biological processes. *Plant J*, **37**, 914-939.

Thony, B., Fischer, H.M., Anthamatten, D., Bruderer, T. and Hennecke, H. (1987) The symbiotic nitrogen fixation regulatory operon (fixRnifA) of Bradyrhizobium japonicum is expressed aerobically and is subject to a novel, nifA-independent type of activation. *Nucleic Acids Res*, **15**, 8479-8499.

Thumfort, P.P., Layzell, D.B. and Atkins, C.A. (2000) A simplified approach for modeling diffusion into cells. *Journal of Theoretical Biology*, **204**, 47-65.

Thummler, F. and Verma, D.P.S. (1987) Nodulin-100 of Soybean Is the Subunit of Sucrose Synthase Regulated by the Availability of Free Heme in Nodules. *Journal of Biological Chemistry*, **262**, 14730-14736.

Thykjaer, T., Finnemann, J., Schauser, L., Christensen, L., Poulsen, C. and Stougaard, J. (1997) Gene targeting approaches using positive-negative selection and large flanking regions. *Plant Mol Biol*, **35**, 523-530.

Tjepkema, J.D. and Yocum, C.S. (1974) Measurement of oxygen partial pressure within soybean nodules by oxygen microelectrodes. *Planta*, **119**, 351-360.

Trent, J.T., 3rd, Watts, R.A. and Hargrove, M.S. (2001) Human neuroglobin, a hexacoordinate hemoglobin that reversibly binds oxygen. *J Biol Chem*, **276**, 30106-30110.

Trepp, G.B., Plank, D.W., Gantt, J.S. and Vance, C.P. (1999a) NADH-glutamate synthase in alfalfa root nodules. Immunocytochemical localization. *Plant Physiology*, **119**, 829-837.

Trepp, G.B., van de Mortel, M., Yoshioka, H., Miller, S.S., Samac, D.A., Gantt, J.S. and Vance, C.P. (1999b) NADH-glutamate synthase in alfalfa root nodules. Genetic regulation and cellular expression. *Plant Physiology*, **119**, 817-828.

Trevaskis, B., Watts, R.A., Andersson, C.R., Llewellyn, D.J., Hargrove, M.S., Olson, J.S., Dennis, E.S. and Peacock, W.J. (1997) Two hemoglobin genes in Arabidopsis thaliana: The evolutionary origins of leghemoglobins. *Proceedings of the National Academy of Sciences of the United States of America*, **94**, 12230-12234.

Trieu, A.T., Burleigh, S.H., Kardailsky, I.V., Maldonado-Mendoza, I.E., Versaw, W.K., Blaylock, L.A., Shin, H., Chiou, T.J., Katagi, H., Dewbre, G.R., Weigel, D. and Harrison, M.J. (2000) Transformation of Medicago truncatula via infiltration of seedlings or flowering plants with Agrobacterium. *Plant J*, **22**, 531-541.

Trieu, A.T. and Harrison, M.J. (1996) Rapid transformation of Medicago truncatula: regeneration via shoot organogenesis. *Plant Cell Reports*, **6**, 6-11.

Uchiumi, T., Shimoda, Y., Tsuruta, T., Mukoyoshi, Y., Suzuki, A., Senoo, K., Sato, S., Kato, T., Tabata, S., Higashi, S. and Abe, M. (2002) Expression of symbiotic and nonsymbiotic globin genes responding to microsymbionts on Lotus japonicus. *Plant and Cell Physiology*, **43**, 1351-1358.

Udvardi, M., Day, D.A. and Gresshoff, P.M. (1986) Stimulation of respiration and nitrogenase in bacteroids of Siratro (Macroptilium atropurpureum) by plant nodule cytosol. *Plant Cell Rep*, **3**, 207-209.

Udvardi, M.K. and Day, D.A. (1997) Metabolite transport across symbiotic membranes of legume nodules. *Annual Review of Plant Physiology and Plant Molecular Biology*, **48**, 493-523.

Umemura, Y., Ishiduka, T., Yamamoto, R. and Esaka, M. (2004) The Dof domain, a zinc finger DNA-binding domain conserved only in higher plants, truly functions as a Cys2/Cys2 Zn finger domain. *Plant J*, **37**, 741-749.

Van de Velde, W., Mergeay, J., Holsters, M. and Goormachtig, S. (2003) Agrobacterium rhizogenes-mediated transformation of Sesbania rostrata. *Plant Sci*, **165**, 1281-1288.

van Dongen, J.T., Roeb, G.W., Dautzenberg, M., Froehlich, A., Vigeolas, H., Minchin, P.E. and Geigenberger, P. (2004) Phloem import and storage metabolism are highly coordinated by the low oxygen concentrations within developing wheat seeds. *Plant Physiol*, **135**, 1809-1821.

van Slooten, J.C., Bhuvaneswari, T.V., Bardin, S. and Stanley, J. (1992) Two C4-dicarboxylate transport systems in Rhizobium sp. NGR234: Rhizobial dicarboxylate transport is essential for nitrogen fixation in tropical legumes. *Molecular Plant-Microbe Interactions*, **5**, 179-186.

Vanacker, H., Carver, T.L. and Foyer, C.H. (1998) Pathogen-induced changes in the antioxidant status of the apoplast in barley leaves. *Plant Physiol*, **117**, 1103-1114.

Vance, C.P. and Gantt, J.S. (1992) Control of nitrogen and carbon metabolism in root nodules. *Physiol Plant*, **85**, 266-274.

Vance, C.P. and Johnson, E.B. (1983) Plant determined ineffective nodules in alfalfa (Medicago sativa): structural and biochemical comparison. *Canadian Journal of Botany-Revue Canadienne De Botanique*, **61**, 49-61.

Vaucheret, H., Beclin, C. and Fagard, M. (2001) Post-transcriptional gene silencing in plants. *J Cell Sci*, **114**, 3083-3091.

Vaucheret, H. and Fagard, M. (2001) Transcriptional gene silencing in plants: targets, inducers and regulators. *Trends Genet*, **17**, 29-35.

Vitoursek, P.M., Aber, J.D., Howarth, R.W., Likens, G.E., Matson, P.A., Schindler, D.W., Schlesinger, W.H. and Tilman, D.G. (1997) Human alteration of the global nitrogen cycle: causes and consequences. *Issues in Ecology*, **1**, 1-15.

Waterhouse, P.M., Graham, M.W. and Wang, M.B. (1998) Virus resistance and gene silencing in plants can be induced by simultaneous expression of sense and antisense RNA. *Proc Natl Acad Sci U S A*, **95**, 13959-13964.

Waterhouse, P.M., Wang, M.B. and Finnegan, E.J. (2001a) Role of short RNAs in gene silencing. *Trends in Plant Science*, **6**, 297-301.

Waterhouse, P.M., Wang, M.B. and Lough, T. (2001b) Gene silencing as an adaptive defence against viruses. *Nature*, **411**, 834-842.

Watts, R.A., Hunt, P.W., Hvitved, A.N., Hargrove, M.S., Peacock, W.J. and Dennis, E.S. (2001) A hemoglobin from plants homologous to truncated hemoglobins of microorganisms. *Proceedings of the National Academy of Sciences of the United States of America*, **98**, 10119-10124.

Webb, J. and Sheehy, J.E. (1991) Legume Nodule Morphology with Regard to Oxygen Diffusion and Nitrogen-Fixation. *Annals of Botany*, **67**, 77-83.

Webb, K.J., Gibbs, M.J., Mizen, S., Skot, L. and Gatehouse, J.A. (1996) Genetic transformation of Lotus corniculatus with Agrobacterium tumefaciens and the analysis of the inheritance of transgenes in the T1 generation. *Transgenic Res*, **5**, 303-312.

Wienkoop, S. and Saalbach, G. (2003) Proteome analysis. Novel proteins identified at the peribacteroid membrane from Lotus japonicus root nodules. *Plant Physiology*, **131**, 1080-1090.

Wittenberg, J.A., Bergersen, F.J., Appleby, C.A. and Turner, G.L. (1974) Facilitated oxygen diffusion. The role of leghemoglobin in nitrogen fixation by bacteroids isolated from soybean root nodules. *J Biol Chem*, **249**, 4057-4066.

Wittenberg, J.B. and Wittenberg, B.A. (1990) Mechanisms of Cytoplasmic Hemoglobin and Myoglobin Function. *Annual Review of Biophysics and Biophysical Chemistry*, **19**, 217-241.

Wittenberg, J.B., Wittenberg, B.A. and Appleby, C.A. (1972) Kinetics of Reactions of Leghemoglobin with Oxygen and Carbon-Monoxide. *J Biol Chem*, **247**, 527-536.

Witty, J.F. and Minchin, F.R. (1994) A new method to detect the presence of continuous gas-filled pathways for oxygen diffusion in legume nodules. *J Exp Bot*, **45**, 967-978.

Witty, J.F. and Minchin, F.R. (1998) Hydrogen measurements provide direct evidence for a variable physical barrier to gas diffusion in legume nodules. *Journal of Experimental Botany*, **49**, 1015-1020.

Xu, W.X., Zhou, Y. and Chollet, R. (2003) Identification and expression of a soybean nodule-enhanced PEP-carboxylase kinase gene (NE-PpcK) that shows striking up-/down-regulation in vivo. *Plant Journal*, **34**, 441-452.

Yoshioka, H., Gregerson, R.G., Samac, D.A., Hoevens, K.C.M., Trepp, G., Gantt, J.S. and Vance, C.P. (1999) Aspartate aminotransferase in alfalfa nodules: Localization of mRNA during effective and ineffective nodule development and promoter analysis. *Molecular Plant-Microbe Interactions*, **12**, 263-274.

Yu, J.P. and Shao, Q.Q. (1991) Transfromation of Lotus corniculatus L. mediated by Agrobacterium tumefasciens. *Sci China B*, **34**, 932-937.

9.0 Appendix

Primers used for qRT-PCR

EST Accession	TC number	Forward primer	Reverse primer	Gene annotation
LjNEST20b12	TC14054	TTCACCTTGTGCTCCGTCTTC	AACAACAGCACACACAGCCAATCC	Ubiquitin
AB042716	TC14055	TTTGAGCACTGCTTGGGGAGTAGCT	CTGCAATTAAGAAGGCAATG	Leghemoglobin, LjLb1
AB042717	TC14065	ATTGAGCACTGCTTGGGGAGTAGCC	CTGCAATTAAGAAGGCAATG	Leghemoglobin, LjLb2
AB088224	TC14039	CTTGAGCACCGCTTGGGAAGGAGCA	CTGCAATTAAGAAGGCAATG	Leghemoglobin, LjLb3
	see above	CTCCAAGCCCATGCTGAAAA	TGGCATCTGCAAGTGTCACTTC	Symbiotic leghemoglobins (LjLbtotal)
LjNEST67g11	TC16046	TTGGCTGGGGTGATTAAAAAGGG	CATCACCAGTTTAACAAGTTTTAG	Non-symbiotic hemoglobin, LjNSG1
LjNEST35c7	TC10713	CAAGCCTCATGCCATGTCTGT	CAGTGACTTTTCCAGCCTTCCGC	Non-symbiotic hemoglobin, LjNSG2
NC_002678	None	TCCAAGGTCATCCACTTCGTG	GCGCATACTGGATTACCGTCA	Nitrogenase (NifH, Fe-protein)
NC_002678	None	AATTGCTTGCATCCTCGTCC	AAACAGCAGCGAACGCATC	Nitrogenase (NifD, FeMo protein)
NC_004463	None	GCCCTCTGCTCGACCTTTCC	AGCATCGCCATCGTGTCCTC	sigA
LjNEST98c11	TC11125	GCCACATGCTAGAGTTTCCCAAA	TGTGGTTTTTGCGGAGGCT	Ascorbate oxidase
LjNEST8d4	singleton	GATTCCCAAATAGTCCTCTTCCGTC	GTAAAGCGGCGATGTCACGAGACC	Potassium transporter LjKUP
LjNEST11A11	TC18767	GATGCTGAGGATCAGCCTTCTG	CCCATCCTCCTGTTCTGCAAT	unknown
LjNEST25D11	TC8629	TTCTACAAACGCCACGCTTGT	TGTCCTTGAAAAATGCACCCC	carbonic anhydrase
LjNEST3E1	TC14306	TCCCTAGTGAACCTGCACACAT	AAAGAGCCCTAACCCCTTGCT	carbonic anhydrase
LjNEST7c12	TC8366	TGAAGAGCCATACTCATTCCGC	CCAATCACATTTACTGCGAGGC	MtN24
LjNEST12h12	TC8309	TGCATCAGCAAACTCTGCC	CTCATGATCCTTCAATGAAGCC	NJ21
LjNEST2h5	TC13004	TGTGGAAATGGCATCCCCTA	ATCCTGGAAGCCAGCCACTTA	Lysophospholipase
LjNEST15A11	TC14525	CTGCCAGAAGATCCAGAAAACTAC	CCAGAGCGCTTGCCCAAACACTC	isoliquiritigenin 2'-O-methyltransferase (cOMT)
LjNEST12H12	TC19016	TGCATCAGCAAACTCTGCC	CTCATGATCCTTCAATGAAGCC	Ent-kaurene synthase A
LjNEST12C4	TC8045	TCTTGGACTGGTCTTCCTTGCT	TGGTCTCTTGTTCCTCACGTGT	Sulphate transporter
LjNEST16B9	TC8129	GACATGCAAGCCCACAAACT	CTATGAGTGTTTTGGCCTCAGG	GA 2-oxidase
AJ271788	TC14488	TCACACACACTCCTCTGCATCC	ATCCACAACTGCAAGTGCGAC	ENOD40
LjNEST96a9	TC14124	CCAGAATGGCGTGCTTTGATGG	GTAGCCAGGCGGAAATACTCAA	Phosphoenolpyruvate carboxylase
LjNEST7c7	TC14491	TGCATGCGCTCATAACCCTAC	CCTAATCTGCTCCCATTGCTCA	Aspartate aminotransferase
AW409409	TC14272	GCCTTATTGAAGCCCATGTTGA	TCCTTCAGAATAGCCGCACCT	Ferredoxin dependent GOGAT
LjNEST60e4	TC8427	CAGCATATGGAACAGGCAATGA	GGTGTGGATGTCAGCTGTTTCA	Glutamine sythase
LjNEST18a5	TC7991	AGGAGGTGTTGCATTGGCTATG	GGAAGCCTCAGCAAAAGAACG	NADPH-specific isocitrate dehydrogenase

10.0 Publications and presentations of the projects

Peer-reviewed papers and book articles

1. Guilhem Desbrosses, Claudia Kopka, **Thomas Ott**, and Michael K. Udvardi (2004); "*Lotus japonicus LjKUP* is induced late during nodule development and encodes a potassium transporter of the plasma membrane"; Mol Plant Microbe Int 17 (7): 789-797
2. Gillian Colebatch, Guilhem Desbrosses, **Thomas Ott**, Lene Krusell, Sebastian Kloska, Joachim Kopka, and Michael Udvardi (2004); "Global changes in transcription orchestrate metabolic differentiation during symbiotic nitrogen fixation in *Lotus japonicus*"; The Plant Journal, 39 (4): 487-512
3. **Thomas Ott**, Lene Krusell and Michael Udvardi (2005): "*Lotus* transcriptome analysis using cDNA arrays"; in: *Lotus japonicus* handbook (Márquez AJ, Ed.), Kluwer, Dordrecht (*in press*)
4. Makoto Hayashi, Myra L. Tansengco, Norio Suganuma, Krzysztof Szczyglowski, Lene Krusell, **Thomas Ott**, Michael Udvardi (2005): "Methods for studying nodule development and function"; in: *Lotus japonicus* handbook (Márquez AJ, Ed.), Kluwer, Dordrecht (*in press*)
5. **Thomas Ott,** Joost van Dongen, Catrin Günther, Lene Krusell, Guilhem Desbrosses, Vivien Bock, Helene Vigeolas, Tomasz Czechowski, Peter Geigenberger and Michael Udvardi (2005): "Plant hemoglobins reduce free-oxygen concentrations in legume root nodules and are indispensable for symbiotic nitrogen fixation ", Current Biology, Mar 29;15(6):531-5.
6. Lene Krusell, Katja Krause, **Thomas Ott**, Guilhem Desbrosses, Ute Kraemer, Shusei Sato, Yasukazu Nakamura, Satoshi Tabata, Euan James, Niels Sandal, Jens Stougaard, Masayoshi Kawaguchi, Ai Miyamoto, Norio Suganuma and Michael Udvardi (2005): "The sulfate transporter SST1 is crucial for symbiotic nitrogen fixation in *Lotus japonicus* root nodules" , The Plant Cell, Vol. 17, 1625–1636.
7. **Thomas Ott,** Lene Krusell, Manolis Flementakis, Michael Udvardi; "Cell-specific expression of ascorbate oxidase reveals its role in nodule development" (*in preparation*)

Conference contributions (proceedings, posters, talks) and seminar talks

1. **Thomas Ott** (2003); "Redox control of rhizobial infection in the model legume *Lotus japonicus*";12th May 2003; University of Göttingen, Germany (**seminar speaker**)
2. **Thomas Ott**, Lene Krusell, Guilhem Desbrosses, Michael Udvardi (2003); "Functional genomics of redox metabolism and nodulation in Lotus japonicus"; MPMI-11th International Congress; 18th-26th July 2003, St. Petersburg, Russia (**poster**)
3. **Thomas Ott** (2004); "New insights and final proofs: The importance of oxygen during symbiotic nitrogen fixation and nodule development in *Lotus japonicus*"; 16th April 2004, INRA Toulouse, France (**seminar speaker**)
4. Lene Krusell, **Thomas Ott**, Katja Krause, Gillian Colebatch, Guilhem Desbrosses, Sebastian Kloska, and Joachim Kopka, Niels Sandal, Jens Stougaard, Norio Suganuma, and Michael Udvardi ; "Legume Transcriptomics

and the Renaissance in Symbiotic Nitrogen Fixation Research"; (**proceeding**, *in press*)

5. **Thomas Ott**, Joost van Dongen, Catrin Günther, Lene Krusell, Guilhem Desbrosses, Vivien Bock, Tomasz Czechowski, Peter Geigenberger and Michael Udvardi; "RNAi silencing of leghemoglobin increases steady-state oxygen concentrations and prohibits symbiotic nitrogen fixation in *Lotus japonicus* nodules"; 6th European Nitrogen Fixation Congress, 24th 27th July 2004, Toulouse, France (**talk and poster**)
6. **Thomas Ott**, Joost van Dongen, Catrin Günther, Lene Krusell, Guilhem Desbrosses, Vivien Bock, Tomasz Czechowski, Peter Geigenberger and Michael Udvardi; "Testing a decades old hypothesis: RNAi silencing of leghemoglobin increases steady-state oxygen concentrations and prohibits symbiotic nitrogen fixation in *Lotus japonicus* nodules"; Botanikertagung, 05th 10th September 2004, Braunschweig, Germany (**talk**)
7. **Thomas Ott** (2004); "Functional genomics on nodulins in the model legume Lotus japonicus"; 10th November 2004, University of San Martin, INTECH, Buenos Aires, Argentina (**seminar speaker**)
8. Michael Udvardi, Vivien Bock, Gillian Colebatch, Guilhem Desbrosses, Sebastian Kloska, Katja Krause, Lene Krusell, **Thomas Ott**, Ben Trevaskis, Maren Wandrey (2004); "Genetic reorganisation of legume transport and metabolism during symbiotic nitrogen fixation"; Biology of Plant-Microbe Interactions, Volume 4, Igor Tikhonovich, Ben Lugtenberg and Nikolai Provorov (Eds.), pp 490-492 (**proceeding**)
9. **Thomas Ott**, Joost van Dongen, Catrin Günther, Lene Krusell, Guilhem Desbrosses, Helene Vigeolas, Vivien Bock, Diana Sahid, Tomasz Czechowski, Peter Geigenberger, John Sullivan, Clive Ronson, Euan James and Michael K. Udvardi (2005): "Symbiotic leghemoglobins are crucial for nitrogen fixation in legume root nodules but not for general plant growth and development"; XIIth International Congress on Molecular Plant-Microbe Interactions, July 17-22, 2005, Cancun, Mexico (**talk**)